

1 **Mass balance of the ice sheets and glaciers – progress since AR5 and challenges**

2 **EARTH SCIENCE REVIEWS invited review/synthesis paper**

3 **30 September 2019 revised version**

4  
5 Edward Hanna<sup>1</sup>, Frank Pattyn<sup>2</sup>, Francisco Navarro<sup>3</sup>, Vincent Favier<sup>4</sup>, Heiko Goelzer<sup>2,5</sup>,  
6 Michiel R. van den Broeke<sup>5</sup>, Miren Vizcaino<sup>6</sup>, Pippa L. Whitehouse<sup>7</sup>, Catherine Ritz<sup>4</sup>, Kevin  
7 Bulthuis<sup>8,2</sup>, Ben Smith<sup>9</sup>

8

9 <sup>1</sup>School of Geography and Lincoln Centre for Water and Planetary Health, University of  
10 Lincoln, Lincoln, UK, ehanna@lincoln.ac.uk

11 <sup>2</sup>Laboratoire de Glaciologie, Université Libre de Bruxelles, Brussels, Belgium

12 <sup>3</sup>Departamento de Matemática Aplicada a las Tecnologías de la Información y las  
13 Comunicaciones, Universidad Politécnica de Madrid, Madrid, Spain

14 <sup>4</sup>CNRS, Univ. Grenoble Alpes, Institut des Géosciences de l'Environnement (IGE), 38000  
15 Grenoble, France

16 <sup>5</sup>Institute for Marine and Atmospheric Research, Utrecht University, Utrecht, The  
17 Netherlands

18 <sup>6</sup>Department of Geoscience and Remote Sensing, Delft University of Technology, Delft, The  
19 Netherlands

20 <sup>7</sup>Department of Geography, University of Durham, Durham, UK

21 <sup>8</sup>Computational and Stochastic Modeling, Aerospace and Mechanical Engineering, Université  
22 de Liège, Liège, Belgium

23 <sup>9</sup>Polar Science Center, Applied Physics Lab, University of Washington, Seattle, USA

24  
25  
26  
27 **Abstract.** Recent research shows increasing decadal ice mass losses from the Greenland and  
28 Antarctic Ice Sheets and more generally from glaciers worldwide in the light of continued  
29 global warming. Here, in an update of our previous ISMASS paper (Hanna et al., 2013), we  
30 review recent observational estimates of ice sheet and glacier mass balance, and their related  
31 uncertainties, first briefly considering relevant monitoring methods. Focusing on the response  
32 to climate change during 1992-2018, and especially the post-IPCC AR5 period, we discuss  
33 recent changes in the relative contributions of ice sheets and glaciers to sea-level change. We  
34 assess recent advances in understanding of the relative importance of surface mass balance  
35 and ice dynamics in overall ice-sheet mass change. We also consider recent improvements in  
36 ice-sheet modelling, highlighting data-model linkages and the use of updated observational  
37 datasets in ice-sheet models. Finally, by identifying key deficiencies in the observations and  
38 models that hamper current understanding and limit reliability of future ice-sheet projections,  
39 we make recommendations to the research community for reducing these knowledge gaps.  
40 Our synthesis aims to provide a critical and timely review of the current state of the science  
41 in advance of the next Intergovernmental Panel on Climate Change Assessment Report that is  
42 due in 2021.

## 51 1.0 Introduction

52

53 Major uncertainties in predicting and projecting future sea-level rise are due to the  
54 contribution of the two major ice sheets on Earth, Greenland and Antarctica (Pattyn et al.,  
55 2018). These uncertainties essentially stem from the fact that both ice sheets may reach a  
56 tipping point, in this context defined as (regionally) irreversible mass loss, with a warming  
57 climate and that the timing of the onset of such a tipping point is difficult to assess. This is  
58 particularly true for the Antarctic Ice Sheets (AIS), where two instability mechanisms  
59 potentially operate, allowing a large divergence in timing of onset and mass loss in model  
60 projections, while the Greenland Ice Sheet (GrIS) is also particularly susceptible to increased  
61 mass loss from surface melting and associated feedbacks under anthropogenic warming.

62 The Expert Group on Ice Sheet Mass Balance and Sea Level (ISMAS; <http://www.climate-cryosphere.org/activities/groups/ismass>) convened a one-day workshop  
63 as part of POLAR2018 in Davos, Switzerland, on 15 June 2018, to discuss advances in ice-  
64 sheet observations and modelling since the Fifth Assessment Report of the Intergovernmental  
65 Panel on Climate Change (IPCC AR5). The talks and discussions are summarised here in an  
66 update of our previous review (Hanna et al., 2013) where we synthesised material from a  
67 similar workshop held in Portland, Oregon, USA, in July 2012. Here we focus, in the light of  
68 advances in the last six years, on what we need to know in order to make improved model  
69 projections of ice-sheet change. Apart from providing an update of recent observational  
70 estimates of ice-sheet mass changes, we also set this in a wider context of global glacier  
71 change. The paper is arranged as follows. In section (2) we discuss recent advances in ice-  
72 sheet observations, while section (3) focuses on advances in modelling and identifies  
73 remaining challenges – including links with observational needs - that need to be overcome  
74 in order to make better projections. Section (4) discusses recent and projected mass-balance  
75 rates for glaciers and ice caps, comparing these with recent ice-sheet changes, setting the  
76 latter in a broader context of global glacier change. Finally, in section (5) we summarise our  
77 findings and make key recommendations for stimulating further research.

78

## 80 2.0 Observational estimates of ice-sheet total and surface mass balance

81

82 In this section we summarise recent observation-based estimates of the total mass balance of  
83 the Antarctic and Greenland ice sheets, also considering changes in surface mass balance  
84 (SMB; net snow accumulation minus surface meltwater runoff) and – for marine-terminating  
85 glaciers – ice dynamics (solid ice dynamical discharge across the grounding line – the contact  
86 of an ice sheet with the ocean where the ice mass becomes buoyant and floats – and  
87 subsequent calving of icebergs) where appropriate (**Figure 1**). **Figure 2** shows mean SMB  
88 for the ice sheets for recent periods, while mean surface ice flow velocity maps can be found  
89 in Rignot et al. (2019) and Mouginot et al. (2019) (Fig. 1A in both papers). Satellite, airborne  
90 and in situ observational techniques and modelling studies have provided a detailed  
91 representation of recent ice-sheet mass loss and increases in ice melt and discharge (Moon et  
92 al., 2012; Enderlin et al., 2014, Bigg et al., 2014; Shepherd et al., 2012, 2018; Trusel et al.  
93 2018; Rignot et al., 2019; Mouginot et al., 2019).

94 There are three main methods of estimating ice-sheet mass changes. Firstly, radar and  
95 laser altimetry (mainly using CryoSat, Envisat, ERA and ICESat satellites), which measure  
96 changes in height of the surface over repeat surveys that are interpolated over the surface area  
97 of interest to estimate a volume change which is converted into a mass change. This latter is  
98 typically done using knowledge or assumptions of the radar return depth and/or near-surface  
99 density. Alternatively Zwally et al. (2015) use knowledge of the accumulation-driven mass  
100 anomaly during the period of observation, together with the associated accumulation-driven

101 elevation anomaly corrected for the accumulation-driven firn compaction, to derive the total  
102 mass change and its accumulation- and dynamic-driven components Secondly, satellite  
103 gravimetry effectively weighs the ice sheets through their gravitational pull on a pair of  
104 orbiting satellites called GRACE (or, since May 2018, the subsequent GRACE Follow On  
105 mission). Thirdly, the mass budget or component method compares SMB model output with  
106 multi-sensor satellite radar observations of ice velocity across a position on or close to the  
107 grounding line, from which ice discharge can be inferred if the thickness and vertical velocity  
108 profile of ice at that point are also assumed/known. All three methods have their strengths and  
109 weaknesses (e.g. Hanna et al., 2013; Bamber et al., 2018). Altimetry and, especially,  
110 gravimetry, require accurate quantification of Glacial Isostatic Adjustment (GIA; Section 2.3)  
111 which contaminates the ice-sheet mass loss signals. Gravimetry is limited by a relatively  
112 short time series (since 2002) and low spatial resolution (~300 km) compared with the other  
113 methods but is the method that most directly measures mass change.

114 Altimetry surveys, which date relatively far back to the early 1990s, provide elevation  
115 changes that need to be converted into volume and then mass changes, requiring knowledge  
116 of near-surface density which is often highly variable and uncertain for ice sheets. In  
117 addition, radar altimeter surveys do not adequately sample relatively steeper-sloping ice-sheet  
118 margins and require correction for the highly-variable radar-reflection depth that has strong  
119 seasonal variations and interannual trends and complex interactions between linearly-  
120 polarized radar signals and the direction of the surface slope. Successful corrections have  
121 been developed and applied to radar altimeter data from ERS1 and ERS2 using crossover  
122 analysis data (Wingham et al., 1998; Davis and Ferguson, 2004; Zwally et al., 2005; Yi et al.,  
123 2011; Khvorostovsky, 2012) and to Envisat data using repeat track analysis and an advanced  
124 correction algorithm (Filament and Remy, 2012). However, the corrections applied by others  
125 to Envisat and CryoSat data have been questioned due to complex interaction of the cross-  
126 track linearly-polarized radar signal of Envisat and CryoSat with the surface slope that affects  
127 the highly-variable penetration/reflection depth (Zwally et al., 2016; Nilsson et al., 2016).  
128 Also, allowance must be made for firn-compaction changes arising from temperature and/or  
129 accumulation variations, especially in the context of a warming ice-sheet, which significantly  
130 affect surface elevation without mass change (e.g. Li and Zwally, 2015; Zwally et al., 2015).  
131 A number of the altimetry studies included here have used a regionally-varying, temporally  
132 constant effective density value to convert observed volume changes to mass change  
133 estimates. In many cases, a low effective density is assigned for inland areas, and a high  
134 effective density in coastal errors. Because in Greenland and much of Antarctica, coastal  
135 areas are thinning while inland areas are in neutral balance or thickening, this can produce  
136 negative biases in estimated ice-sheet mass-change rates if the changes in the interior are  
137 associated with long-term imbalance between ice flow and snow accumulation.

138 The mass-budget method involves subtracting two large quantities (SMB and  
139 discharge) and needs detailed and complete regional information on these components, which  
140 is recently available from satellite radar data for discharge. SMB cannot be directly measured  
141 at the ice-sheet scale but is instead estimated using regional climate models that are evaluated  
142 and calibrated using in-situ climate and SMB observations. These RCM/SMB models can  
143 have significant uncertainties in derived accumulation and runoff (of the order of 15%, e.g.  
144 Fettweis, 2018). Deriving discharge requires knowledge of bathymetry and the assumption of  
145 an internal velocity profile in order to determine ice flux across the grounding line, and there  
146 are also errors in determining the position of the grounding line. Further uncertainty arises in  
147 estimating the discharge from the areas where the ice velocity is not measured. Despite these  
148 significant uncertainties, an advantage of this method is that the mass change can be  
149 partitioned into its (sub-)components.

150

151 A more recent group use combinations of measurement strategies to minimize the  
152 disadvantages of each, such as by combining altimetric with gravimetric data (Sasgen et al,  
153 2019) or mass-budget data with gravimetric data (e.g. Talpe et al, 2017) to simultaneously  
154 estimate GIA rates and ice-sheet mass-balance rates. These studies typically report errors  
155 comparable to those reported by single-technique studies, but their results may be seen as  
156 more credible because they provide self-consistent solutions for the most important error  
157 sources affecting other studies.

158 A major international research programme called the Ice-sheet Mass Balance Inter-  
159 comparison Exercise (IMBIE; <http://imbie.org/>) has attempted to reconcile differences  
160 between these various methods, and its second phase IMBIE2 has recently reported an  
161 updated set of reconciled total mass balance estimates for Antarctica (Shepherd et al., 2018)  
162 and is shortly expected to update previous results for Greenland. However, despite recent  
163 improvements in coverage and accuracy, modern satellite-based records are too short for  
164 attribution studies aiming to separate the contributions from anthropogenic greenhouse gas  
165 warming signal and background climate variability to the contemporary mass loss (Wouters  
166 et al., 2013), and proxy data such as ice cores are therefore used to overcome this limitation.

167 We have compiled recent estimates of mass balance using available (at the time of  
168 writing) published references from 2014 to 2019 (**Figure 3**), in an update of Figure 1 in  
169 Hanna et al. (2013). Our new box plots clearly show continuing significant mass losses from  
170 both ice sheets, with approximately double the recent rate of mass loss for Greenland  
171 compared with Antarctica. However, the boxes tend to suppress the considerable interannual  
172 variability of mass fluctuations, e.g. the record loss of mass from the GrIS in 2012, and this  
173 shorter-term variability is strikingly shown by annually-resolved time series based on the  
174 mass-budget method [Figure 3 of Rignot et al. (2019) for Antarctica and Figure 3 of  
175 Mougnot et al. (2019) for GrIS].

176

## 177 *2.1 Antarctic ice sheets*

178

179 Recent work agrees on significant and steadily growing mass losses from the West Antarctic  
180 Ice Sheet (WAIS) and the Antarctic Peninsula but highlights considerable residual  
181 uncertainty regarding the recent contribution of the East Antarctic Ice Sheet (EAIS) to global  
182 sea-level rise (SLR) (Shepherd et al., 2018; Rignot et al., 2019). For Antarctica there is  
183 relatively little surface melt and subsequent runoff, and surface accumulation has been  
184 relatively stable, although recent reports show an increase in AIS snowfall (Medley and  
185 Thomas, 2019). In Antarctica, the main sustained mass losses are through ice dynamics,  
186 expressed as increased ice discharge across the grounding line. Mass loss through this  
187 mechanism occurs primarily through increased flow speeds of marine terminating glaciers in  
188 the Amundsen and Bellingshausen Sea sectors, which are sensitive to ocean warming,  
189 although superimposed on these relatively gradual changes there are significant short-term,  
190 i.e. interannual to decadal, SMB variations (Rignot et al., 2019). As a key output of the  
191 IMBIE2 project, Shepherd et al. (2018) built on Shepherd et al. (2012) by significantly  
192 extending the study period and reconciling the results of 24 independent estimates of  
193 Antarctic ice-sheet mass balance using satellite altimetry, gravimetry and the mass budget  
194 methods encompassing thirteen satellite missions and approximately double the number of  
195 studies previously considered. They found that between 1992-2017 the Antarctic ice sheets  
196 lost  $2725 \pm 1400$  Gt of ice, therefore contributing  $7.6 \pm 3.9$  mm to SLR, principally due to  
197 increased mass loss from the WAIS and the Antarctic Peninsula. However, they also found  
198 that EAIS was close to balance, i.e.  $5 \pm 46$  Gt yr<sup>-1</sup> averaged over the 25 years, although this  
199 was the least certain region, attributed to its enormous area and relatively poorly constrained  
200 GIA (Section 2.3) compared with other regions. Shepherd et al. (2018) found that WAIS

201 mass loss steadily increased from  $53\pm 29$  Gt yr<sup>-1</sup> for 1992-1996 to  $159\pm 26$  Gt yr<sup>-1</sup> during  
202 2013-2017, and that Antarctic Peninsula mass losses increased by 15 Gt yr<sup>-1</sup> since 2000,  
203 while the EAIS had little overall trend in mass balance during the period of study. The overall  
204 reconciled sea-level contribution from Antarctica rose correspondingly from 0.2 to 0.6 mm  
205 yr<sup>-1</sup>. These authors also reported no systematic Antarctic SMB trend, and they therefore  
206 attributed WAIS mass loss to increased ice discharge. Of particular concern is the case of  
207 ongoing grounding line retreat in the Amundsen Sea in West Antarctica, as well as basal melt  
208 of ice shelves through polynya-related feedbacks, e.g. in the Ross Sea (Stewart et al., 2019).

209 Rignot et al. (2019) used the mass budget method to compare Antarctic snow  
210 accumulation with ice discharge for 1979-2017, using improved, high-resolution datasets of  
211 ice-sheet velocity and thickness, topography and drainage basins and modelled SMB. Within  
212 uncertainties their total mass balance estimates for WAIS and the Antarctic Peninsula agreed  
213 with those of Shepherd et al. (2018) but they derived a  $-57\pm 2$  Gt yr<sup>-1</sup> mass balance for East  
214 Antarctica for 1992-2017, compared with the  $+5\pm 46$  Gt yr<sup>-1</sup> for the same period derived in  
215 IMBIE2. Possible reasons for this difference include uncertainties in ice thickness and  
216 modelled SMB in the mass budget method, together with further uncertainties in the IMBIE-  
217 2 EAIS mass estimates arising from volume to mass conversions within the altimetry data  
218 processing and significantly uncertain GIA corrections when processing GRACE data.  
219 Zwally et al. (2015) found significant EAIS mass gains of  $136 \pm 50$  Gt yr<sup>-1</sup> for 1992-2001  
220 from ERS radar altimetry and  $136 \pm 28$  Gt yr<sup>-1</sup> for 2003-2008 based on ERS radar altimetry  
221 and ICESat laser altimetry, dynamic thickening of  $147 \pm 55$  Gt yr<sup>-1</sup> and  $147 \pm 34$  Gt yr<sup>-1</sup>  
222 respectively, and accumulation-driven losses of  $11 \pm 6$  Gt yr<sup>-1</sup> in both periods with respect to  
223 a 27-year mean. They attributed the dynamic thickening to a long-term dynamic response  
224 arising from a 67-266% increase in snow accumulation during the Holocene, as derived from  
225 six ice cores (Siegert, 2003), rather than contemporaneous increases in accumulation.  
226 However, because the results of Zwally et al. (2015) differ from most others, they have been  
227 questioned by other workers (Scambos and Shuman, 2016; Martín-Español et al., 2017),  
228 although see Zwally et al. (2016) for a response. Bamber et al. (2018) describe “reasonable  
229 consistency between [EAIS mass balance] estimates” if they discount the outlier of Zwally et  
230 al. (2015). Notwithstanding, as highlighted by Hanna et al. (2013) and Shepherd et al. (2018)  
231 and clearly shown here in **Figure 3** which clearly shows ‘outliers’ on both sides of the  
232 IMBIE-reconciled means, disparate estimates of the mass balance of East Antarctica, which  
233 vary by  $\sim 100$  Gt yr<sup>-1</sup>, have not yet been properly resolved. Furthermore, the range of  
234 differences does not appear to be narrowing with time, which indicates a lack of advancement  
235 in one or more of the mass-balance determination methods.

## 236 237 *2.2 Greenland Ice Sheet*

238  
239 According to several recent estimates, the GrIS lost  $257\pm 15$  Gt yr<sup>-1</sup> of mass during 2003-  
240 2015 (Box et al., 2018),  $262\pm 21$  Gt yr<sup>-1</sup> during 2007-2011 (Andersen et al., 2015),  $269\pm 51$   
241 Gt yr<sup>-1</sup> during 2011-2014 (McMillan et al., 2016),  $247$  Gt yr<sup>-1</sup> of mass – representing 37% of  
242 the overall land ice contribution to global sea-level rise – during 2012-2016 (Bamber et al.  
243 2018), and  $286\pm 20$  Gt yr<sup>-1</sup> during 2010-2018 (Mouginot et al., 2019). A slightly greater mass  
244 loss of  $308\pm 12$  Gt yr<sup>-1</sup> based on GRACE gravimetric satellite data for 2007-2016 was given  
245 by Zhang et al. (2019). Some of the difference between these numbers can be attributed to  
246 different methods considering either just the contiguous ice sheet or also including  
247 disconnected peripheral glaciers and ice caps, the latter being the case for GRACE-based  
248 estimates. However, GrIS mass loss approximately quadrupled during 2002/3 to 2012/13  
249 (Bevis et al., 2019). The GrIS sea-level contribution over 1992-2017 was approximately one

250 and a half times the sea-level contribution of Antarctica (Box et al., 2018). However this kind  
251 of average value masks very significant interannual variability of  $\pm 228 \text{ Gt yr}^{-1}$ , and even 5-  
252 year mean values can vary by  $\pm 102 \text{ Gt yr}^{-1}$ , based on 2003-2016 data; for example recent  
253 annual mass losses ranged from  $>400 \text{ Gt}$  in 2012 (a record melt year caused by jet-stream  
254 changes, e.g. Hanna et al., 2014) to  $<100 \text{ Gt}$  just one year later (Bamber et al., 2018).

255 McMillan et al. (2016) found that high interannual (1991-2014) mass balance  
256 variability was mainly due to changes in runoff of  $102 \text{ Gt yr}^{-1}$  (standard deviation,  $\sim 28\%$  of  
257 the mean annual runoff value) with lesser contributions from year-to-year snowfall variations  
258 of  $\sim 61 \text{ Gt yr}^{-1}$  ( $\sim 9\%$  of the mean snowfall value) and solid ice discharge of  $\sim 20 \text{ Gt yr}^{-1}$  ( $\sim 5\%$   
259 of the mean annual discharge). Their interpretation of transient mass changes was supported  
260 by Zhang et al. (2019) who attributed big short-term ( $\sim 3$ -year) fluctuations in surface mass  
261 balance to changes in atmospheric circulation, specifically the Greenland Blocking Index  
262 (GBI; Hanna et al. 2016), with opposite GBI phases in 2010-2012 (highly positive GBI) and  
263 2013-2015 (less blocked Greenland). Also, in the MODIS satellite record since the year 2000,  
264 Greenland albedo was relatively high from 2013-2018 after reaching a record low in 2012  
265 (Tedesco et al., 2018). The relatively low GrIS mass loss in 2013-14 was termed the “pause”  
266 (Bevis et al., 2019). However, Zhang et al. (2019) inferred an acceleration of  $18 \pm 9 \text{ Gt yr}^{-2}$  in  
267 GrIS mass loss over 2007-2016. Given this pronounced recent short-term variability, for  
268 example the recent slowdown of rapid mass loss increases in the 2000s and very early 2010s,  
269 such trends should only be extrapolated forward with great caution.

270 Greenland mass loss is mainly driven by atmospheric warming, and – based on ice-  
271 core-derived melt information and regional model simulations – surface meltwater runoff  
272 increased by  $\sim 50\%$  since the 1990s, becoming significantly higher than pre-industrial levels  
273 and being unprecedented in the last 7000 years (Trusel et al., 2018). Enderlin et al. (2014)  
274 found an increasingly important role of runoff on total mass annual losses during their 2000-  
275 2012 study period and concluded that SMB changes were the main driver of long-term  
276 (decadal or longer) mass loss.

277 However, just five marginal glacier near-termini regions, covering  $<1\%$  of the GrIS  
278 by area were responsible for 12% of the net ice loss (McMillan et al., 2016), highlighting the  
279 potentially important role and sensitivity of ice dynamics; these authors alongside Tedesco et  
280 al. (2016) also found an atmospheric warming signal on mass balance in the northernmost  
281 reaches of the ice sheet. Taking a longer perspective from 1972-2018, using extended  
282 datasets of outlet glacier velocity and ice thickness, improved bathymetric and gravity  
283 surveys and newly-available high resolution SMB model output, Mouginit et al. (2019)  
284 reported that dynamical losses from the GrIS have continuously increased since 1972,  
285 dominating mass changes except for the last 20 years, estimating that over this longer period  
286  $66 \pm 8\%$  of the overall mass losses were from dynamics and  $34 \pm 8\%$  from SMB. They  
287 concluded that dynamics are likely to continue to be important in future decades, apart from  
288 the southwest where runoff/SMB changes predominate, and that the northern parts of GrIS –  
289 where outlet glaciers could lose their buttressing ice shelves – are likely to be especially  
290 sensitive to future climate warming.

### 291 292 *2.3 Glacial Isostatic Adjustment*

293  
294 Processes associated with GIA must be accounted for when quantifying contemporary ice-  
295 sheet change (Shepherd et al., 2018) and also when predicting the dynamics of future change  
296 (Adhikari et al., 2014; Gomez et al., 2015; Konrad et al., 2015). Specifically, ongoing  
297 changes to the height of the land surface and the shape of Earth’s gravitational field, in  
298 response to past ice-mass change, will bias gravimetry- and altimeter-based measurements of  
299 contemporary ice mass balance and alter the boundary conditions for ice sheet dynamics. Due

300 to density differences between the ice sheet and the solid Earth, the impact of GIA on  
301 gravimetry measurements will be 4-5 times greater than the impact on altimetry  
302 measurements (Wahr et al., 2000).

303 Numerical models can be used to estimate the geodetic signal associated with GIA  
304 (Whitehouse et al., 2012; Ivins et al., 2013; Argus et al., 2014) or it can be inferred via data  
305 inversion (Gunter et al., 2014; Martín-Español et al., 2016; Sasgen et al., 2017). Both  
306 approaches would benefit from better spatial coverage of GPS observations of land  
307 deformation, while the first approach strongly depends on past ice sheet change, for which  
308 constraints are severely lacking, particularly across the interior of the Greenland and  
309 Antarctic ice sheets. Both approaches also typically rely on the assumption that mantle  
310 viscosity beneath the major ice sheets is spatially uniform and high enough that the signal due  
311 to past ice-mass change is constant in time. However, recent work has revealed regions in  
312 both Greenland and Antarctica where mantle viscosity is much lower than the global average  
313 (e.g. Nield et al., 2014; Khan et al., 2016; Barletta et al., 2018; Mordret, 2018). This has two  
314 important implications. First, in regions where upper mantle viscosity is less than  $\sim 10^{19}$  Pa s  
315 the response to recent (decadal to centennial) ice-mass change will dominate the GIA signal,  
316 and may not be steady in time. In such regions a time-varying GIA correction, which  
317 accounts for both the viscous and elastic response to contemporary ice-mass change, should  
318 be applied to gravimetry, altimetry and other geodetic observations. Secondly, since GIA acts  
319 to reduce the water depth adjacent to a shrinking marine-based ice sheet, this can act to slow  
320 (Gomez et al., 2010) or reverse (Kingslake et al., 2018) the rate of ice loss, with the  
321 stabilising effect being stronger in regions with low upper mantle viscosity (Gomez et al.,  
322 2015; Konrad et al., 2015). To better understand the behaviour and likely future of marine-  
323 based ice masses it will be necessary to quantify the spatially-varying strength of this  
324 stabilising effect and account for feedbacks between GIA and ice dynamics within a coupled  
325 modelling framework (e.g. Pollard et al., 2017; Gomez et al., 2018; Larour et al., 2019;  
326 Whitehouse et al., 2019).

327

### 328 **3.0 Recent advances and challenges in modelling including links with observational** 329 **needs**

330

#### 331 *3.1 Modelling ice-sheet instabilities*

332

333 The marine ice-sheet instability (MISI; **Figure 4**) hypothesises a possible collapse of West  
334 Antarctica as a consequence of global warming. This process, first proposed in the 1970s  
335 (Weertman, 1974; Thomas and Bentley, 1978), was recently theoretically confirmed and  
336 demonstrated in numerical models (Schoof, 2007; Pattyn et al., 2012). It arises from thinning  
337 and eventually flotation of the ice near the grounding line, which moves the latter into deeper  
338 water where the ice is thicker. Thicker ice results in increased ice flux, which further thins  
339 (and eventually floats) the ice, resulting in further retreat into deeper water (and thicker ice)  
340 and so on. This instability is activated when the bedrock deepens toward the interior of the  
341 ice sheet, i.e., a retrograde bed slope, as is the case for most of the West Antarctic ice sheet.  
342 The possibility that some glaciers, such as Pine Island Glacier and Thwaites Glacier, are  
343 already undergoing MISI has been suggested (Rignot et al., 2014; Christianson et al., 2016).  
344 Thwaites Glacier is currently in a less-buttressed state, and several simulations using state-of-  
345 the-art ice-sheet models indicate continued mass loss and possibly MISI or MISI-like  
346 behaviour even under present climatic conditions (Joughin et al., 2014; Nias et al., 2016;  
347 Seroussi et al., 2017). However, rapid grounding line retreat due to MISI or MISI-like  
348 behaviour remains highly dependent on the subtleties of subglacial topography (Waibel et al.,

349 2018) and feedbacks associated with GIA (section 2.3), limiting the predictive behaviour of  
350 the onset of MISI. In other words, geography matters.

351 The marine ice cliff instability (MICI) hypothesises (**Figure 4**) collapse of ice cliffs  
352 that become unstable and fail if higher than  $\sim 90$  m above sea level, leading to the rapid  
353 retreat of ice sheets during past warm (e.g., Pliocene and last interglacial) periods (Pollard et  
354 al., 2015; DeConto and Pollard, 2016). MICI is a process that facilitates and enhances MISI  
355 once the ice shelf has completely disappeared but can also act alone, for instance where the  
356 bed is not retrograde (which prevents MISI). MICI relies on the assumption of perfect plastic  
357 rheology to represent failure. Cliff instability requires an a priori collapse of ice shelves and  
358 is facilitated by hydro-fracturing through the increase of water pressure in surface crevasses  
359 which deepens the latter (Bassis and Walker, 2012; Nick et al., 2013; Pollard et al., 2015).  
360 Whether MICI is necessary to explain Pliocene sea-level high stands has been questioned  
361 recently (Edwards et al., 2019).

362 The introduction of MICI in one ice-sheet model (DeConto and Pollard, 2016) has  
363 profoundly shaken the modelling community, as the mechanism potentially results in future  
364 sea-level rise estimates of almost an order of magnitude larger compared with other studies  
365 (Figure 5 and Table 1). While projected contributions of the Antarctic ice sheet to sea-level  
366 rise by the end of this century for recent studies hover between 0 and 0.45 m (5%-95%  
367 probability range), the MICI model occupies a range of 0.2-1.7 m (Figure 5a). The  
368 discrepancy is even more pronounced for 2300, where the MICI results and other model  
369 estimates no longer agree within uncertainties. Edwards et al. (2019) discuss in detail the  
370 results of DeConto and Pollard (2016), related to cliff collapse but also the sensitivity of the  
371 driving climate model that overestimates surface melt compared to other CMIP5 models.  
372 MICI is a plausible mechanism and is observed on tidewater and outlet glaciers in Greenland  
373 and the Arctic. However, whether and how it applies to very large outlet glaciers of the  
374 Antarctic ice sheet will require further scrutiny. Evidence from paleo-shelf breakup in the  
375 Ross Sea shows that ice-sheet response may be more complicated, including significant lags  
376 in the response of grounding line retreat (Bart et al., 2018). In order to accurately model ice-  
377 sheet instabilities, motion of the grounding line must be accurately represented. International  
378 model inter-comparisons of marine ice-sheet models (MISMIP; MISMIP3d) greatly  
379 improved those models in terms of representing grounding-line migration numerically by  
380 conforming them to known analytical solutions (Pattyn et al., 2012, 2013). These numerical  
381 experiments demonstrated that in order to resolve grounding-line migration in marine ice-  
382 sheet models, a sufficiently high spatial resolution needs to be applied, since membrane  
383 stresses need to be resolved across the grounding line to guarantee mechanical coupling. The  
384 inherent change in basal friction occurring across the grounding line – zero friction below the  
385 ice shelf – requires high spatial resolution (e.g.,  $< 1$  km for Pine Island Glacier; Gladstone et  
386 al., 2012) for an accurate representation of grounding-line migration. Therefore, a series of  
387 ice-sheet models have implemented a spatial grid refinement, mainly for the purpose of  
388 accurate data assimilation (Cornford et al., 2015; Gillet-Chaulet et al., 2012; Morlighem et  
389 al., 2010), but also for further transient simulations where the adaptive mesh approach  
390 enables the finest grid to follow the grounding-line migration (Cornford et al., 2013, 2016).  
391 These higher spatial resolutions of the order of hundreds of meters in the vicinity of  
392 grounding lines also pose new challenges concerning data management for modelling  
393 purposes (Durand et al., 2011).

394

### 395 *3.2 Model initialisation, uncertainty and inter-comparison*

396

397 Despite major improvements in ice-sheet model sophistication, major uncertainties still  
398 remain pertaining to model initialisation as well as the representation of critical processes



399 such as basal sliding and friction, ice rheology, ice damage (such as calving and MICI) and  
400 sub-shelf melting. New developments in data assimilation methods led to improved  
401 initialisations in which the initial ice-sheet geometry and velocity field are kept as close as  
402 possible to observations by optimising other unknown fields, such as basal friction coefficient  
403 and ice stiffness (accounting for crevasse weakening and ice anisotropy; Arthern and  
404 Hindmarsh, 2006; Arthern and Gudmundsson, 2010; Cornford et al., 2015; MacAyeal, 1992;  
405 Morlighem et al., 2010, 2013). Motivated by the increasing ice-sheet imbalance of the  
406 Amundsen Sea Embayment glaciers over the last 20 years (Shepherd et al., 2018), and  
407 supported by the recent boom in satellite data availability, data-assimilation methods are  
408 progressively used to evaluate unknown time-dependent fields such as basal drag by using  
409 time-evolving states accounting for the transient nature of observations and model dynamics  
410 (Gillet-Chaulet et al., 2016; Goldberg et al., 2013, 2015, 2016).

411 Ensemble model runs equally improve the predictive power of models by translating  
412 uncertainty in a probabilistic framework. The use of statistical emulators thereby increases  
413 the confidence in sampling parameter space (Bulthuis et al., 2019) and helps to reduce  
414 uncertainties in ice dynamical contributions to future sea-level rise (Ritz et al., 2015;  
415 Edwards et al., 2019). Probability distributions for Antarctica are usually not Gaussian and  
416 have a long tail towards high values, especially for high greenhouse warming scenarios  
417 (**Figure 5** and **Table 1**).

418 An important step forward since the Fifth Assessment Report of the IPCC (IPCC,  
419 2013) is that process-based projections of sea-level contributions from both ice sheets are  
420 now organised under the Ice Sheet Model Intercomparison Project for CMIP6 (ISMIP6) and  
421 form an integral part of the CMIP process (Eyring et al., 2016; Nowicki et al., 2016; Goelzer  
422 et al., 2018a; Seroussi et al., 2019). ISMIP6 is working towards providing projections of  
423 future ice-sheet mass changes for the next Assessment Report of the IPCC (AR6). It has  
424 recently finished its first set of experiments focussing on the initial state of the ice sheets as a  
425 starting point for future projections (Goelzer et al., 2018a; Seroussi et al., 2019), which has  
426 seen an unprecedented return from ice-sheet modelling groups globally. With ISMIP6, the  
427 ice-sheet modelling community has engaged to evolve to new standards in availability,  
428 accessibility and transparency of ice-sheet model output data (e.g. Goelzer et al., 2018b),  
429 facilitating model-model and data-model comparison and analysis.

430 ISMIP6 has strengthened the links between the ice-sheet modelling community and  
431 other communities of global and regional climate modellers, ocean modellers and remote  
432 sensing and observations of ice, ocean and atmosphere.

433

### 434 *3.3 Ice sheet model-climate model coupling*

435

436 Fully coupled simulations based on state of the art AOGCMs and ISMs are an emerging field  
437 of active research (e.g. Fyke et al., 2014a; Fischer et al., 2014; Vizcaino et al., 2015; Reerink  
438 et al., 2016; Fyke et al., 2018). This development will help to improve our understanding of  
439 processes and feedbacks due to climate-ice sheet coupling in consistent modelling  
440 frameworks. However, coupling is challenging due to differences in resolution between  
441 climate and ice-sheet models, the computational expense of global climate models, and the  
442 need for advanced snow/firn schemes, etc. (a review of these challenges and recent advances  
443 is given by Vizcaino, 2014). ISMIP6 is also leading and supporting current coupled  
444 modelling efforts (Nowicki et al., 2016).

445 Coupling approaches between atmosphere/ice/ocean/sea ice for the Antarctic ice sheet  
446 have been considerably developed since the AR5 (Asay-Davis et al., 2017; Pattyn et al.,  
447 2017; Favier et al., 2017; Donat-Magnin et al., 2017) but there is still an important need to  
448 document the processes occurring at the interface between ocean and ice. Due to the

449 computational cost, these are limited to a single basin (Seroussi et al., 2017) or intermediate  
450 coupling for the whole ice sheet (Golledge et al., 2019). Observations are currently being  
451 developed to study the ocean characteristics below the ice shelves using autonomous  
452 underwater vehicle (AUVs) or remotely operated vehicle (ROVs) (Jenkins et al., 2010;  
453 Kimura et al., 2016; Nicholls et al., 2006) and should offer critical information for modellers.

454 For the Greenland ice sheet, coupled models have been applied to investigate several  
455 outstanding questions regarding ice-climate interaction, particularly on multi-century and  
456 multi-millennia timescales. Some examples of the topics already addressed include the  
457 impacts of meltwater on ocean circulation (Golledge et al., 2019), regional impact of ice-  
458 sheet area change (Vizcaino et al., 2008, 2010), effect of albedo and cloud change on future  
459 SMB (Vizcaino et al., 2014), and elevation-SMB feedback (Vizcaino et al., 2015). Ongoing  
460 work aims to include more interaction processes, such as the effects of ocean warming on ice-  
461 sheet stability (Straneo et al., 2013).

462 Due to their high computational cost, simulation ensembles (for ice-sheet parameters  
463 as well as climate forcing) are rare in coupled modelling. These ensembles are essential tools  
464 for the attribution of on-going mass loss and to constrain uncertainty in century projections.  
465 Vizcaino et al. (2015) compared 1850-2300 Greenland ice-sheet evolution with a coupled  
466 model forced with three different Representative Concentration Pathways (RCP2.6, RCP4.5  
467 and RCP8.5). For the historical and RCP8.5 scenarios, they performed a small ensemble (size  
468 three). They found a relatively high uncertainty from climate variability in the simulation of  
469 contemporary mass loss. However, this uncertainty was relatively small for the projections as  
470 compared with the uncertainty from greenhouse gas scenario.

471

### 472 *3.4 Earth system/regional climate modelling and surface mass balance modelling: advances* 473 *and challenges*

474

#### 475 3.4.1 General

476

477 The accuracy of SMB model output naturally depends on observations that are available to  
478 evaluate the models. Recent efforts to collect, synthesise and quality-control in-situ  
479 observations of SMB over the AIS and GrIS have greatly improved our confidence in these  
480 measurements (Favier et al., 2013; Machguth et al., 2016; Montgomery et al., 2018), yet the  
481 observational density remains too low to estimate ice-sheet wide SMB based on interpolation  
482 of these data alone. Uncertainties remain especially large along the ice-sheet margins, where  
483 SMB gradients are steepest and data density lowest because of adverse climate conditions  
484 (Arthern et al., 2006; Bales et al., 2009). Moreover, most in-situ observations constitute an  
485 integrated measurement, providing little insight in SMB component partitioning and seasonal  
486 evolution. Suitable co-located meteorological observations enable time-dependent estimates  
487 of SMB and surface energy balance components such as snow accumulation, sublimation and  
488 melt (van den Broeke et al., 2004, 2011), but especially on the AIS surprisingly few  
489 (automatic) weather stations collect sufficient data to do so. In the GrIS ablation zone, the  
490 PROMICE automatic weather station (AWS) network has recently resolved this problem  
491 (Citterio et al., 2015).

492 Although their performance in simulating ice-sheet SMB is continually improving  
493 (Cullather et al., 2014; Vizcaino et al., 2014; Lenaerts et al., 2016; van Kampenhout et al.,  
494 2017), Earth System Models (ESMs) currently have insufficient (50-100 km) horizontal  
495 resolution in the atmosphere to properly resolve marginal SMB gradients, although  
496 downscaling via elevation classes (Lipscomb et al., 2013; Alexander et al., 2019; Sellevold et  
497 al., submitted), and upcoming variable-resolution ESMs may alleviate this. Moreover, as they  
498 do not assimilate observations, ESMs do not simulate realistic weather. Atmospheric

499 reanalyses have similar low resolution, although this is improved in the recently released  
500 ERA5 reanalysis, but do assimilate meteorological observations, and hence can be used to  
501 force regional climate models (RCMs) at their boundaries. As a result, RCMs provide  
502 reasonably realistic ice-sheet weather at acceptable resolutions: typically 25 km for the full  
503 AIS (van Wessem et al., 2018; Agosta et al., 2019) and 5 km for AIS sub-regions (van  
504 Wessem et al., 2015; Lenaerts et al., 2012; Lenaerts et al., 2018; Datta et al., 2019) and the  
505 GrIS (Lucas-Picher et al., 2012; Fettweis et al., 2017; van den Broeke et al., 2016). Further  
506 statistical downscaling to 1 km resolution is required to resolve SMB over narrow GrIS outlet  
507 glaciers (Noël et al., 2018a). The resulting gridded SMB products cover multiple decades  
508 (1979/1958-present for AIS/GrIS, respectively) at (sub-)daily timescales, allowing synoptic  
509 case studies at the SMB component level but also multidecadal trend analysis. RCM products  
510 also helped to extend ice-sheet SMB time series further back in time by guiding the  
511 interpolation between firn cores (Thomas et al., 2017; Box, 2013).

512 Further improvements are needed: RCMs struggle to realistically simulate (mixed-  
513 phase) clouds (van Tricht et al., 2016) and (sub-) surface processes, such as drifting snow  
514 (Lenaerts et al., 2017), bio-albedo (Stibal et al., 2017) and heterogeneous meltwater  
515 percolation (Steger et al., 2017). A powerful emerging observational technique for dry snow  
516 zones is airborne accumulation radar (Koenig et al., 2016; Lewis et al., 2017), which together  
517 with improved re-analyses products such as MERRA (Cullather et al., 2016) will further  
518 improve our knowledge of contemporary ice-sheet SMB.

519

### 520 3.4.2 Greenland

521

522 Despite considerable advances with RCMs and SMB models, there are significant remaining  
523 biases in absolute values between GrIS SMB simulations for the last few decades. However,  
524 these are expected to be at least partly reconciled through a new SMB Model Intercomparison  
525 Project (SMB\_MIP; Fettweis, 2018) which is standardising model comparisons and  
526 evaluation using in-situ and satellite data (e.g. Machguth et al., 2016). The results of this  
527 exercise should help to improve the models as well as inform on what are the more reliable  
528 model outputs. This exercise may help to resolve significant disagreement between model  
529 reconstructions of GrIS SMB, and especially accumulation, for the last 50-150 years (van den  
530 Broeke et al., 2017).

531 The elevation classes downscaling method has been applied to 1850-2100 GrIS SMB  
532 simulations in several studies with the Community Earth System Model (CESM): these  
533 encompass regional climate and SMB projections (Vizcaino et al., 2014), a freshwater  
534 forcing reconstruction and effect on ocean circulation (Lenaerts et al., 2015), the relationship  
535 between SMB variability and future climate change (Fyke et al., 2014b), and the time of  
536 emergence of an anthropogenic SMB signal from background SMB variability (Fyke et al.,  
537 2014c). The latter study assesses the point in time when the anthropogenic trend in the SMB  
538 becomes larger than the “noise”, and addresses an observational gap given the short records  
539 and/or limited density of remote-sensing/in-situ observations and high GrIS SMB variability  
540 (Wouters et al., 2013). Fyke et al. (2014c) identified a bimodal emergence pattern, with  
541 upward emergence (positive SMB trend) in the interior due to increased accumulation,  
542 downward emergence (negative SMB trend) in the margins due to increased ablation, and an  
543 intermediate area of no emergence due to compensating elevated ablation and accumulation.  
544 This study suggests the Greenland summit as an interesting area to monitor emergence, due  
545 to its high signal-to-noise ratio and resulting early emergence. This high ratio is due to low  
546 SMB variability from drier and colder conditions relative to the margins. These results should  
547 be revisited with further simulations, e.g., from an ensemble and/or multiple models.  
548 Additionally, they should be confronted with available observations of the recent strong SMB

549 decline to identify whether the models adequately represent the causes of this trend (e.g.,  
550 Greenland Blocking, Hanna et al., 2018).

551

### 552 3.4.3 Antarctica

553

554 Shepherd et al. (2018) reveal that present sub-decadal to decadal precipitation and SMB  
555 variations significantly dominate EAIS mass balance variability (Gardner et al., 2018)  
556 justifying the need for further SMB model improvements, validations, and inter-comparisons  
557 (Agosta et al., 2019; Favier et al., 2017). Thanks to observations, the inclusion of several key  
558 processes have been improved in models since AR5, including the roles of the stable  
559 atmospheric boundary layer (Vignon et al., 2017), drifting snow, (Amory et al., 2017; van  
560 Wessem et al., 2018) and supraglacial hydrology (Kingslake et al., 2015, 2017; Hubbard et  
561 al., 2016).

562 A persistent problem is that climate reanalyses used to force regional climate models  
563 still present biases (Bromwich et al., 2011), most noticeably in moisture transport (Dufour et  
564 al., 2019). Constraining atmospheric moisture and cloud microphysics with ground-based  
565 techniques in Antarctica [ceilometer, infrared pyrometer, vertically profiling precipitation  
566 radar (Gorodetskaya et al., 2015), polarimetric weather radar, micro rain radar, weighing  
567 gauges, multi-angle snowflake cameras (Grazioli et al., 2017a), etc.] is necessary to  
568 accurately model cloud evolution and precipitation. Ground-based estimates of cloud  
569 properties and precipitation are only obtained at a few sites, which calls for the use of  
570 distributed remote-sensing techniques to characterise Antarctic precipitation statistics and  
571 rates [e.g., Cloudsat products (Palerm et al., 2014)]. However, processes occurring within 1  
572 km above the surface remain undetected by satellite sensors. In this critical layer for SMB,  
573 sublimation impacts precipitating snowflakes (Grazioli et al., 2017b) and drifting snow  
574 particles (Amory et al., 2017; van Wessem et al., 2018), reducing surface accumulation and  
575 leading to potential feedbacks on atmospheric moisture (Barral et al., 2014). Thus  
576 continental-scale sublimation may be underestimated, suggesting mass balance and SMB  
577 agreement likely relies on some degree of error compensation in models (Agosta et al., 2019).

578 Recent progress has shown that an improved description of the atmospheric structure  
579 is needed during precipitation events; several studies present site-specific results on  
580 precipitation origins [precipitation from synoptic scale systems, hoar frost, diamond dust  
581 (Dittmann et al., 2016; Stenni et al., 2016; Schlosser et al., 2016)] and their impact on the  
582 local SMB. Synoptic-scale precipitation is known to control the inter-annual variability of  
583 accumulation in Dronning Maud Land (Gorodetskaya et al., 2014), Dome C, and Dome F  
584 (Schlosser et al., 2016) through high-intensity precipitation events, but continental-scale  
585 studies for Antarctica are still rare (Turner et al., 2019). High precipitation events are related  
586 to warm and moist air mass intrusions linked to mid-tropospheric planetary waves (Turner et  
587 al. 2016) that are connected with the main modes of atmospheric circulation variability at  
588 southern high-latitudes (Thompson et al., 2011; Turner et al., 2016; Nicolas et al., 2017;  
589 Bromwich et al., 2012). Low-elevation surface melt in West Antarctica (Nicolas et al., 2017;  
590 Scott et al., 2019) and on the Larsen ice shelves (Kuipers Munneke et al., 2018; Bozkurt et  
591 al., 2018) occurs during increased foehn events (Cape et al., 2015) and moisture intrusions  
592 favoured by large synoptic blockings (Scott et al., 2019). These melt-related moisture  
593 intrusions generally occur in the form of atmospheric rivers (Wille et al., 2019). However, the  
594 synoptic causes of these events are still poorly known. Moreover, the feedbacks between  
595 melting and albedo, which may be critical for processes prior to ice shelf collapse (Kingslake  
596 et al., 2017; Bell et al., 2018), are poorly observed in the field. Currently, there is a major gap  
597 between the large scale on which models and remote sensing typically operate (Lenaerts et  
598 al., 2016; Kuipers Munneke et al., 2018) and the local scale, especially regarding snow

599 erosion and redistribution (Amory et al., 2017). These latter processes typically occur at a  
600 decametre scale (Libois et al., 2014; Souverijns et al., 2018), which is not matched by space-  
601 and airborne microwave radar (e.g., between 4 and 6 GHz) or ground penetrating radar  
602 (GPR) (Fujita et al., 2011; Verfaillie et al., 2012; Medley et al., 2013, 2015; Frezzotti et al.,  
603 2007) observations on the kilometre scale that are used to evaluate regional climate models  
604 (Agosta et al., 2019; van Wessem et al., 2018).

605 Despite improvements in regional-scale models, assessing the future SMB of  
606 Antarctica will rely on our capability to produce accurate future projections of the moisture  
607 fluxes towards Antarctica, e.g. linked to changes in sea-ice cover (Bracegirdle et al., 2017;  
608 Krinner et al., 2014; Palerme et al., 2017), and the westerly circulation and atmospheric  
609 blocking patterns around Antarctica (Massom et al., 2004). These aspects are still poorly  
610 represented in CMIP5 simulations (Bracegirdle et al., 2017; Favier et al., 2016). To resolve  
611 this, bias corrections based on nudging approaches or data assimilation schemes have been  
612 proposed, in addition to ensemble approaches (Beaumet et al., 2019; Krinner et al., 2014,  
613 Krinner et al. 2019). To aid these efforts, paleo-climate information on the westerlies  
614 (Saunders et al., 2018), sea ice characteristics (Campagne et al., 2015), temperature (Jones et  
615 al., 2016), and SMB (Thomas et al., 2017) may be useful for constraining the models (Jones  
616 et al., 2016; Abram et al., 2014) and attributing SMB changes to anthropogenic warming.  
617 Emergence of this signal from the natural climate variability of Antarctica is currently  
618 expected between 2020-2050 (Previdi and Polvani, 2016).

619

#### 620 **4.0. Recent and projected mass-balance rates for glaciers and ice caps**

621

622 In this section we target valley glaciers or mountain glaciers and ice caps (<50,000 km<sup>2</sup>). We  
623 here review the advances, since the IPCC AR5, in the estimate of the contribution to SLR of  
624 wastage from these smaller glaciers and ice caps (henceforth, glaciers), as well as its  
625 projections to the end of the 21<sup>st</sup> century. At the time of AR5, the first consensus estimate of  
626 this contribution had just been published (Gardner et al., 2013), and it was estimated to be  
627  $259 \pm 28 \text{ Gt yr}^{-1}$  ( $0.94 \pm 0.08 \text{ mm yr}^{-1}$  SLE) for 2003–2009, including the contribution from the  
628 glaciers in the periphery of Greenland and Antarctica (henceforth, peripheral glaciers). For  
629 the longer period of 1993–2010, AR5 attributed 27% of the SLR to wastage from glaciers  
630 (Church et al., 2013). This was above the combined contribution of the ice sheets of  
631 Antarctica and Greenland (21%), despite the fact that global glacier volume is only ~0.6% of  
632 the combined volume of both ice sheets (Vaughan et al., 2013). Since then, the contribution  
633 to SLR from the ice sheets has accelerated, as discussed in earlier sections, which has  
634 resulted in a current dominance of the ice-sheet contribution despite the contribution from  
635 glaciers having also increased in absolute terms, as will be discussed in this section.

636

##### 637 *4.1 Methods used to estimate the global glacier mass balance*

638

639 For estimating the global mass balance of glaciers, in addition to the techniques already  
640 discussed for ice sheets, such as repeated altimetry (e.g. Moholdt et al., 2010), gravity  
641 observations (e.g. Luthcke et al., 2008), or the mass budget method (e.g. Deschamps-Berger  
642 et al., 2019), other methods are commonly used, which are sometimes variations of those  
643 mentioned above. Purely observation-based techniques include the extrapolation of both in-  
644 situ direct observations by the glaciological method and geodetic mass balance estimates  
645 (Cogley, 2009), as well as reconstructions based on glacier length changes (Leclercq et al.,  
646 2011, 2012, 2014). The glaciological method relies on point measurements of surface mass  
647 balance, which are then integrated to the entire glacier surface (Cogley et al., 2011). Such  
648 measurements are available for a reduced sample of <300 glaciers (Zemp et al., 2015) out of

649 more than 200,000 glaciers inventoried worldwide (Pfeffer et al., 2014), which introduces a  
650 bias when extrapolating to the whole glacierized area of undersampled regions (Gardner et al.,  
651 2013). The geodetic mass balance, in turn, is determined using volume changes from DEM  
652 differencing and then converting to mass changes using an appropriate assumption for the  
653 density (Huss, 2013). The reconstructions based on observed glacier length changes convert  
654 these, upon normalization and averaging to a global mean, to normalized global volume  
655 change. The latter is converted into global glacier mass change using a calibration against  
656 global glacier mass change over a certain period (Leclercq et al., 2011).

657 Finally, the modelling-based approaches for estimating past or current changes are  
658 mostly based on the use of climatic mass balance models forced by either climate  
659 observations or climate model output, calibrated and validated using surface mass-balance  
660 observations. As these techniques are based on a statistical scaling relationship, they are  
661 commonly referred to as statistical modelling, to distinguish them from the use of an RCM to  
662 estimate, directly, the surface mass balance of an ice mass. The latter works well for ice caps,  
663 but not for glaciers, due to their complex topography and corresponding micro-climatological  
664 effects (Bamber et al., 2018). Based on statistical modelling, an analysis of the processes and  
665 feedbacks affecting the global sensitivity of glaciers to climate change can be found in  
666 Marzeion et al. (2014a), while the attribution of the observed mass changes to anthropogenic  
667 and natural causes has been addressed by Marzeion et al. (2014b).

#### 668 669 *4.2 20th century and current estimates*

670  
671 Much of the work done since AR5 has focused on improving the estimates for the reference  
672 period 2003–2009 (or some earlier periods), and on producing new estimates for more recent  
673 (or extended) periods. Both the reanalyses and the new estimates have been based on  
674 improvements in the number of mass balance or glacier length changes observations, and on  
675 the use of an increased set of gridded climate observations, and of more complete and  
676 accurate global glacier inventories and global DEMs. These improvements allowed Marzeion  
677 et al. (2015) to achieve the agreement, within error bounds, of the global reconstructions of  
678 the mass losses from glacier wastage for the periods 1961–2005, 1902–2005 and 2003–2009  
679 produced using the various methods available. In spite of the agreement at the global level,  
680 strong disagreements persisted for particular regions such as Svalbard and the Canadian  
681 Arctic, likely because of the omission of calving in the statistical models. Marzeion et al.  
682 (2017), using a yet more extended set of glaciological and geodetic measurements (Zemp et  
683 al., 2015), gave a global glacier mass-change rate estimate of  $-0.61 \pm 0.07$  mm SLE yr<sup>-1</sup> for  
684 2003–2009 (including Greenland peripheral glaciers, but not those of the Antarctic  
685 periphery), obtained by averaging various recent GRACE-based studies (Jacob et al., 2012;  
686 Chen et al., 2013; Yi et al., 2015; Schrama et al., 2014) and several studies combining  
687 GRACE with other datasets (Gardner et al., 2013, and an update of it; Dieng et al., 2015;  
688 Reager et al., 2016; Rietbroek et al., 2016). The studies based on GRACE data consistently  
689 give less negative glacier mass balances than those obtained using other methods.  
690 Uncertainties in the GRACE-derived estimates remain important especially due to the small  
691 size of glaciers compared with the GRACE footprint of ~300 km. Associated problems  
692 include the leakage of the gravity signal into the oceans, or the difficulty of distinguishing  
693 between mass changes due to glacier mass changes or to land water storage changes. In  
694 regional and global studies, however, the problem of the footprint and related leakage is not  
695 relevant, as individual glaciers need not to be resolved and GRACE has been shown to be  
696 effective in providing measurements of mass changes for clusters of glaciers (Luthcke et al.,  
697 2008). Uncertainties in the GIA correction also remain, and the effects of rebound from the  
698 Little Ice Age (LIA) deglaciation have to be accounted for.

699 Parkes and Marzeion (2018) have analysed the contribution to SLR from uncharted  
700 glaciers (glaciers melted away and small glaciers not inventoried) during the 21<sup>st</sup> century.  
701 Although they will play a minimal role in SLR in the future, the important finding is that their  
702 contribution is sufficient to close the historical sea-level budget, for which undiscovered  
703 physical processes are then no longer required.

704 Bamber et al. (2018) have updated the glacier mass-change rates presented in  
705 Marzeion et al. (2017) by adding new estimates of mass trends for the Arctic glaciers and ice  
706 caps and the glaciers of High-Mountain Asia and Patagonia, which together contribute to  
707 84% of the SLR from glacier wastage. They combine the most recent observations (including  
708 CryoSat2 radar altimetry) and the latest results from statistical modelling, as well as regional  
709 climate modelling for the Arctic ice caps (Noël et al., 2018b) and stereo photogrammetry for  
710 High-Mountain Asia (Brun et al., 2017). They find poor agreement between the estimates  
711 based on statistical modelling and all other methods (altimetry/gravimetry/RCM) for Arctic  
712 Canada, Svalbard, peripheral Greenland, the Russian Arctic and the Andes, which are all  
713 regions with significant marine- or lake-terminating glaciers, where statistical modelling,  
714 which does not account for frontal ablation, is expected to perform worse than the  
715 observational-based approaches. Bamber et al. (2018) also present pentadal mass balance  
716 rates for the period 1992-2016, which are shown in **Table 2** and clearly illustrate the increase  
717 in global glacier mass losses. If we add to the mass budget for the last pentad (2012-2016) in  
718 **Table 2** the mass budget of  $-33 \text{ Gt yr}^{-1}$  for the Greenland peripheral glaciers estimated by  
719 averaging the CryoSat and RCM values for 2010-2014 given in Table 1 of Bamber et al.  
720 (2018), and the mass budget of  $-6 \text{ Gt yr}^{-1}$  for the Antarctic peripheral glaciers over 2003-  
721 2009 estimated by Gardner et al. (2013), we get an estimate of the current global glacier  
722 mass budget of  $-266 \pm 33 \text{ Gt yr}^{-1}$  ( $0.73 \pm 0.09 \text{ mm SLE yr}^{-1}$ ).

723 The most recent studies to highlight are those of Zemp et al. (2019) and Wouters et al.  
724 (2019). The former is based on glaciological and geodetic measurements but uses a much-  
725 extended dataset (especially for the geodetic measurements), the most updated glacier  
726 inventory (RGI 6.0) and a novel approach. The latter combines, for each glacier region, the  
727 temporal variability from the glaciological sample with the glacier-specific values of the  
728 geodetic sample. The calibrated annual time series is then extrapolated to the whole set of  
729 regional glaciers to assess regional mass changes, considering the rates of area change in the  
730 region. The authors claim that this procedure has overcome the earlier reported negative bias  
731 in the glaciological sample (Gardner et al., 2013). Nevertheless, for large glacialised regions  
732 (e.g. RGI regions), large differences remain between different mass-loss estimates, for  
733 example in the Southern Andes where two recent studies have found reduced mass loss  
734 compared to Zemp et al. (2019) and Wouters et al. (2019) using differencing of digital  
735 elevation models (Braun et al., 2019; Dussaillant et al., 2019). However, the global glacier  
736 mass loss estimate by Zemp et al. (2019), of  $0.74 \pm 0.05 \text{ mm SLE yr}^{-1}$  during 2006-2016,  
737 excluding the peripheral glaciers ( $0.92 \pm 0.39 \text{ mm SLE yr}^{-1}$  if included), is still large compared  
738 to that by Bamber et al. (2018), of  $0.59 \pm 0.11 \text{ mm SLE yr}^{-1}$  for the same period, which is very  
739 similar to the most recent gravimetry-based estimate by Wouters et al. (2019), of  $0.55 \pm 0.10$   
740  $\text{mm SLE yr}^{-1}$ , again for the same period (from their Table S1). This estimate is an  
741 improvement over earlier ones, by using longer time series, an updated glacier inventory  
742 (RGI 6.0), the latest GRACE releases (RL06), which are combined in an ensemble to further  
743 reduce the noise, a new GIA model (Caron et al., 2018) and new hydrology models (GLDAS  
744 V2.1 (Rodell et al., 2004; Beaudoin and Rodell, 2016), and PCR-GLOBW 2 (Sutanudjaja et  
745 al., 2018)) to remove the signal from continental hydrology.

746  
747  
748

#### 749 4.3 Projected estimates to the end of the 21<sup>st</sup> century

750

751 Among the post-AR5 studies on projected global estimates of mass losses by glaciers to the  
752 end of the 21<sup>st</sup> century, we highlight those of Radić et al. (2014), Huss and Hock (2015) and  
753 Marzeion et al. (2018), together with the main results from the recent model intercomparison  
754 by Hock et al. (2019). An account of other pre- and post-AR5 (up to 2016) projections can be  
755 found in the review by Slangen et al. (2017). While the first two mentioned projections share  
756 many common features (glacier inventory, global climate models and emission scenarios, a  
757 temperature-index mass balance model, similar climate forcing for the calibration period and  
758 similar global DEMs), they have two remarkable differences. First, Radić et al. (2014) rely on  
759 volume-area scaling for the initial volume estimate and to account for the dynamic response  
760 to modelled mass change, while Huss and Hock (2015) derive the initial ice-thickness  
761 distribution using the inverse method by Huss and Farinotti (2012), and the modelled glacier  
762 dynamic response to mass changes is based on an empirical relation between thickness  
763 change and normalized elevation range (Huss et al., 2010). Second, the Huss and Hock  
764 (2015) model accounts for frontal ablation of marine-terminating glaciers, dominated by  
765 calving losses and submarine melt. The results by Radić et al. (2014) suggest SLR  
766 contributions of  $155\pm 41$  (RCP4.5) and  $216\pm 44$  (RCP8.5) mm, similar to the projections of  
767 Marzeion et al. (2012), and to the projections of Slangen and van de Wal (2011) updated in  
768 Slangen et al. (2017). However, the more updated and complete model by Huss and Hock  
769 (2015) predicts lower contributions, of  $79\pm 24$  (RCP2.6),  $108\pm 28$  (RCP4.5), and  $157\pm 31$   
770 (RCP8.5) mm. Of these glacier mass losses, ~10% correspond to frontal ablation globally,  
771 and up to ~30% regionally. In both models, the most important contributors to SLR are the  
772 Canadian Arctic, Alaska, the Russian Arctic, Svalbard, and the periphery of Greenland and  
773 Antarctica. Both models are highly sensitive to the initial ice volume. Regarding Marzeion et  
774 al. (2018), while they use basically the same statistical model as in Marzeion et al. (2012,  
775 2014a,b, 2015, 2017), the use of a newer version (5.0) of the RGI, as well as updated DEMs  
776 and SMB calibration datasets, led to lower SLR contributions from glacier wastage to the end  
777 of the 21<sup>st</sup> century, similar to those by Huss and Hock (2015): 84 [54–116] (RCP2.6), 104  
778 [58–136] (RCP4.5) and 142 [83–165] (RCP8.5) mm (the numbers in brackets indicate the  
779 fifth and ninety-fifth percentiles of the glacier model ensemble distribution).

780 A recent intercomparison of six global-scale glacier mass-balance models,  
781 GlacierMIP (Hock et al., 2019), has provided a total of 214 projections of annual glacier mass  
782 and area, to the end of the 21<sup>st</sup> century, forced by 25 GCMs and four RCPs. Global glacier  
783 mass loss (including Greenland and Antarctic peripheries) by 2100 relative to 2015, averaged  
784 over all model runs, varies between  $94\pm 25$  (RCP2.6) and  $200\pm 44$  (RCP8.5) mm SLE. Large  
785 differences are found between the results from the various models even for identical RCPs,  
786 particularly for some glacier regions. These discrepancies are attributed to differences in  
787 model physics, calibration and downscaling procedures, input data and initial glacier volume,  
788 and the number and ensembles of GCMs used.

789 Although only a regional study, the modelling by Zekollari et al. (2019) is a good  
790 example of one of the lines of improvements expected for the future generation of models for  
791 projecting the future evolution of glaciers. Zekollari et al. (2019) have added ice dynamics to  
792 the model by Huss and Hock (2015), in which glacier changes are imposed based on a  
793 parameterization of the changes in surface elevation at a regional scale. The inclusion of ice  
794 dynamics results in a reduction of the projected mass loss, especially for the low-emission  
795 scenarios such as RCP2.6, and this effect increases with the glacier elevation range, which is  
796 typically broader for the largest glaciers.

797 The contribution from glaciers to SLR is expected to continue to increase during most  
798 of the 21<sup>st</sup> century. Note e.g. that the projections by Huss and Hock (2015) give average rates,



799 over their 90-yr modelled period, between  $0.88\pm 0.27$  and  $1.74\pm 0.34$  mm SLE  $\text{yr}^{-1}$ , depending  
800 on the emission scenario, which are larger than the current rates. However, this contribution  
801 is expected to decay as the total ice volume stored in glaciers becomes smaller as the low-  
802 latitude and low-altitude glaciers disappear and those remaining become confined to the  
803 higher latitudes and altitudes. The projections by Huss and Hock (2015) yield a global glacier  
804 volume loss of 25–48% between 2010 and 2100, depending on the scenario. In parallel, the  
805 contribution from the ice sheets is increasing (e.g. Shepherd et al., 2013, 2018; this paper),  
806 and thus the sea-level rise caused by mass losses from land ice masses will more and more be  
807 dominated by losses from the ice sheets (**Table 3**).

808

## 809 **5.0 Summary and outlook**

810

811 Never before have there been so much new observational, especially satellite, data for  
812 assessing the state of mass balance of ice sheets and glaciers and their sensitivity to ongoing  
813 climate change. However, the usable satellite record is still relatively short in climate terms.  
814 One of the main remaining challenges is that satellite observations date back only 2-3  
815 decades, which is a very short period for the reference and evaluation of century-scale  
816 projections. Therefore, further extension of the ice-sheet satellite record into the past, for  
817 example through revised processing of earlier albeit lower quality observations following the  
818 method of Trusel et al. (2018), would greatly inform modellers. Also in the same line, and for  
819 the sake of ice-sheet mass and regional climate change detection and attribution, model  
820 evaluation and improved projections, the maintenance and extension of current automatic  
821 weather stations (e.g. Hermann et al., 2018; Smeets et al. 2018) across the ice sheets is of key  
822 interest, with particular emphasis on energy balance stations able to quantify melt energy.

823 Our review highlights that, despite recent efforts, significant discrepancies remain  
824 with respect to absolute mass balance values for the EAIS, and so further studies are  
825 recommended to resolve this matter. Compared to the AIS, for the GrIS, there is a higher  
826 level of agreement, but absolute values vary by  $\sim 100\text{--}300$  Gt  $\text{yr}^{-1}$  between recent years. These  
827 significant fluctuations are mainly due to SMB variability (precipitation and runoff) that are  
828 in turn linked to fluctuations in atmospheric circulation. Ice dynamics may also have an  
829 important role to play in future changes of the GrIS, especially in regions away from the  
830 southwest, and the relative contributions of SMB and dynamics to future mass change remain  
831 unclear.

832 Continued monitoring is vital to resolve these open questions. Apart from ensuring  
833 the continuity of key satellite data provided by missions including GRACE Follow On  
834 (gravimetry) and ICESat2 (altimetry), and carrying out more frequent (annual)  
835 comprehensive inter-comparison assessments of ice-sheet mass balance, the cryospheric and  
836 climate science communities need to enhance existing collaborations on improving regional  
837 climate model and SMB simulations of Antarctica and Greenland (SMB\_MIP being a key  
838 example), and also make further significant improvements to GIA models, as these are some  
839 of the key sources of residual uncertainty underlying current ice-sheet mass balance  
840 estimates.

841 Recent advances in ice-sheet models show major improvements in terms of  
842 understanding of physics and rheology and model initialization, especially thanks to the  
843 wealth of satellite data that has recently become available. However, recent model  
844 intercomparisons (Goelzer et al., 2018a; Seroussi et al., 2019) still point to large process and  
845 parameter uncertainties. Nevertheless, new techniques need to be further explored to improve  
846 initialization methods using both surface elevation and ice velocity changes, allowing for  
847 improved understanding of underlying friction laws and rheological conditions of marine-  
848 terminating glaciers (e.g. Gillet-Chaulet et al., 2016; Gillet-Chaulet, 2019). Given that marine

849 outlet glaciers are especially sensitive to small-change topographic variations, multi-  
850 parameter ensemble modelling and the use of novel emulation methods to evaluate  
851 uncertainty will become an essential tool in ice-sheet modelling. There is a corresponding  
852 need to acquire additional high resolution subglacial topography data to help with  
853 predictions. Several paleo-studies have also emphasized the importance of subglacial  
854 topography in controlling grounding zone location. Jamieson et al. (2012), Batchelor and  
855 Dowdeswell (2015), and Danielson and Bart (2019) all demonstrate that the post-LGM  
856 Antarctic grounding line preferentially stabilized in regions where there are vertical or lateral  
857 topographic restrictions. Meanwhile, in recognition of the remaining limitations of ice-sheet  
858 models, despite significant recent progress, alternative novel approaches including structured  
859 expert judgment are useful to assess the likely impact of ongoing ice-sheet melt on SLR. For  
860 example, Bamber et al. (2019) indicate that a high-emissions greenhouse warming scenario  
861 gives a not insignificant chance of a total  $>2$  m SLR by 2100.

862 Regarding glaciers other than the ice sheets, in spite of recent improvements the  
863 observational database needs to be further extended in space and time. As suggested by Zemp  
864 et al. (2019), emphasis should be on closing data gaps in: 1) regions where glaciers dominate  
865 runoff during warm/dry seasons (tropical Andes and Central Asia), and 2) regions expected to  
866 dominate the future glacier contribution to SLR (Alaska, Arctic Canada, the Russian Arctic  
867 and Greenland and Antarctica peripheries). ICESat-2 and GRACE follow-on missions are  
868 likely to have revolutionary impacts on our knowledge of the mass changes of glaciers and  
869 ice caps, though GIA corrections and LIA deglaciation effects still have room for  
870 improvement. ICESat-2 especially, with its multiple laser beams and precise repeat-track  
871 pointing capability, has the potential to revolutionise our knowledge of mass changes on  
872 small glaciers worldwide. However, there is an unfortunate conflict that is seriously limiting  
873 ICESat-2 collection of precise repeat-track data globally. The current mission operation for  
874 ICESat-2 has systematic off-nadir pointing outside of polar regions to provide denser  
875 mapping of vegetation biomass for a vegetation inventory, despite the fact that such data is  
876 also being collected by the GEDI laser altimeter on the International Space Station. After one  
877 year of ICESat-2 vegetation-inventory mapping, it would be advisable that the mission  
878 operation plan be changed to precise-repeat track pointing to reference tracks globally for  
879 studies of mass changes of glaciers and ice caps, which will also provide improved vegetation  
880 measurements for studies of seasonal and interannual vegetation changes. DEM differencing  
881 from sub-metre resolution optical satellites such as Quickbird, WorldView and Pléiades will  
882 play a key role in geodetic mass-balance estimates (Kronenberg et al. 2016; Melkonian et al.,  
883 2016; Berthier et al., 2014). The discrepancy between the GlacierMIP mass-change  
884 projections from the various models, even under identical emission scenarios, calls for further  
885 standardized intercomparison experiments, where common glacier inventory version, initial  
886 glacier volume, ensemble of GCMs and RCP emission scenarios are prescribed for all models  
887 (Hock et al., 2019). Finally, projections of future contributions to SLR will benefit from  
888 inclusion in the models of ice dynamics, as done by Zekollari et al. (2019).

## 889 **Acknowledgements**

891 The authors are grateful to WCRP CliC, SCAR and IASC for sponsoring the ISMASS  
892 workshop in Davos, Switzerland, on 15 June 2018 that led to this paper. FN received funding  
893 from grant CTM2017-84441-R of the Spanish State Plan for R&D. KB acknowledges  
894 support from the Fonds de la Recherche Scientifique de Belgique (F.R.S.-FNRS). HG  
895 received funding from the programme of the Netherlands Earth System Science Centre  
896 (NESSC), financially supported by the Dutch Ministry of Education, Culture and Science  
897 (OCW) under grant no. 024.002.001. MV acknowledges support from the European Research  
898

899 Council ERC-StG-678145-CoupledIceClim. EH thanks Jay Zwally for permission to  
900 reproduce Figure 1, and Holly Garner for help with final checking.

901  
902  
903  
904  
905  
906  
907  
908  
909  
910  
911  
912  
913  
914  
915  
916  
917  
918  
919  
920  
921  
922  
923  
924  
925  
926  
927  
928  
929  
930  
931  
932  
933  
934  
935  
936  
937  
938  
939  
940  
941  
942  
943  
944  
945  
946  
947  
948

949 **References**

950

951 Abram, N.J., Mulvaney, R., Vimeux, F., Phipps, S.J., Turner, J., England, M.H., 2014.  
952 Evolution of the Southern Annular Mode during the past millennium. *Nat. Clim. Change* 4,  
953 564–569, doi:10.1038/nclimate2235.

954

955 Adhikari, S., Ivins, E.R., Larour, E., Seroussi, H., Morlighem, M., Nowicki, S., 2014. Future  
956 Antarctic bed topography and its implications for ice sheet dynamics. *Solid Earth* 5, 569-584.

957

958 Agosta, C., Amory, C., Kittel, C., Orsi, A., Favier, V., Gallée, H., van den Broeke, M.R.,  
959 Lenaerts, J.T.M., van Wessem, J.M., Fettweis, X., 2019. Estimation of the Antarctic surface  
960 mass balance using the regional climate model MAR (1979–2015) and identification of  
961 dominant processes, *The Cryosphere* 13, 281-296.

962

963 Alexander, P. M., LeGrande, A. N., Fischer, E., Tedesco, M., Fettweis, X., Kelley, M.,  
964 Nowicki, S. M. J., Schmidt, G. A., 2019. Simulated Greenland surface mass balance in the  
965 GISS ModelE2 GCM: Role of the ice sheet surface. *Journal of Geophysical Research: Earth*  
966 *Surface* 124, 750–765.

967

968 Amory, C., Gallée, H., Naaim-Bouvet, F., Favier, V., Vignot, E., Picard, G., Trouvillez, A.,  
969 Picard, L., Genthon, C., Bellot, H., 2017. Seasonal Variations in Drag Coefficient over a  
970 Sastrugi-Covered Snowfield in Coastal East Antarctica. *Bound.-Layer Meteorol.* 164, 107-  
971 133.

972

973 Andersen, M.L., Stenseng, L., Skourup, H., Colgan, W., Khan, S.A., Kristensen, S.S.,  
974 Andersen, S.B., Box, J.E., Ahlstrøm, A.P., Fettweis, X., Forsberg, R., 2015. Basin-scale  
975 partitioning of Greenland ice sheet mass balance components (2007-2011). *Earth Planet. Sci.*  
976 *Lett.* 409, 89-95.

977

978 Argus, D.F., Peltier, W.R., Drummond, R., Moore, A.W., 2014. The Antarctica component of  
979 postglacial rebound model ICE-6G\_C (VM5a) based on GPS positioning, exposure age  
980 dating of ice thicknesses, and relative sea level histories. *Geophysical Journal International*  
981 198(1), 537-563.

982

983 Arthern, R.J., Gudmundsson G.H., 2010. Initialization of ice-sheet forecasts viewed as an  
984 inverse Robin problem. *J. Glaciol.* 56 (197), 527–33, doi:10.3189/002214310792447699.

985

986 Arthern, R.J., Hindmarsh, R.C.A., 2006. Determining the contribution of Antarctica to sea-  
987 level rise using data assimilation methods. *Philos. Transact. A Math. Phys. Eng. Sci.*  
988 364(1844):1841–65, doi:10.1098/rsta.2006.1801.

989

990 Arthern, R.J., Winebrenner, D.P., Vaughan, D.G., 2006. Antarctic snow accumulation  
991 mapped using polarization of 4.3-cm wavelength microwave emission. *J. Geophys. Res.*  
992 *Atmos.* 111(6):1-10. doi:10.1029/2004JD005667.

993

994 Asay-Davis, X. S., Jourdain, N.C., and Nakayama, Y., 2017. Developments in Simulating  
995 and Parameterizing Interactions Between the Southern Ocean and the Antarctic Ice Sheet.  
996 *Curr. Clim. Change Rep.* 3, 316–329, doi:10.1007/s40641-017-0071-0.

997

998 Bales, R.C., Guo, Q., Shen, D., McConnell, J.R., Du., G., Burkhart, J.F., Spikes, V.B.,

999 Hanna, E., Cappelen, J., 2009. Annual accumulation for Greenland updated using ice core  
1000 data developed during 2000-2006 and analysis of daily coastal meteorological data. *J.*  
1001 *Geophys. Res. Atmos.* 114(6), D06116, doi:10.1029/2008JD011208.  
1002

1003 Bamber, J.L., Westaway, R.M., Marzeion, B., Wouters, B., 2018. The land ice contribution to  
1004 sea level during the satellite era. *Environmental Research Letters* 13, 063008.  
1005 doi:10.1088/1748-9326/aac2f0.  
1006

1007 Bamber, J.L., Oppenheimer, M., Kopp, R.E., Aspinnall, W.P., Cooke, R.M., 2019. Ice sheet  
1008 contributions to future sea-level rise from structured expert judgment. *PNAS* 116 (23),  
1009 11195-11200, <https://doi.org/10.1073/pnas.1817205116>.  
1010

1011 Barletta, V.R., Bevis, M., Smith, B.E., Wilson, T., Brown, A., Bordoni, A., Willis, M., Khan,  
1012 S.A., Rovira-Navarro, M., Dalziel, I., Smalley, R., Kendrick, E., Konfal, S., Caccamise, D.J.,  
1013 Aster, R.C., Nyblade, A., Wiens, D.A., 2018. Observed rapid bedrock uplift in Amundsen  
1014 Sea Embayment promotes ice-sheet stability. *Science*, 360(6395): 1335-1339.  
1015

1016 Barral, H., Genthon, C., Trouvilliez, A., Brun, C., Amory, C., 2014. Blowing snow in coastal  
1017 Adélie Land, Antarctica: three atmospheric-moisture issues. *The Cryosphere* 8, 1905–1919,  
1018 doi:10.5194/tc-8-1905-2014.  
1019

1020 Bart, P.J., DeCesare, M., Rosenheim, B.E., Majewski, W., McGlannan, A., 2018. A  
1021 centuries-long delay between a paleo-ice-shelf collapse and grounding-line retreat in the  
1022 Whales Deep Basin, eastern Ross Sea, Antarctica. *Scientific Reports* 8, 12392.  
1023

1024 Bassis, J.N., Walker, C.C., 2012. Upper and lower limits on the stability of calving glaciers  
1025 from the yield strength envelope of ice. *Proc. R. Soc. Lond. A Math. Phys. Sci.*  
1026 468(2140):913–31. doi:10.1098/rspa.2011.0422  
1027

1028 Batchelor, C.L., Dowdeswell, J.A., 2015. Ice-sheet grounding-zone wedges (GZWs) on high-  
1029 latitude continental margins. *Marine Geology* 363, 65-92.  
1030

1031 Baur, O., Kuhn, M., Featherstone, W.E., 2013. Continental mass change from GRACE over  
1032 2002-2011 and its impact on sea level. *Journal of Geodesy*, 87(2): 117-125.  
1033

1034 Beaudoin, H., Rodell, M., 2016. GLDAS Noah Land Surface Model L4 monthly 0.25 x 392  
1035 0.25 degree V2.1, doi:10.5067/SXAVCZFAQLNO.  
1036

1037 Beaumet, J., Krinner, G., Déqué, M., Haarsma, R., Li, L., 2019. Assessing bias-corrections of  
1038 oceanic surface conditions for atmospheric models. *Geosci. Model Dev.* 12, 321-342.  
1039 doi:<https://doi.org/10.5194/gmd-2017-247>.  
1040

1041 Bell, R.E., Banwell, A.F., Trusel, L.D., Kingslake, J., 2018. Antarctic surface hydrology and  
1042 impacts on ice-sheet mass balance. *Nature Climate Change* 8, 1044–1052.  
1043

1044 Berthier, E., Vincent, C., Magnússon, E., Gunnlaugsson, Á.P., Pitte, P., Le Meur, E.,  
1045 Masiokas, M., Ruiz, L., Pálsson, F., Belart, J.M.C., Wagnon, P., 2014. Glacier topography  
1046 and elevation changes derived from Pléiades submeter stereo images. *The Cryosphere* 8,  
1047 2275–2291. doi:10.5194/tc-8-2275-2014.  
1048

1049 Bevis, M., Harig, C., Khan, S.A., Brown, A., Simons, F.J., Willis, M., Fettweis, X., van den  
1050 Broeke, M.R., Madsen, F.B., Kendrick, E., Caccamise II, D.J., Van Dam, T., Knudsen, P.,  
1051 Nylen, T., 2019. Accelerating changes in ice mass within Greenland, and the ice sheet's  
1052 sensitivity to atmospheric forcing. *PNAS* 116, 1934-1939.

1053  
1054 Bigg, G.R., Wei, H.L., Wilton, D.J., Zhao, Y., Billings S.A., Hanna, E., Kadiramanathan V.,  
1055 2014. A century of variation in the dependence of Greenland iceberg calving on ice sheet  
1056 surface mass balance and regional climate change. *Proceedings of the Royal Society A:  
1057 Mathematical, Physical and Engineering Sciences* 470, 20130662.

1058  
1059 Box J.E., 2013. Greenland ice sheet mass balance reconstruction. Part II: Surface mass  
1060 balance: 1840-2010. *J. Clim.* 26(18), 6974-6989, doi:10.1175/JCLI-D-12-00518.1.

1061  
1062 Box, J.E., Colgan, W.T., Wouters, B., Burgess, D.O., O'Neel, S., Thomson, L.I., Mernild,  
1063 S.H., 2018. Global sea-level contribution from Arctic land ice: 1971-2017. *Environ. Res.  
1064 Lett.* 13, 125012.

1065  
1066 Bozkurt, D., Rondanelli, R., Marín, J.C., Garreaud, R., 2018. Foehn Event Triggered by an  
1067 Atmospheric River Underlies Record-Setting Temperature Along Continental Antarctica. *J.  
1068 Geophys. Res. Atmos.* 123, 3871–3892, doi:10.1002/2017JD027796.

1069  
1070 Bracegirdle, T.J., Hyder, P., Holmes, C.R., 2017. CMIP5 Diversity in Southern Westerly Jet  
1071 Projections Related to Historical Sea Ice Area: Strong Link to Strengthening and Weak Link  
1072 to Shift. *J. Clim.* 31, 195–211, doi:10.1175/JCLI-D-17-0320.1.

1073  
1074 Braun, M. H., Malz, P., Sommer, C., Farías-Barahona, D., Sauter, T., Casassa, G., Soruco,  
1075 A., Skvarca, P., and Seehaus, T. C., 2019. Constraining glacier elevation and mass changes in  
1076 South America. *Nature Climate Change* 9, 130.

1077  
1078 Bromwich, D.H., Nicolas, J.P., Monaghan, A.J., 2011. An Assessment of Precipitation  
1079 Changes over Antarctica and the Southern Ocean since 1989 in Contemporary Global  
1080 Reanalyses. *J. Clim.* 24, 4189–4209, doi:10.1175/2011JCLI4074.1.

1081  
1082 Bromwich, D.H., Nicolas, J.P., Monaghan, A.J., Lazzara, M.A., Keller, L.M., Weidner, G.A.,  
1083 Wilson, A.B., 2012. Central West Antarctica among the most rapidly warming regions on  
1084 Earth. *Nat. Geosci.* 6, 139–145, doi:10.1038/ngeo1671.

1085  
1086 Brun, F., Berthier, E., Wagnon, P., Kääh, A., Treichler D., 2017. A spatially resolved  
1087 estimate of High Mountain Asia glacier mass balances from 2000–2016. *Nature Geoscience*  
1088 10(9), 668–673, doi:10.1038/NGEO2999.

1089  
1090 Bulthuis, K., Arnst, M., Sun, S., Pattyn, F. 2019. Uncertainty quantification of the multi-  
1091 centennial response of the Antarctic ice sheet to climate change. *The Cryosphere* 13, 1349-  
1092 1380, <https://doi.org/10.5194/tc-13-1349-2019>.

1093  
1094 Campagne, P., Crosta, X., Houssais, M.N., Swingedouw, D., Schmidt, S., Martin, A.,  
1095 Devred, E., Capo, S., Marieu, V., Closset, I., Massé, G., 2015. Glacial ice and atmospheric  
1096 forcing on the Mertz Glacier Polynya over the past 250 years. *Nat. Commun.* 6, 6642,  
1097 doi:10.1038/ncomms7642.

1098 Cape, M.R., Vernet, M., Skvarca, P., Marinsek, S., Scambos, T. Domack, E., 2015. Foehn  
1099 winds link climate-driven warming to ice shelf evolution in Antarctica. *J. Geophys. Res.*  
1100 *Atmospheres* 120, 11037-11057.  
1101

1102 Caron, L., Ivins, E., Larour, E., Adhikari, S., Nilsson, J., Blewitt, G., 2018. GIA Model  
1103 Statistics for Cape, GRACE Hydrology, Cryosphere, and Ocean Science. *Geophysical*  
1104 *Research Letters* 45, 2203–2212, doi:10.1002/2017GL076644.  
1105

1106 Chen, J.L., Wilson, C.R., Tapley, B.D., 2013. Contribution of ice sheet and mountain glacier  
1107 melt to sea level rise. *Nature Geoscience* 6, 549–552, doi:10.1038/NGEO1829.  
1108

1109 Christianson, K., Bushuk, M., Dutrieux, P., Parizek, B.R., Joughin, I.R., Alley, R.B., Shean,  
1110 D.E., Abrahamsen, E.P., Anandakrishnan, S., Heywood, K.J., Kim, T.-W., Lee, S.-H.,  
1111 Nicholls, K., Stanton, T., Truffer, M., Webber, B.G.M., Jenkins, A., Jacobs, S.,  
1112 Bindschadler, R., Holland, D.M., 2016. Sensitivity of Pine Island Glacier to observed  
1113 ocean forcing, *Geophys. Res. Lett.*, 43, 10,817–10,825, doi:10.1002/2016GL070500.  
1114

1115 Church, J.A., Clark, P.U., Cazenave, A., Gregory, J.M., Jevrejeva, S., Levermann, A.,  
1116 Merrifield, M.A., Milne, G.A., Nerem, R.S., Nunn, P.D., Payne, A.J., Pfeffer, W.T.,  
1117 Stammer, D., and Unnikrishnan, A.S., 2013: Sea Level Change, in: Stocker, T.F., Qin, D.,  
1118 Plattner, G.-K., Tignor, M., Allen, S.K., Boschung, J., Nauels, A., Xia, Y., Bex, V., Midgley,  
1119 P.M. (Eds.), *Climate Change 2013: The Physical Science Basis. Contribution of Working*  
1120 *Group I to the Fifth Assessment Report of the Intergovernmental Panel on Climate Change.*  
1121 *Cambridge University Press, Cambridge, United Kingdom and New York, NY, USA, pp.*  
1122 *1137–1216.*  
1123

1124 Citterio, M., van As, D., Ahlstrøm A.P., Andersen, M.L., Andersen, S.B., Box, J.E.,  
1125 Charalampidis, C., Colgan, W.T., Fausto, R.S., Nielsen, S., Veicherts, M., 2015. Automatic  
1126 weather stations for basic and applied glaciological research. *Geol. Surv. Denmark Greenl.*  
1127 *Bull.* 33, 69-72. [http://www.geus.dk/media/10888/nr33\\_p69-72.pdf](http://www.geus.dk/media/10888/nr33_p69-72.pdf).  
1128

1129 Cogley, J.G., 2009. Geodetic and direct mass-balance measurements: comparison and joint  
1130 analysis. *Annals of Glaciology* 50, 96–100. doi:10.3189/172756409787769744.  
1131

1132 Cogley, J.G., Hock, R., Rasmussen, L.A., Arendt, A.A., Bauder, A., Braithwaite, R.J.,  
1133 Jansson, P., Kaser, G., Möller, M., Nicholson, L., and Zemp, M., 2011. Glossary of Glacier  
1134 Mass Balance and Related Terms. IHP-VII Technical Documents in Hydrology No. 86, IACS  
1135 Contribution No. 2, UNESCO-IHP, Paris, 114 pp.  
1136

1137 Cornford, S.L., Martin, D.F., Graves, D.T., Ranken, D.F., Le Brocq, A.M., Gladstone, R.M.,  
1138 Payne, A.J., Ng, E.G., Lipscomb, W.H., 2013. Adaptive mesh, finite volume modeling of  
1139 marine ice sheets. *J. Comput. Phys.* 232, 529–549, doi:10.1016/j.jcp.2012.08.037  
1140

1141 Cornford, S.L., Martin, D.F., Payne, A.J., Ng, E.G., Le Brocq, A.M., Gladstone, R.M.,  
1142 Edwards, T.L., Shannon, S.R., Agosta, C., Van Den Broeke, M.R., Hellmer, H.H., Krinner,  
1143 G., Ligtenberg, S.R.M., Timmermann, R., Vaughan, D.G., 2015. Century-scale simulations  
1144 of the response of the West Antarctic Ice Sheet to a warming climate. *Cryosphere* 9(4), 1579–  
1145 600, doi:10.5194/tc-9-1579-2015.  
1146

1147 Cornford, S.L., Martin, D.F., Lee, V., Payne, A.J., Ng, E.G., 2016. Adaptive mesh refinement  
1148 versus subgrid friction interpolation in simulations of Antarctic ice dynamics. *Ann. Glaciol.*  
1149 *57*(73), 1–9, doi:10.1017/aog.2016.13.  
1150

1151 Csatho, B.M., Schenk, A.F., Van der Veen, C.J., Babonis, G., Duncan, K., Rezvanbehbahani,  
1152 S., Van den Broeke, M.R., Simonsen, S.B., Nagarajan, S., Van Angelen, J.H., 2014. Laser  
1153 altimetry reveals complex pattern of Greenland Ice Sheet dynamics. *Proceedings of the*  
1154 *National Academy of Sciences of the United States of America*, *111*(52): 18478-18483.  
1155

1156 Cullather, R.I., Nowicki, S.M.J., Zhao, B., Suarez, M.J., 2014. Evaluation of the Surface  
1157 Representation of the Greenland Ice Sheet in a General Circulation Model. *J. Clim.* *27*(13),  
1158 4835-4856.  
1159

1160 Cullather, R.I., Nowicki, S.M.J., Zhao, B., Koenig, L.S., 2016. A Characterization of  
1161 Greenland Ice Sheet Surface Melt and Runoff in Contemporary Reanalyses and a Regional  
1162 Climate Model. *Front Earth Sci.* *4*: 10, doi:10.3389/feart.2016.00010.  
1163

1164 Danielson, M., Bart, P.J., 2019. Topographic control on the post-LGM grounding zone  
1165 locations of the West Antarctic Ice Sheet in the Whales Deep Basin, eastern Ross Sea.  
1166 *Marine Geology* *407*, 248-260.  
1167

1168 Datta, R. T., Tedesco, M., Fettweis, X., Agosta, C., Lhermitte, S., Lenaerts, J. T.M., &  
1169 Wever, N. (2019) The effect of Foehn-induced surface melt on firn evolution over the  
1170 northeast Antarctic peninsula. *Geophysical Research Letters* *46*, 3822–3831.  
1171

1172 Davis, C. H., Ferguson, A.C., 2004. Elevation Change of the Antarctic Ice Sheet, 1995–2000,  
1173 From ERS-2 Satellite Radar Altimetry. *IEEE Transactions on Geoscience and Remote*  
1174 *Sensing.* *42*: 2437 - 2445.  
1175

1176 DeConto, R.M., Pollard, D., 2016. Contribution of Antarctica to past and future sea-level rise.  
1177 *Nature* *531*(7596), 591–597, doi:10.1038/nature17145.  
1178

1179 Deschamps-Berger, C., Nuth, C., van Pelt, W., Berthier, E., Kohler, J., Altena, B., 2019.  
1180 Closing the mass budget of a tidewater glacier: the example of Kronebreen, Svalbard. *J.*  
1181 *Glaciol.*, *65*(249), 136-148, doi:10.1017/jog.2018.98.  
1182

1183 Dieng, H.N., Champollion, N., Cazenave, A., Wada, Y., Schrama, E., Meyssignac, B., 2015.  
1184 Total land water storage change over 2003-2013 estimated from a global mass budget  
1185 approach. *Environmental Research Letters* *10*(12), 124010, doi:10.1088/1748-  
1186 9326/10/12/124010.  
1187

1188 Dittmann, A., Schlosser, E., Masson-Delmotte, V., Powers, J.G., Manning, K.W., Werner,  
1189 M., Fujita, K., 2016. Precipitation regime and stable isotopes at Dome Fuji, East Antarctica.  
1190 *Atmospheric Chem. Phys.* *16*, 6883–6900, doi:https://doi.org/10.5194/acp-16-6883-2016.  
1191

1192 Donat-Magnin, M., Jourdain, M.C., Spence, P., Sommer, J.L., Gallée, H., Durand, G., 2017:  
1193 Ice-Shelf Melt Response to Changing Winds and Glacier Dynamics in the Amundsen Sea  
1194 Sector, Antarctica. *J. Geophys. Res. Oceans* *122*, 10206–10224, doi:10.1002/2017JC013059.  
1195



1196 Dufour, A., Charrondière, C., Zolina, O., 2019. Moisture transport in observations and  
1197 reanalysis as a proxy for snow accumulation in East Antarctica. *Cryosphere* 13, 413-425.  
1198

1199 Durand, G., Gagliardini, O., Favier, L., Zwinger, T., Le Meur, E., 2011. Impact of bedrock  
1200 description on modeling ice sheet dynamics. *Geophys. Res. Lett.* 38, L20501,  
1201 doi.org/10.1029/2011GL048892.  
1202

1203 Dussaillant, I., Berthier, E., Brun, F., Masiokas, M., Hugonnet, R., Favier, V., Rabatel, A.,  
1204 Pitte, P., Ruiz, L., 2018. Two decades of glacier mass loss along the Andes, *Nature*  
1205 *Geoscience* 12, 802-808.

1206 Edwards, T.L., Brandon, M.A., Durand, G., Edwards, N.R., Golledge, N.R., Holden, P.H.,  
1207 Nias, I.J., Payne, A.J., Ritz, C., Wernecke, A., 2019. Revisiting Antarctic ice loss due to  
1208 marine ice-cliff instability. *Nature* 566, 58–64.  
1209

1210 Enderlin, E.M., Howat, I.M., Jeong, S., Noh, M.-J., Van Angelen, J.H. and Van den Broeke,  
1211 M.R., 2014. An improved mass budget for the Greenland ice sheet. *Geophysical Research*  
1212 *Letters* 41, 866-872, 2013GL059010.  
1213

1214 Eyring, V., Bony, S., Meehl, G.A., Senior, C.A., Stevens, B., Stouffer, R.J., Taylor, K.E.,  
1215 2016. Overview of the Coupled Model Intercomparison Project Phase 6 (CMIP6)  
1216 experimental design and organization. *Geosci. Model Dev.* 9, 1937-1958, doi:10.5194/gmd-  
1217 9-1937-2016.  
1218

1219 Favier, V., Agosta, C., Parouty, S., Durand, G., Delaygue, G., Gallée, H., Drouet, A.-S.,  
1220 Trouvilliez, A., Krinner, G., 2013. An updated and quality controlled surface mass balance  
1221 dataset for Antarctica. *Cryosphere* 7(2), 583-597, doi:10.5194/tc-7-583-2013.  
1222

1223 Favier, V., Verfaillie, D., Berthier, B., Menegoz, M., Jomelli, V., Kay, J.E., Ducret, L.,  
1224 Malbêteau, Y., Brunstein, D., Gallée, H., Park, Y.-H., Rinterknecht, V., 2016. Atmospheric  
1225 drying as the main driver of dramatic glacier wastage in the southern Indian Ocean. *Sci. Rep.*  
1226 6, 32396, doi:10.1038/srep32396.  
1227

1228 Favier, V., Krinner, G., Amory, C., Gallée, H., Beaumet, J., Agosta, C., 2017. Antarctica-  
1229 Regional Climate and Surface Mass Budget. *Curr. Clim. Change Rep.* 3, 303–315,  
1230 doi:10.1007/s40641-017-0072-z.  
1231

1232 Fettweis, X., 2018. The SMB Model Intercomparison (SMBMIP) over Greenland: first  
1233 results. AGU Fall Meeting 2018, Washington, DC,  
1234 <https://orbi.uliege.be/handle/2268/232923>.  
1235

1236 Fettweis, X., Box J.E., Agosta, C., Amory, C., Kittel, C., Lang, C., van As, D., Machguth, H.,  
1237 Gallée, H., 2017. Reconstructions of the 1900–2015 Greenland ice sheet surface mass  
1238 balance using the regional climate MAR model. *The Cryosphere* 11(2), 1015-1033.  
1239 doi:10.5194/tc-11-1015-2017.  
1240

1241 Filament, T., Rémy, F., 2012. Dynamic thinning of Antarctic glaciers from along-track repeat  
1242 radar altimetry. *J. Glaciol.* 58: 830–840. doi: 10.3189/2012JoG11J11.  
1243

1244 Fischer, R., Nowicki, S., Kelley, M., Schmidt, G.A., 2014. A system of conservative  
1245 regridding for ice-atmosphere coupling in a General Circulation Model (GCM), *Geosci.*  
1246 *Model Dev.* 7, 883-907, doi:10.5194/gmd-7-883-2014.  
1247

1248 Frezzotti, M., Urbini, S., Proposito, M., Sarchilli, C. Gandolfi, S., 2007. Spatial and  
1249 temporal variability of surface mass balance near Talos Dome, East Antarctica. *J. Geophys.*  
1250 *Res. Earth Surf.* 112, F02032, doi:10.1029/2006JF000638.  
1251

1252 Fujita, S., Holmlund, P., Andersson, I., Brown, I., Enomoto, H., Fujii, Y., Fujita, K., Fukui,  
1253 K., Furukawa, T., Hansson, M., Hara, K., Hoshina, Y., Igarashi, M., Iizuka, Y., Imura, S.,  
1254 Ingvander, S., Karlin, T., Motoyama, H., Nakazawa, F., Oerter, H., Sjöberg, L.E., Sugiyama,  
1255 S., Surdyk, S., Ström, J., Uemura, R., Wilhelms, F., 2011. Spatial and temporal variability of  
1256 snow accumulation rate on the East Antarctic ice divide between Dome Fuji and EPICA  
1257 DML. *The Cryosphere* 5, 1057–1081, doi:10.5194/tc-5-1057-2011.  
1258

1259 Fyke, J.G., Sacks, W.J., Lipscomb, W.H., 2014a. A technique for generating consistent ice  
1260 sheet initial conditions for coupled ice sheet/climate models. *Geosci. Model Dev.*, 7, 1183-  
1261 1195, doi:10.5194/gmd-7-1183-2014, 2014.  
1262

1263 Fyke, J.G., Vizcaino, M., Lipscomb, W.H., Price, S., 2014b. Future climate warming  
1264 increases Greenland ice sheet surface mass balance variability. *Geophysical Research Letters*,  
1265 41(2), 470-475.  
1266

1267 Fyke, J.G., Vizcaino, M., Lipscomb, W.H., 2014c. The pattern of anthropogenic signal  
1268 emergence in Greenland Ice Sheet surface mass balance. *Geophysical Research Letters*  
1269 41(16), 6002-6008.  
1270

1271 Fyke, J., Sergienko, O., Löfverström, M., Price, S., Lenaerts, J.T.M., 2018. An Overview of  
1272 Interactions and Feedbacks Between Ice Sheets and the Earth System. *Rev. Geophys.* 56,  
1273 361-408, doi:10.1029/2018RG000600.  
1274

1275 Gao, C.C., Lu, Y., Zhang, Z.Z., Shi, H.L., Zhu, C.D., 2015. Ice sheet mass balance in  
1276 Antarctica measured by GRACE and its uncertainty. *Chinese Journal of Geophysics-Chinese*  
1277 *Edition* 58(3), 780-792.  
1278

1279 Gao, C.C., Lu, Y., Shi, H.L., Zhang, Z.Z., Xu, C.Y. Tan, B., 2019a. Detection and analysis of  
1280 ice sheet mass changes over 27 Antarctic drainage systems from GRACE RLO6 data.  
1281 *Chinese Journal of Geophysics-Chinese Edition* 62(3), 864-882.  
1282

1283 Gao, C.C., Lu, Y., Zhang, Z.Z. Shi, H.L., 2019b. A Joint Inversion Estimate of Antarctic Ice  
1284 Sheet Mass Balance Using Multi-Geodetic Data Sets. *Remote Sens.* 11(6), 653,  
1285 doi:10.3390/rs11060653.  
1286

1287 Gardner, A. S., Moholdt, G., Cogley, J. G., Wouters, B., Arendt, A. A., Wahr, J., Berthier, E.,  
1288 Hock, R., Pfeffer, W. T., Kaser, G., Ligtenberg, S. R. M., Bolch, T., Sharp, M. J., Hagen, J.  
1289 O., van den Broeke, M. R., Paul, F., 2013. A reconciled estimate of glacier contributions to  
1290 sea level rise: 2003 to 2009. *Science* 340, 852–857, doi:10.1126/science.1234532.  
1291

1292 Gardner, A.S., Moholdt, G., Scambos, T., Fahnestock, M., Ligtenberg, S., Van den Broeke,  
1293 M., Nilsson, J., 2018. Increased West Antarctic and unchanged East Antarctic ice discharge

1294 over the last 7 years. *The Cryosphere* 12, 521–547, doi:[https://doi.org/10.5194/tc-12-521-](https://doi.org/10.5194/tc-12-521-1295)  
1295 2018.

1296

1297 Gillet-Chaulet, F., 2019. Assimilation of surface observations in a transient marine ice sheet  
1298 model using an ensemble Kalman filter. *The Cryosphere Discuss*, [https://doi.org/10.5194/tc-](https://doi.org/10.5194/tc-1299)  
1299 2019-54, in review.

1300

1301 Gillet-Chaulet, F., Gagliardini, O., Seddik, H., Nodet, M., Durand, G., Ritz, C., Zwinger, T.,  
1302 Greve, R., Vaughan, D.G., 2012. Greenland ice sheet contribution to sea-level rise from a  
1303 new-generation icesheet model. *Cryosphere* 6(6), 1561–76, doi:10.5194/tc-6-1561-2012.

1304

1305 Gillet-Chaulet, F., Durand, G., Gagliardini, O., Mosbeux, C., Mouginit, J., Rémy, F., Ritz,  
1306 C., 2016. Assimilation of surface velocities acquired between 1996 and 2010 to constrain the  
1307 form of the basal friction law under Pine Island Glacier. *Geophys. Res. Lett.* 43(19), 10311-  
1308 10321, doi:10.1002/2016GL069937.

1309

1310 Gladstone, R.M., Payne, A.J., Cornford, S.L., 2012. Resolution requirements for grounding-  
1311 line modelling: Sensitivity to basal drag and ice-shelf buttressing. *Ann Glaciol.* 53(60), 97–  
1312 105. doi:10.3189/2012AoG60A148.

1313

1314 Goelzer, H., Nowicki, S., Edwards, T., Beckley, M., Abe-Ouchi, A., Aschwanden, A., Calov,  
1315 R., Gagliardini, O., Gillet-Chaulet, F., Golledge, N.R., Gregory, J., Greve, R., Humbert, A.,  
1316 Huybrechts, P., Kennedy, J H., Larour, E., Lipscomb, W.H., Le clec'h, S., Lee, V.,  
1317 Morlighem, M., Pattyn, F., Payne, A.J., Rodehacke, C., Rückamp, M., Saito, F., Schlegel, N.,  
1318 Seroussi, H., Shepherd, A., Sun, S., Van de Wal, R., Ziemen, F.A., 2018a: Design and results  
1319 of the ice sheet model initialisation experiments initMIP-Greenland: an ISMIP6  
1320 intercomparison. *The Cryosphere*, 12, 1433-1460, doi:10.5194/tc-12-1433-2018.

1321

1322 Goelzer, H., Nowicki, S., Edwards, T., Beckley, M., Abe-Ouchi, A., Aschwanden, A., Calov,  
1323 R., Gagliardini, O., Gillet-Chaulet, F., Golledge, N.R., Gregory, J., Greve, R., Humbert, A.,  
1324 Huybrechts, P., Kennedy, J.H., Larour, E., Lipscomb, W.H., Le clec'h, S., Lee, V.,  
1325 Morlighem, M., Pattyn, F., Payne, A.J., Rodehacke, C., Rückamp, M., Saito, F., Schlegel, N.,  
1326 Seroussi, H., Shepherd, A., Sun, S., Van de Wal, R., Ziemen, F.A., 2018b: Results of the ice  
1327 sheet model initialisation experiments initMIP-Greenland: an ISMIP6 intercomparison,  
1328 10.5281/zenodo.1173088.

1329

1330 Goldberg DN, Heimbach P, 2013. Parameter and state estimation with a time-dependent  
1331 adjoint marine ice sheet model. *Cryosphere* 7(6),1659–78. doi:10.5194/tc-7-1659-2013.

1332

1333 Goldberg DN, Heimbach P, Joughin I, Smith B., 2015. Committed retreat of Smith, Pope,  
1334 and Kohler Glaciers over the next 30 years inferred by transient model calibration.  
1335 *Cryosphere* 9(6), 2429–46. doi:10.5194/tc-9-2429-2015.

1336

1337 Goldberg, D.N., Narayanan, S.H.K., Hascoet, L., Utke, J., 2016. An optimized treatment for  
1338 algorithmic differentiation of an important glaciological fixed-point problem. *Geosci. Model*  
1339 *Dev.* 9(5):1891–904, doi:10.5194/gmd-9-1891-2016.

1340

1341 Golledge, N.R., Kowalewski, D.E., Naish, T.R., Levy, R.H., Fogwill, C.J., Gasson, E.G.W.,  
1342 2015. The multi-millennial Antarctic commitment to future sea-level rise. *Nature* 526, 421-  
1343 425, <https://doi.org/10.1038/nature15706>.

1344  
1345 Golledge, N.R., Keller, E.D., Gomez, N., Naughten, K.A., Bernales, J., Trusel, L.D., and  
1346 Edwards, T.L., 2019. Global environmental consequences of twenty-first-century ice-sheet  
1347 melt. *Nature* 566, 65-72, <https://doi.org/10.1038/s41586-019-0889-9>.  
1348  
1349 Gomez, N., Mitrovica, J.X., Huybers, P., Clark, P.U., 2010. Sea level as a stabilizing factor  
1350 for marine-ice-sheet grounding lines. *Nature Geoscience* 3(12), 850-853.  
1351  
1352 Gomez, N., Pollard, D., Holland, D., 2015. Sea-level feedback lowers projections of future  
1353 Antarctic Ice-Sheet mass loss. *Nature Communications*, 6: 8798.  
1354  
1355 Gomez, N., Latychev, K., Pollard, D., 2018. A coupled ice sheet-sea level model  
1356 incorporating 3D Earth structure: Variations in Antarctica during the last deglacial retreat.  
1357 *Journal of Climate* 31(10), 4041-4054.  
1358  
1359 Gorodetskaya, I.V., Tsukernik, M., Claes, K., Ralph, M.F., Neff, W.D., Van Lipzig, N.P.M.,  
1360 2014. The role of atmospheric rivers in anomalous snow accumulation in East Antarctica.  
1361 *Geophys. Res. Lett.* 41, 6199–6206, doi:10.1002/2014GL060881.  
1362  
1363 Gorodetskaya, I.V., Kneifel, S., Maahn, M., Thiery, W., Schween, J.H., Mangold, A.,  
1364 Crewell, S., Van Lipzig, N.P.M., 2015. Cloud and precipitation properties from ground-based  
1365 remote-sensing instruments in East Antarctica. *The Cryosphere* 9, 285–304, doi:10.5194/tc-9-  
1366 285-2015.  
1367  
1368 Grazioli, J., Genthon, C., Boudevillain, B., Duran-Alarcon, C., Del Guasta, M., Madeleine,  
1369 J.-B., Berne, A., 2017a. Measurements of precipitation in Dumont d’Urville, Adélie  
1370 Land, East Antarctica. *The Cryosphere* 11, 1797–1811, doi:10.5194/tc-11-1797-2017.  
1371  
1372 Grazioli, J., Madeleine, J.-B., Gallée, H., Forbes, R.M., Genthon, C., Krinner, G., Berne, A.,  
1373 2017b. Katabatic winds diminish precipitation contribution to the Antarctic ice mass balance.  
1374 *Proc. Natl. Acad. Sci.* 114, 10858–10863, doi:10.1073/pnas.1707633114.  
1375  
1376 Groh, A., Ewert, H., Fritsche, M., Rulke, A., Rosenau, R., Scheinert, M., Dietrich, R., 2014a.  
1377 Assessing the Current Evolution of the Greenland Ice Sheet by Means of Satellite and  
1378 Ground-Based Observations. *Surveys in Geophysics* 35(6), 1459-1480.  
1379  
1380 Groh, A., Ewert, H., Rosenau, R., Fagiolini, E., Gruber, C., Floricioiu, D., Jaber, W.A.,  
1381 Linow, S., Flechtner, F., Eineder, M., Dierking, W. and Dietrich, R., 2014b. Mass, Volume  
1382 and Velocity of the Antarctic Ice Sheet: Present-Day Changes and Error Effects. *Surveys in*  
1383 *Geophysics* 35(6), 1481-1505.  
1384  
1385 Gunter, B.C., Didova, O., Riva, R.E.M., Ligtenberg, S.R.M., Lanaerts, J.T.M., King, M., van  
1386 den Broeke, M.R., Urban, T., 2014. Empirical estimation of present-day Antarctic glacial  
1387 isostatic adjustment and ice mass change. *The Cryosphere* 8(2), 743-760.  
1388  
1389 Hanna, E., Navarro, F.J., Pattyn, F., Domingues, C.M., Fettweis, X., Ivins, E.R., Nicholls,  
1390 R.J., Ritz, C., Smith, B., Tulaczyk, S., Whitehouse, P.L., Zwally, H.J., 2013. Ice-sheet mass  
1391 balance and climate change. *Nature* 498 (7452), 51-59.  
1392

1393 Hanna, E., Fettweis, X., Mernild, S.H., Cappelen, J., Ribergaard, M.H., Shuman, C.A.,  
1394 Steffen, K., Wood, L., Mote, T.L., 2014. Atmospheric and oceanic climate forcing of the  
1395 exceptional Greenland ice sheet surface melt in summer 2012. *International Journal of*  
1396 *Climatology* 34, 1022-1037.

1397  
1398 Hanna, E., Cropper, T.R., Hall, R.J., Cappelen, J., 2016. Greenland Blocking Index 1851-  
1399 2015: a regional climate change signal. *International Journal of Climatology* 36, 4847-4861.

1400  
1401 Hanna, E., Fettweis, X. and Hall R.J., 2018: Brief communication: Recent changes in  
1402 summer Greenland blocking captured by none of the CMIP5 models. *The Cryosphere* 12(10),  
1403 3287-3292.

1404  
1405 Harig, C., Simons, F.J., 2015. Accelerated West Antarctic ice mass loss continues to outpace  
1406 East Antarctic gains. *Earth and Planetary Science Letters* 415, 134-141.

1407  
1408 Hermann, M., Box, J.E., Fausto, R.S., Colgan, W.T., Langen, P.L., Mottram, R., Wuite, J.,  
1409 Noël, B., Van den Broeke, M.R., Van As, D., 2018. Application of PROMICE Q-Transect in  
1410 Situ Accumulation and Ablation Measurements (2000-2017) to Constrain Mass Balance at  
1411 the Southern Tip of the Greenland Ice Sheet. *J. Geophys. Res.-Earth* 123(6), 1235-1256.

1412  
1413 Hock, R., Bliss, A., Marzeion, B., Giesen, R., Hirabayashi, Y., Huss, M., Radić, V., Slangen,  
1414 A., 2019. GlacierMIP – A model intercomparison of global-scale glacier mass-balance  
1415 models and projections. *Journal of Glaciology* 65, 453-467, doi:10.1017/jog.2019.22.

1416  
1417 Hubbard, B., Luckman, A., Ashmore, D.W., Bevan, S., Kulesa, B., Kuipers Munneke, P.,  
1418 Philippe, M., Jansen, D., Booth, A., Sevestre, H., Tison, J.-L., O’Leary, M., Rutt, I., 2016.  
1419 Massive subsurface ice formed by refreezing of ice-shelf melt ponds. *Nat. Commun.* 7,  
1420 11897, doi:10.1038/ncomms11897.

1421  
1422 Hurkmans, R., Bamber, J.L., Davis, C.H., Joughin, I.R., Khvorostovsky, K.S., Smith, B.S.,  
1423 Schoen, N., 2014. Time-evolving mass loss of the Greenland Ice Sheet from satellite  
1424 altimetry. *Cryosphere* 8(5), 1725-1740.

1425  
1426 Huss, M., 2013. Density assumptions for converting geodetic glacier volume change to mass  
1427 change. *The Cryosphere* 7, 877–887, doi:10.5194/tc-7-877-2013.

1428  
1429 Huss, M., Farinotti, D., 2012. Distributed ice thickness and volume of all glaciers around the  
1430 globe. *Journal of Geophysical Research* 117, F04010, doi:10.1029/2012JF002523.

1431  
1432 Huss, M., Hock, R., 2015. A new model for global glacier change and sea-level rise.  
1433 *Frontiers in Earth Science* 3, 54, doi:10.3389/feart.2015.00054.

1434  
1435 Huss, M., Juvet, G., Farinotti, D., Bauder, A., 2010. Future high-mountain hydrology: a new  
1436 parameterization of glacier retreat. *Hydrology and Earth System Sciences* 14, 815–829,  
1437 doi:10.5194/hess-14-815-2010.

1438  
1439 IPCC, 2013. *Climate Change 2013: The Physical Science Basis. Contribution of Working*  
1440 *Group I to the Fifth Assessment Report of the Intergovernmental Panel on Climate Change*,  
1441 edited by: Stocker, T. F., Qin, D., Plattner, G.-K., Tignor, M., Allen, S. K., Boschung, J.,

1442 Nauels, A., Xia, Y., Bex, V., and Midgley, P. M., Cambridge University Press, Cambridge,  
1443 United Kingdom and New York, NY, USA.  
1444

1445 Ivins, E.R., James, T.S., Wahr, J., Schrama, E.J.O., Landerer, F.W., Simon, K.M., 2013.  
1446 Antarctic Contribution to Sea-Level Rise Observed by GRACE with Improved GIA  
1447 Correction. *Journal of Geophysical Research: Solid Earth* 118(6), 3126-3141.  
1448

1449 Jacob, T., Wahr, J., Pfeffer, W.T., Swenson, S., 2012. Recent contributions of glaciers and ice  
1450 caps to sea level rise. *Nature* 482(7386), 514–518. doi:10.1038/nature10847.  
1451

1452 Jamieson, S.S.R., Vieli, A., Livingstone, S.J., Ó Cofaigh, C., Stokes, C., Hillenbrand, C.-D.,  
1453 Dowdeswell, J.A. 2012. Ice-stream stability on a reverse bed slope. *Nature Geoscience* 5,  
1454 799-802.  
1455

1456 Jenkins, A., Dutrieux, P., Jacobs, S.S., McPhail, S.D., Perrett, J.R., Webb, A.T., White, D.,  
1457 2010. Observations beneath Pine Island Glacier in West Antarctica and implications for its  
1458 retreat. *Nat. Geosci.* 3, 468–472, doi:10.1038/ngeo890.  
1459

1460 Jin, S., Abd-Elbaky, M., Feng, G., 2016. Accelerated ice-sheet mass loss in Antarctica from  
1461 18-year satellite laser ranging measurements. *Annals of Geophysics* 59(1), doi: 10.4401/ag-  
1462 6782.  
1463

1464 Jones, J.M., Gille, S.T., Goosse, H., Abram, N.J., Canziani, P.O., Charman, D.J., Clem, K.R.,  
1465 Crosta, X., de Lavergne, C., Eisenman, I., England, M.H., Fogt, R.L., Frankcombe, L.M.,  
1466 Marshall, G.J., Masson-Delmotte, V., Morrison, A.K., Orsi, A.J., Raphael, M.N., Renwick  
1467 J.A., Schneider, D.P., Simpkins, G.R., Steig, E.J., Stenni, B., Swingedouw, D., Vance, T.R.,  
1468 2016. Assessing recent trends in high-latitude Southern Hemisphere surface climate. *Nat.*  
1469 *Clim. Change* 6, 917–926, doi:10.1038/nclimate3103.  
1470

1471 Joughin, I., Smith, B.E., Medley, B., 2014. Marine ice sheet collapse potentially under way  
1472 for the Thwaites Glacier Basin, West Antarctica. *Science* 344, 735–738.  
1473

1474 Khan, S.A., Sasgen, I., Bevis, M., van Dam, T., Bamber, J.L., Wahr, J., Willis, M., Kjaer,  
1475 K.H., Wouters, B., Helm, V., Csatho, B., Fleming, K., Bjork, A.A., Aschwanden, A.,  
1476 Knudsen, P., Munneke, P.K., 2016. Geodetic measurements reveal similarities between post-  
1477 Last Glacial Maximum and present-day mass loss from the Greenland ice sheet. *Science*  
1478 *Advances* 2(9), doi:10.1126/sciadv.1600931.  
1479

1480 Khvorostovsky, K. S., 2012. Merging and analysis of elevation time series over Greenland  
1481 Ice Sheet from satellite radar altimetry, *IEEE Trans. Geosci. Remote Sens.* 50: 23–36,  
1482 doi:10.1109/TGRS.2011.2160071.  
1483

1484 Kimura, S., Jenkins, A., Dutrieux, P., Forryan, A., Garabato, A.C.N., Firing, Y., 2016. Ocean  
1485 mixing beneath Pine Island Glacier ice shelf, West Antarctica. *J. Geophys. Res. Oceans* 121,  
1486 8496–8510, doi:10.1002/2016JC012149.  
1487

1488 King, M.A., Bingham, R.J., Moore, P., Whitehouse, P.L., Bentley, M.J., Milne, G.A., 2012.  
1489 Lower satellite-gravimetry estimates of Antarctic sea-level contribution. *Nature* 491(7425),  
1490 586-589.  
1491

1492 Kingslake, J., Ng, F., Sole, A., 2015. Modelling channelized surface drainage of supraglacial  
1493 lakes. *J. Glaciol.* 61, 185–199.

1494

1495 Kingslake, J., Ely, J.C., Das, I., Bell, R.E., 2017. Widespread movement of meltwater onto  
1496 and across Antarctic ice shelves. *Nature* 544, 349–352, doi:10.1038/nature22049.

1497

1498 Kingslake, J., Scherer, R.P., Albrecht, T., Coenen, J., Powell, R.D., Reese, R., Stansell, N.D.,  
1499 Tulaczyk, S., Wearing, M.G., Whitehouse, P.L., 2018. Extensive retreat and re-advance of  
1500 the West Antarctic Ice Sheet during the Holocene. *Nature*, 558(7710): 430-434.

1501

1502 Kjeldsen, K.K., Korsgaard, N.J., Bjørk, A.A., Khan, S.A., Box, J.E., Funder, S., Larsen,  
1503 N.K., Bamber, J.L., Colgan, W., Van den Broeke, M., Siggaard-Andersen, M.-L., Nuth, C.,  
1504 Schomacker, A., Andresen, C.S., Willerslev, E., Kjaer, K.H., 2015. Spatial and temporal  
1505 distribution of mass loss from the Greenland Ice Sheet since AD 1900. *Nature* 528, 396-400.

1506

1507 Koenig, L.S., Ivanoff, A., Alexander, P.M., MacGregor, J.A., Fettweis, X., Panzer, B., Paden,  
1508 J. D., Forster, R.R., Das, I., McConnell, J.R., Tedesco, M., Leuschen, C., and Gogineni, P.,  
1509 2016. Annual Greenland accumulation rates (2009–2012) from airborne snow radar, *The*  
1510 *Cryosphere* 10, 1739-1752, <https://doi.org/10.5194/tc-10-1739-2016>

1511

1512 Konrad, H., Sasgen, I., Pollard, D., Klemann, V., 2015. Potential of the solid-Earth response  
1513 for limiting long-term West Antarctic Ice Sheet retreat in a warming climate. *Earth Planet.*  
1514 *Sci. Lett.* 432, 254-264.

1515

1516 Krinner, G., Langeron, C., Ménégoz, M., Agosta, C., Brutel-Vuilmet, C., 2014. Oceanic  
1517 Forcing of Antarctic Climate Change: A Study Using a Stretched-Grid Atmospheric General  
1518 Circulation Model. *J. Clim.* 27, 5786–5800, doi:10.1175/JCLI-D-13-00367.1.

1519

1520 Krinner, G., Beaumet, J., Favier, V., Déqué, M., Brutel-Vuilmet, C., 2019. Empirical run -  
1521 time bias correction for Antarctic regional climate projections with a stretched-grid AGCM.  
1522 *Journal of Advances in Modeling Earth Systems* 11, 64–82.

1523

1524 Kronenberg, M., Barandun, M., Hoelzle, M., Huss, M., Farinotti, D., Azisov, E., Usabaliev,  
1525 R., Gafurov, A., Petrakov, D., Kääh, A., 2016. Mass-balance reconstruction for Glacier No.  
1526 354, Tien Shan, from 2003 to 2014. *Annals of Glaciology* 57(71), 92–102.  
1527 doi:10.3189/2016AoG71A032.

1528

1529 Kuipers Munneke, P., Luckman, A.J., Bevan, S.L., Smeets, C.J.P.P., Gilbert, E., Van den  
1530 Broeke, M.R., Wang, W., Zender, C., Hubbard, B., Ashmore, D., Orr, A., King, J.C.,  
1531 Kulesa, B., 2018. Intense winter surface melt on an Antarctic ice shelf. *Geophys. Res. Lett.*  
1532 45 (15), 7615-7623, <https://doi.org/10.1029/2018GL077899>.

1533

1534 Larour, E., Seroussi, H., Adhikari, Z., Ivins, E., Caron, L., Morlighem, M., Schlegel, N.,  
1535 2019: Slowdown in Antarctic mass loss from solid Earth and sea-level feedbacks. *Science*  
1536 364 (6444), 10.1126/science.aav7908.

1537

1538 Leclercq, P.W., Oerlemans, J., Cogley, J. G., 2011. Estimating the glacier contribution to sea-  
1539 level rise for the period 1800–2005. *Surv. Geophys.* 32, 519–535. doi:10.1007/s10712-011-  
1540 9121-7.

1541

1542 Leclercq, P.W., Weidick, A., Paul, F., Bolch, T., Citterio, M., Oerlemans, J., 2012. Brief  
1543 communication “Historical glacier length changes in West Greenland”. *The Cryosphere* 6,  
1544 1339–1343, doi:10.5194/tc-6-1339-2012.  
1545

1546 Leclercq, P.W., Oerlemans, J., Basagic, H.J., Bushueva, I., Cook, A.J., Le Bris, R., 2014. A  
1547 data set of worldwide glacier length fluctuations. *The Cryosphere* 8, 659–672.  
1548 doi:10.5194/tc-8-659-2014.  
1549

1550 Lenaerts, J.T.M., van Den Broeke, M.R., Scarchilli, C., Agosta, C., 2012. Impact of model  
1551 resolution on simulated wind, drifting snow and surface mass balance in Terre Adélie, East  
1552 Antarctica. *J. Glaciol.* 58(211), 821–829. doi:10.3189/2012JoG12J020.  
1553

1554 Lenaerts, J.T.M., Le Bars, D., Kampenhout, L., Vizcaino, M., Enderlin, E.M., van den  
1555 Broeke, M.R., 2015. Representing Greenland ice sheet freshwater fluxes in climate models,  
1556 *Geophys. Res. Lett.* 42, 6373– 6381, doi:10.1002/2015GL064738.  
1557

1558 Lenaerts J.T.M., Vizcaino M., Fyke J., van Kampenhout L., van den Broeke M.R., 2016.  
1559 Present-day and future Antarctic ice sheet climate and surface mass balance in the  
1560 Community Earth System Model. *Climate Dynamics* 47(5-6), 1367–1381.  
1561 doi:10.1007/s00382-015-2907-4.  
1562

1563 Lenaerts, J.T.M., Lhermitte, S., Drews, R., Ligtenberg, S.R.M., Berger, S., Helm, V., Smeets,  
1564 C.J.P.P., van den Broeke, M.R., van de Berg, W.J., van Meijgaard, E., Eijkelboom, M., Elsen,  
1565 O., Pattyn, F., 2017. Meltwater produced by wind-albedo interaction stored in an East  
1566 Antarctic ice shelf. *Nature Climate Change* 7(1), 58–62. doi:10.1038/nclimate3180.  
1567

1568 Lenaerts, J., Ligtenberg, S.R.M., Medley, B., van de Berg, W.J., Konrad, H., Nicolas, J.P.,  
1569 van Wessem, J.M., Trusel, L.D., Mulvaney, R., Tuckwell, R.J., Hogg, A.E., Thomas, E.R.,  
1570 2018. Climate and surface mass balance of coastal West Antarctica resolved by regional  
1571 climate modelling. *Ann. Glaciol.* 59(76), 29–41, doi:10.1017/aog.2017.42.  
1572

1573 Levermann, A., Winckelmann, R., Nowicki, S., Fastook, J. L., Frieler, K., Greve, R., Hellmer,  
1574 H.H., Martin, M.A., Meinshausen, M., Mengel, M., Payne, A.J., Pollard, D., Sato, T.,  
1575 Timmermann, R., Wang, W.L., Bindschadler, R.A., 2014. Projecting Antarctic ice discharge  
1576 using response functions from SeaRISE ice-sheet models. *Earth System Dynamics* 5, 271-  
1577 293, <https://doi.org/10.5194/esd-5-271-2014>.  
1578

1579 Lewis, G., Osterberg, E., Hawley, R., Whitmore, B., Marshall, H.P., Box, J., 2017. Regional  
1580 Greenland accumulation variability from Operation IceBridge airborne accumulation radar.  
1581 *Cryosphere* 11(2), 773-788, doi:10.5194/tc-11-773-2017.  
1582

1583 Li, J., Zwally, H.J., 2015. Response times of ice-sheet surface heights to changes in the rate  
1584 of Antarctic firn compaction caused by accumulation and temperature variations. *J. Glaciol.*,  
1585 61, 1037–1047, doi: 10.3189/2015JoG14J082.  
1586

1587 Li, F., Yuan, L.X., Zhang, S.K., Yang, Y.D., E, D.C., Hao, W.F., 2016. Mass change of the  
1588 Antarctic ice sheet derived from ICESat laser altimetry. *Chinese Journal of Geophysics-  
1589 Chinese Edition* 59(1), 93-100.  
1590



1591 Libois, Q., Picard, G., Arnaud, L., Morin, S., Brun, E., 2014. Modeling the impact of snow  
1592 drift on the decameter-scale variability of snow properties on the Antarctic Plateau. *J.*  
1593 *Geophys. Res. Atmospheres* 119, 11,662–11,681, doi:10.1002/2014JD022361.

1594 Lipscomb, W., Fyke, J.G., Vizcaino, M., Sacks, W., Wolfe, J., Vertenstein, M., Craig, A.,  
1595 Kluzek, E., Lawrence D., 2013. Implementation and Initial Evaluation of the Glimmer  
1596 Community Ice Sheet Model in the Community Earth System Model. *Journal of Climate*  
1597 26(19), 7352-7371.

1598  
1599 Lucas-Picher, P., Wulff-Nielsen, M., Christensen, J.H., Adalgeirsdóttir, G., Mottram, R.H.,  
1600 Simonsen, S.B., 2012. Very high resolution regional climate model simulations over  
1601 Greenland: Identifying added value. *J. Geophys. Res.* 117, D02108.  
1602 doi:10.1029/2011JD016267.

1603 Luthcke, S.B., Arendt, A.A., Rowlands, D.D., Mccarthy, J.J., Larsen C.F., 2008. Recent  
1604 glacier mass changes in the Gulf of Alaska region from GRACE mascon solutions. *J.*  
1605 *Glaciol.*, 54(188), 767-777.

1606  
1607 MacAyeal, D.R., 1992. The basal stress distribution of Ice Stream E, Antarctica, inferred by  
1608 control methods. *J. Geophys. Res.* 97(B1), 595-603, doi:10.1029/91JB02454.

1609  
1610 Machguth, H., Thomsen, H.H., Weidick, A., Ahlstrøm, A.P., Abermann, J., Andersen, M.L.,  
1611 Andersen, S.B., Bjørk, A.A., Box, J.E., Braithwaite, R.J., Bøggild, C.E., Citterio, M.,  
1612 Clement, P., Colgan, W., Fausto, R.S., Gleie, K., Gubler, S., Hasholt, B., Hynek, B.,  
1613 Knudsen, N.T., Larsen, S.H., Mernild, S.H., Oerlemans, J., Oerter, H., Olesen, O.B., Smeets,  
1614 C.J.P.P., Steffen, K., Stober, M., Sugiyama, S., van As, D., van den Broeke, M.R., van de  
1615 Wal, R.S.W., 2016. Greenland surface mass-balance observations from the ice-sheet ablation  
1616 area and local glaciers. *J Glaciol.* 62(235), 861-887, doi:10.1017/jog.2016.75.

1617  
1618 Martín-Español, A., Zammit-Mangion, A., Clarke, P.J., Flament, T., Helm, V., King, M.A.,  
1619 Luthcke, S.B., Petrie, E., Remy, F., Schon, N., Wouters, B., Bamber, J.L., 2016. Spatial and  
1620 temporal Antarctic Ice Sheet mass trends, glacio-isostatic adjustment, and surface processes  
1621 from a joint inversion of satellite altimeter, gravity, and GPS data. *J. Geophys. Res.: Earth*  
1622 *Surface* 121(2), 182-200.

1623  
1624 Martín-Español, A., Bamber, J.L., Zammit-Mangion, A., 2017. Constraining the mass  
1625 balance of East Antarctica. *Geophys. Res. Lett.* 44, 4168-4175, doi:10.1002/2017GL072937.

1626  
1627 Marzeion, B., Jarosch, A. H., Hofer, M., 2012. Past and future sea-level change from the  
1628 surface mass balance of glaciers. *The Cryosphere* 6, 1295–1322, doi:10.5194/tc-6-1295-2012.

1629  
1630 Marzeion, B., Cogley, J.G., Richter, K., Parkes, D., 2014a. Attribution of global glacier mass  
1631 loss to anthropogenic and natural causes. *Science* 345(6199), 919–921.  
1632 doi:10.1126/science.1254702.

1633  
1634 Marzeion, B., Jarosch, A.H., Gregory, J.M., 2014b. Feedbacks and mechanisms affecting the  
1635 global sensitivity of glaciers to climate change. *The Cryosphere* 8, 59–71, doi: 10.5194/tc-8-  
1636 59-2014.

1637

1638 Marzeion, B., Leclercq, P.W., Cogley, J.G., Jarosch, A.H., 2015. Brief communication:  
1639 global reconstructions of glacier mass change during the 20th century are consistent. *The*  
1640 *Cryosphere* 9, 2399–2404, doi:10.5194/tc-9-2399-2015.

1641

1642 Marzeion, B., Champollion, N., Haerberli, W., Langley, K., Leclercq, P., Paul, F., 2017.  
1643 Observation-based estimates of global glacier mass change and its contribution to sea-level  
1644 change. *Surv. Geophys.* 38, 105–30, doi:10.1007/s10712-016-9394-y.

1645

1646 Marzeion, B., Kaser, G., Maussion, F., Champollion, N., 2018. Limited influence of climate  
1647 change mitigation on short-term glacier mass loss. *Nature Climate Change* 8, 305–308, doi:  
1648 10.1038/s41558-018-0093-1.

1649

1650 Massom, R.A., Pook, M.J., Comiso, J.C., Adams, N., Turner, J., Lachlan-Cope, T., Gibson,  
1651 T.T., 2004. Precipitation over the interior East Antarctic Ice Sheet related to midlatitude  
1652 blocking-high activity. *J. Clim.* 17, 1914–1928.

1653

1654 McMillan, M., Shepherd, A., Sundal, A., Briggs, K., Muir, A., Ridout, A., Hogg, A.,  
1655 Wingham, D., 2014. Increased ice losses from Antarctica detected by CryoSat-2. *Geophys.*  
1656 *Res. Lett.* 41(11), 3899-3905.

1657

1658 McMillan, M., Leeson, A., Shepherd, A., Briggs, K., Armitage, T.W.K., Hogg, A., Kuipers  
1659 Munneke, P., van den Broeke, M., Noël, B., van de Berg, W.J., Ligtenberg, S., Horwath, M.,  
1660 Groh, A., Muir, A., Gilbert, L., 2016. A high-resolution record of Greenland mass balance.  
1661 *Geophys. Res. Lett.* 43, 7002-7010.

1662

1663 Medley, B., Thomas, E.R., 2019. Increased snowfall over the Antarctic Ice Sheet mitigated  
1664 twentieth-century sea-level rise. *Nature Climate Change* 9, 34-39.

1665

1666 Medley, B., Joughin, I., Das, S.B., Steig, E.J., Conway, H., Gogineni, S., Criscitiello, A.S.,  
1667 McConnell, J.R., Smith, B.E., van den Broeke, M.R., Lenaerts, J.T.M., Bromwich, D.H.,  
1668 Nicolas J.P., 2013. Airborne-radar and ice-core observations of annual snow accumulation  
1669 over Thwaites Glacier, West Antarctica confirm the spatiotemporal variability of global and  
1670 regional atmospheric models. *Geophys. Res. Lett.* 40, 3649–3654, doi:10.1002/grl.50706.

1671

1672 Medley, B., Ligtenberg, S.R.M., Joughin, I., van den Broeke, M.R., Gogineni, S. and  
1673 Nowicki, S., 2015. Antarctic firn compaction rates from repeat-track airborne radar data: I.  
1674 *Methods. Ann. Glaciol.* 56, 155–166, doi:10.3189/2015AoG70A203.

1675

1676 Melkonian, A.K., Willis, M.J., Pritchard M.E., Stewart A.J., 2016. Recent changes in glacier  
1677 velocities and thinning at Novaya Zemlya. *Remote Sensing of the Environment* 174, 244–  
1678 257, doi:10.1016/j.rse.2015.11.001.

1679

1680 Memin, A., Flament, T., Remy, F., Llubes, M., 2014. Snow- and ice-height change in  
1681 Antarctica from satellite gravimetry and altimetry data. *Earth Planet. Sci. Lett.* 404, 344-353.

1682

1683 Moholdt, G., Nuth, C., Hagen, J.O., Kohler, J., 2010. Recent elevation changes of Svalbard  
1684 glaciers derived from ICESat laser altimetry. *Remote Sens. Environ.*, 114(11), 2756-2767,  
1685 doi:10.1016/j.rse.2010.06.008.

1686

- 1687 Montgomery, L., Koenig, L., and Alexander, P., 2018. The SUMup dataset: compiled  
1688 measurements of surface mass balance components over ice sheets and sea ice with analysis  
1689 over Greenland. *Earth Syst. Sci. Data* 10, 1959-1985.
- 1690 Moon, T., Joughin, I., Smith, B., Howat, I., 2012. 21st-century evolution of Greenland outlet  
1691 glacier velocities. *Science* 336(6081), 576-578.
- 1692
- 1693 Mordret, A., 2018. Uncovering the Iceland hot spot track beneath Greenland. *J. Geophys.*  
1694 *Res.-Solid Earth*, 123(6), 4922-4941.
- 1695
- 1696 Morlighem, M., Rignot, E., Seroussi, H., Larour, E., Ben Dhia, H., Aubry, D., 2010. Spatial  
1697 patterns of basal drag inferred using control methods from a full-Stokes and simpler models  
1698 for Pine Island Glacier, West Antarctica. *Geophys Res Lett.* 37(14), 1–6,  
1699 doi:10.1029/2010GL043853.
- 1700
- 1701 Morlighem, M., Seroussi, H., Larour, E., Rignot, E., 2013. Inversion of basal friction in  
1702 Antarctica using exact and incomplete adjoints of a higher-order model. *J. Geophys. Res.*  
1703 *Earth Surf.* 118 (3), 1746–53, doi:10.1002/jgrf.20125.
- 1704
- 1705 Mouginit, J., Rignot, E., Bjørk, A., van den Broeke, M., Millan, R., Morlighem, M., Noël,  
1706 B., Scheuchl, B., Wood, M., 2019. Forty-six years of Greenland Ice Sheet mass balance:  
1707 1972 to 2018. *PNAS* 116 (19), 9239-9244, doi.org/10.1073/pnas.1904242116.
- 1708
- 1709 Nias, I. J., Cornford, S.L., Payne, A.J., 2016. Contrasting the modelled sensitivity of the  
1710 Amundsen Sea embayment ice streams. *J. Glaciol.* 62, 552–562.
- 1711
- 1712 Nicholls, K.W., Abrahamsen, E.P., Buck, J.J.H., Dodd, P.A., Goldblatt, C., Griffiths, G.,  
1713 Heywood, K.J., Hughes, N.E., Kaletzký, A., Lane-Serff, G.F., McPhail, S.D., Millard, N.W.,  
1714 Oliver, K.I.C.; Perrett, J.; Price, M.R.; Pudsey, C.J.; Saw, K.; Stansfield, K.; Stott, M.J.;  
1715 Wadhams, P., Webb, A.T., Wilkinson, J.P., 2006. Measurements beneath an Antarctic ice  
1716 shelf using an autonomous underwater vehicle. *Geophys. Res. Lett.* 33, L08612,  
1717 doi:10.1029/2006GL025998.
- 1718
- 1719 Nick, F.M., Vieli, A., Andersen, M.L., Joughin, I., Payne, A., Edwards, T.L., Pattyn, F., Van  
1720 De Wal, R.S.W., 2013. Future sea-level rise from Greenland’s main outlet glaciers in a  
1721 warming climate. *Nature.* 497(7448), 235–238, doi:10.1038/nature12068.
- 1722
- 1723 Nicolas, J.P., Vogelmann, A.M., Scott, R.C., Wilson, A.B., Cadeddu, M.P., Bromwich, D.H.,  
1724 Verlinde, J., Lubin, D., Russell, L.M., Jenkinson, C., Powers, H.H., Ryczek, M., Stone, G.,  
1725 Wille, J.D., 2017. January 2016 extensive summer melt in West Antarctica favoured by  
1726 strong El Niño. *Nat. Commun.* 8, 15799, doi:10.1038/ncomms15799.
- 1727
- 1728 Nield, G.A., Barletta, V.R., Bordoni, A., King, M.A., Whitehouse, P.L., Clarke, P.J.,  
1729 Domack, E., Scambos, T.A., Berthier, E., 2014. Rapid bedrock uplift in the Antarctic  
1730 Peninsula explained by viscoelastic response to recent ice unloading. *Earth Planet. Sci. Lett.*  
1731 397, 32-41.
- 1732
- 1733 Nilsson, J., Gardner, A., Sørensen, L.S., Forsberg, R., 2016. Improved retrieval of land ice  
1734 topography from CryoSat-2 data and its impact for volume-change estimation of the  
1735 Greenland Ice Sheet. *The Cryosphere* 10, 2953-2969.

1736  
1737 Noël, B., van de Berg, W. J., van Wessem, J. M., van Meijgaard, E., van As, D., Lenaerts, J.  
1738 T. M., Lhermitte, S., Kuipers Munneke, P., Smeets, C. J. P. P., van Ulf, L. H., van de Wal,  
1739 R. S. W., van den Broeke, M. R., 2018a. Modelling the climate and surface mass balance of  
1740 polar ice sheets using RACMO2 – Part 1: Greenland (1958–2016). *The Cryosphere* 12, 811-  
1741 831.  
1742  
1743 Noël, B., van de Berg, W.J., Lhermitte, S., Wouters, B., Schaffer, N., and van den Broeke,  
1744 M.R., 2018b. Six decades of glacial mass loss in the Canadian Arctic Archipelago. *J.*  
1745 *Geophys. Res.: Earth Surface* 123, 1430–1449. doi: 10.1029/2017JF004304.  
1746  
1747 Nowicki, S. M. J., Payne, A., Larour, E., Seroussi, H., Goelzer, H., Lipscomb, W., Gregory,  
1748 J., Abe-Ouchi, A., Shepherd, A., 2016. Ice Sheet Model Intercomparison Project (ISMIP6)  
1749 contribution to CMIP6, *Geosci. Model Dev.* 9, 4521-4545, doi:10.5194/gmd-9-4521-2016.  
1750  
1751 Palerme, C., J. E. Kay, C. Genthon, T. L’Ecuyer, N. B. Wood, C. Claud, 2014. How much  
1752 snow falls on the Antarctic ice sheet? *The Cryosphere* 8, 1577–1587, doi:10.5194/tc-8-1577-  
1753 2014.  
1754  
1755 Palerme, C., C. Genthon, C. Claud, J. E. Kay, N. B. Wood, T. L’Ecuyer, 2017. Evaluation of  
1756 current and projected Antarctic precipitation in CMIP5 models. *Clim. Dyn.* 48, 225–239,  
1757 doi:10.1007/s00382-016-3071-1.  
1758  
1759 Parkes, D., Marzeion, B., 2018. Twentieth-century contribution to sea-level rise from  
1760 uncharted glaciers. *Nature* 563, 551-554, doi:10.1038/s41586-018-0687-9.  
1761  
1762 Pattyn, F., Schoof, C., Perichon, L, Hindmarsh, R.C.A., Bueler, E., De Fleurian, B., Durand,  
1763 G., Gagliardini, O., Gladstone, R., Goldberg, D., Gudmundsson, G.H., Huybrechts, P., Lee,  
1764 V., Nick, F.M., Payne, A.J., Pollard, D., Rybak, O., Saito, F., Vieli, A., 2012. Results of the  
1765 marine ice sheet model intercomparison project, MISMIP. *Cryosphere* 6(3), 573–88,  
1766 doi:10.5194/tc-6-573-2012.  
1767  
1768 Pattyn, F., Perichon, L., Durand, G., Favier, L., Gagliardini, O., Hindmarsh, R.C.A., Zwinger,  
1769 T., Albrecht, T., Cornford, S., Docquier, D., Furst, J.J., Goldberg, D., Gudmundsson, G.H.,  
1770 Humbert, A., Hütten, M., Huybrechts, P., Jouvét, G., Kleiner, T., Larour, E., Martin, D.,  
1771 Morlighem, M., Payne, A.J., Pollard, D., Rückamp, M., Rybak, O., Seroussi, H., Thoma, M.,  
1772 Wilkens, N., 2013. Grounding-line migration in plan-view marine ice-sheet models: Results  
1773 of the ice2sea MISMIP3d intercomparison. *J Glaciol.* 59(215), 410–22,  
1774 doi:10.3189/2013JoG12J129.  
1775  
1776 Pattyn, F., Favier, L., Sun, S., Durand, G., 2017. Progress in Numerical Modeling of  
1777 Antarctic Ice-Sheet Dynamics. *Curr. Clim. Change Rep.* 3, 174–184, doi:10.1007/s40641-  
1778 017-0069-7.  
1779  
1780 Pattyn, F., Ritz, C., Hanna, E., Asay-Davis, X., DeConto, R., Durand, G., Favier, L.,  
1781 Fettweis, X., Goelzer, H., Golledge, N.R., Munneke, P.K., Lenaerts, J.T.M., Nowicki, S.,  
1782 Payne, A.J., Robinson, A., Seroussi, H., Trusel, L.D., van den Broeke, M., 2018. The  
1783 Greenland and Antarctic ice sheets under 1.5°C global warming. *Nature Climate Change* 8,  
1784 1053-1061.  
1785

1786 Peng, P., Zhu, Y.Z., Zhong, M., Kang, K.X., Du, Z.L., Yan, H.M., 2016. Ice mass variation  
1787 in Antarctica from GRACE over 2002-2011. *Marine Geodesy* 39(2), 178-194.  
1788

1789 Pfeffer, W.T., Arendt, A.A., Bliss, A., Bolch, T., Cogley, J.G., Gardner, A.S., Hagen, J.O.,  
1790 Hock, R., Kaser, G., Kienholz, C., Miles, E.S., Moholdt, G., Mölg, N., Paul, F., Radić, V.,  
1791 Rastner, P., Raup, B.H., Rich, J., Sharp, M.J., and the Randolph Consortium, 2014. The  
1792 Randolph Glacier Inventory: a globally complete inventory of glaciers. *J. Glaciol.* 60, 537–  
1793 552, doi:10.3189/2014JoG13J176.  
1794

1795 Pollard, D., DeConto, R.M., Alley, R.B., 2015. Potential Antarctic Ice Sheet retreat driven by  
1796 hydrofracturing and ice cliff failure. *Earth Planet Sci Lett.* 412, 112–121.  
1797 doi:10.1016/j.epsl.2014.12.035  
1798

1799 Pollard, D., Gomez, N., DeConto, R.M., 2017. Variations of the Antarctic Ice Sheet in a  
1800 coupled ice sheet-Earth-sea level model: sensitivity to viscoelastic Earth properties. *J.*  
1801 *Geophys. Res.: Earth Surface* 122, 2124-2138.  
1802

1803 Previdi, M., L. M. Polvani, 2016. Anthropogenic impact on Antarctic surface mass balance,  
1804 currently masked by natural variability, to emerge by mid-century. *Environ. Res. Lett.* 11,  
1805 094001, doi:10.1088/1748-9326/11/9/094001.  
1806

1807 Radić, V., Bliss, A., Beedlow, A.C., Hock, R., Miles, E., Cogley, J.G., 2014. Regional and  
1808 global projections of twenty-first century glacier mass changes in response to climate  
1809 scenarios from global climate models. *Clim. Dynam.* 42, 37–58, doi:10.1007/s10712-013-  
1810 9262-y.  
1811

1812 Reager, J.T., Gardner, A.S., Famiglietti, J.S., Wiese, D.N., Eicker, A., Lo, M.H., 2016. A  
1813 decade of sea level rise slowed by climate-driven hydrology. *Science* 351(6274), 699–703.  
1814 doi:10.1126/science.aad8386.  
1815

1816 Reerink, T. J., van de Berg, W. J., and van de Wal, R. S. W., 2016. OBLIMAP 2.0: a fast  
1817 climate model–ice sheet model coupler including online embeddable mapping routines,  
1818 *Geosci. Model Dev.* 9, 4111-4132, doi:10.5194/gmd-9-4111-2016.  
1819

1820 Rietbroek, R., Brunnabend, S.E., Kusche, J., Schröter, J., Dahle, C., 2016. Revisiting the  
1821 contemporary sea-level budget on global and regional scales. *Proceedings of the National*  
1822 *Academy of Sciences* 113(6), 1504–1509, doi:10.1073/pnas.1519132113.  
1823

1824 Rignot, E., Mouginot, J., Morlighem, M., Seroussi, H., Scheuchl, B., 2014. Widespread, rapid  
1825 grounding line retreat of Pine Island, Thwaites, Smith, and Kohler glaciers, West Antarctica,  
1826 from 1992 to 2011. *Geophys. Res. Lett.* 41(10), 3502-3509.  
1827

1828 Rignot, E., Mouginot, J., Scheuchl, B., van den Broeke, M., van Wessem, M.J., Morlighem,  
1829 M., 2019. Four decades of Antarctic Ice Sheet mass balance from 1979-2017. *PNAS* 116 (4),  
1830 1095-1103.  
1831

1832 Ritz, C., Edwards, T.L., Durand, G, Payne, A.J., Peyaud, V., Hindmarsh, R.C.A., 2015.  
1833 Potential sea-level rise from Antarctic ice-sheet instability constrained by observations.  
1834 *Nature* 528, 115-118.  
1835

1836 Rodell, M., Houser, P. R., Jambor, U., Gottschalck, J., Mitchell, K., Meng, C.-J., Arsenault,  
1837 K., Cosgrove, B., Radakovich, J., Bosilovich, M., Entin, J.K., Walker, J.P., Lohmann, D.,  
1838 Toll, D., 2004. The Global Land Data Assimilation System. *Bull. Amer. Meteorol. Soc.* 85,  
1839 381–394, doi:10.1175/BAMS-85-3-381.

1840  
1841 Sasgen, I., Konrad, H., Ivins, E.R., Van den Broeke, M.R., Bamber, J.L., Martinec, Z.,  
1842 Klemann, V., 2013. Antarctic ice-mass balance 2003 to 2012: regional reanalysis of GRACE  
1843 satellite gravimetry measurements with improved estimate of glacial-isostatic adjustment  
1844 based on GPS uplift rates. *Cryosphere*, 7(5), 1499-1512.

1845  
1846 Sasgen, I., Martín-Español, A., Horvath, A., Klemann, V., Petrie, E.J., Wouters, B., Horvath,  
1847 M., Pail, R., Bamber, J.L., Clarke, P.J., Konrad, H., Drinkwater, M.R., 2017. Joint inversion  
1848 estimate of regional glacial isostatic adjustment in Antarctica considering a lateral varying  
1849 Earth structure (ESA STSE Project REGINA). *Geophysical Journal International*, 211(3),  
1850 1534-1553.

1851  
1852 Sasgen, I., Konrad, H., Helm, V., Grosfeld, K., 2019. High-resolution mass trends of the  
1853 Antarctic ice sheet through a spectral combination of satellite gravimetry and radar altimetry  
1854 observations. *Remote Sensing* 11, 144.

1855  
1856 Saunders, K.M., Roberts, S.J., Perren, B., Butz, C., Sime, L., Davies, S., Van Nieuwenhuyze,  
1857 W., Grosjean, M., Hodgson, D.A., 2018. Holocene dynamics of the Southern Hemisphere  
1858 westerly winds and possible links to CO<sub>2</sub> outgassing. *Nature Geoscience* 11 (9), 650-655.

1859  
1860 Scambos, T., C. Shuman, 2016. Comment on “Mass gains of the Antarctic ice sheet exceed  
1861 losses” by H.J. Zwally and others. *J. Glaciol.* 62, 599-603.

1862  
1863 Schlosser, E., Stenni, B., Valt, M., Cagnati, A., Powers, J.G., Manning, K.W., Raphael, M.,  
1864 Duda, M.G., 2016. Precipitation and synoptic regime in two extreme years 2009 and 2010 at  
1865 Dome C, Antarctica – implications for ice core interpretation. *Atmospheric Chem. Phys.* 16,  
1866 4757–4770.

1867  
1868 Schoof, C., 2007. Ice sheet grounding line dynamics: steady states, stability, and hysteresis. *J.*  
1869 *Geophys. Res. Earth Surf.* 112, F03S28.

1870  
1871 Schrama, E.J.O., Wouters, B., Rietbroek, R., 2014. A mascon approach to assess ice sheet  
1872 and glacier mass balances and their uncertainties from GRACE data. *J. Geophys. Res.: Solid*  
1873 *Earth* 119, 6048–6066, doi:10.1002/2013JB010923.

1874  
1875 Schroder, L., Horvath, M., Dietrich, R., Helm, V., van den Broeke, M.R., Ligtenberg,  
1876 S.R.M., 2019. Four decades of Antarctic surface elevation changes from multi-mission  
1877 satellite altimetry. *Cryosphere* 13, 427-449.

1878  
1879 Scott, R.C., Nicolas, J.P., Bromwich, D., Norris, J.R., Lubin, D., 2019. Meteorological  
1880 drivers and large-scale climate forcing of West Antarctic surface melt. *J. Clim.* 32, 665– 684.

1881  
1882 Seroussi, H., Nakayama, Y., Larour, E., Menemenlis, D., Morlighem, M., Rignot, E.,  
1883 Khazendar, A., 2017. Continued retreat of Thwaites Glacier, West Antarctica, controlled by  
1884 bed topography and ocean circulation. *Geophys. Res. Lett.* 44, 6191–6199.

1885

1886 Seroussi, H., Nowicki, S., Simon, E., Ouchi, A. A., Albrecht, T., Brondex, J., Cornford, S.,  
1887 Dumas, C., Gillet-Chaulet, F., Gladstone, R., Goelzer, H., Golledge, N., Gregory, J., Greve,  
1888 R., Hoffman, M., Humbert, A., Huybrechts, P., Kleiner, T., Larour, E., Leguy, G., Lipscomb,  
1889 W., Lowry, D., Mengel, M., Morlighem, M., Pattyn, F., Payne, A., Pollard, D., Price, S.,  
1890 Quiquet, A., Reerink, T., Reese, R., Rodehacke, C., Schlegel, N., Shepherd, A., Sun, S.,  
1891 Sutter, J., Breedam, J. V., Wal, R. v. d., Winkelmann, R., Zhang, T., 2019. initMIP-  
1892 Antarctica: An ice sheet model initialization experiment of ISMIP6. *The Cryosphere* 13,  
1893 1441-1471.

1894  
1895 Shepherd, A., Ivins, E.R., Barletta, V.R., Bentley, M.J., Bettadpur, S., Briggs, K.H.,  
1896 Bromwich, D.H., Forsberg, R., Galin, N., Horwath, M., Jacobs, S., Joughin, I., King, M.A.,  
1897 Lenaerts, J.T.M., Li, J., Ligtenberg, S.R.M., Luckman, A., Luthcke, S.B., McMillan, M.,  
1898 Meister, R., Milne, G., Mouginot, J., Muir, A., Nicolas, J.P., Paden, J., Payne, A.J., Pritchard,  
1899 H., Rignot, E., Rott, H., Sørensen, L.S., Scambos, T.A., Scheuchl, B., Schrama, E.J.O.,  
1900 Smith, B., Sundal, A.V., van Angelen, J.H., van de Berg, W.J., van den Broeke, M.R.,  
1901 Vaughan, D.G., Velicogna, I., Wahr, J., Whitehouse, P.L., Wingham, D.J., Yi, D., Young, D.  
1902 & Zwally, H.J., 2012. A Reconciled Estimate of Ice-Sheet Mass Balance. *Science* 338  
1903 (6111), 1183-1189.

1904  
1905 Shepherd, A., Ivins, E., Rignot, E., Smith, B., van den Broeke, M., Velicogna, I.,  
1906 Whitehouse, P., Briggs, K., Joughin, I., Krinner, G., Nowicki, S., Payne, T., Scambos, T.,  
1907 Schlegel, N., Geruo, A., Agosta, C., Ahlstrom, A., Babonis, G., Barletta, V., Blazquez, A.,  
1908 Bonin, J., Csatho, B., Cullather, R., Felikson, D., Fettweis, X., Forsberg, R., Gallee, H.,  
1909 Gardner, A., Gilbert, L., Groh, A., Gunter, B., Hanna, E., Harig, C., Helm, V., Horwath, A.,  
1910 Horwath, M., Khan, S., Kjeldsen, K.K., Konrad, H., Langen, P., Lecavalier, B., Loomis, B.,  
1911 Luthcke, S., McMillan, M., Melini, D., Mernild, S., Mohajerani, Y., Moore, P., Mouginot, J.,  
1912 Moyano, G., Muir, A., Nagler, T., Nield, G., Nilsson, J., Noël, B., Ootaka, I., Pattle, M.E.,  
1913 Peltier, W.R., Pie, N., Rietbroek, R., Rott, H., Sandberg-Sorensen, L., Sasgen, I., Save, H.,  
1914 Scheuchl, B., Schrama, E., Schroder, L., Seo, K.W., Simonsen, S., Slater, T., Spada, G.,  
1915 Sutterley, T., Talpe, M., Tarasov, L., van de Berg, W.J., van der Wal, W., van Wessem, M.,  
1916 Vishwakarma, B.D., Wiese, D., Wouters, B., The IMBIE team, 2018. Mass balance of the  
1917 Antarctic Ice Sheet from 1992 to 2017. *Nature* 558, 219-222.

1918  
1919 Siegert, M.J., 2003. Glacial-interglacial variations in central East Antarctic ice accumulation  
1920 rates. *Quaternary Science Reviews* 22, 741-750.

1921  
1922 Slangen, A.B.A., van de Wal, R.S.W., 2011. An assessment of uncertainties in using volume-  
1923 area modelling for computing the twenty-first century glacier contribution to sea-level  
1924 change. *Cryosphere* 5, 673–686, doi:10.5194/tc-5-673-2011.

1925  
1926 Slangen, A.B.A., Adloff, F., Jevrejeva, S., Leclercq, P.W., Marzeion, B., Wada, Y.,  
1927 Winkelmann, R., 2017. A review of recent updates of sea level projections at global and  
1928 regional scales. *Surv. Geophys.* 38(1), 385–406, doi:10.1007/s10712-016-9374-2.

1929  
1930 Smeets, C.J.P.P., Kuipers Munneke, P., van As, D., van den Broeke, M.R., Boot, W.,  
1931 Oerlemans, J., Snellen, H., Reijmer, C.H., van de Wal, R.S.W., 2018. The K-transect in west  
1932 Greenland: Automatic weather station data (1993-2016). *Arctic, Antarctic and Alpine*  
1933 *Research* 50 (1), e1420954, doi: 10.1080/15230430.2017.1420954

1934

1935 Souverijns, N., Gossart, A., Gorodetskaya, I.V., Lhermitte, S., Mangold, A., Laffineur, Q.,  
1936 Delcloc, A., van Lipzig, N.P.M., 2018. How does the ice sheet surface mass balance relate to  
1937 snowfall? Insights from a ground-based precipitation radar in East Antarctica. *The*  
1938 *Cryosphere* 12, 1987–2003, doi:<https://doi.org/10.5194/tc-12-1987-2018>.  
1939  
1940 Steger, C.R., Reijmer, C.H., van den Broeke, M.R., Wever, N., Forster, R.R., Koenig, L.S.,  
1941 Kuipers Munneke, P., Lehning, M., Lhermitte, S., Ligtenberg, S.R.M, Miège, C., Noël,  
1942 B.P.Y., 2017. Firn meltwater retention on the Greenland ice sheet: A model comparison.  
1943 *Front Earth Sci.* 5:3, doi:10.3389/feart.2017.00003.  
1944  
1945 Stenni, B., Scarchilli, C., Masson-Delmotte, V., Schlosser, E., Ciardini, V., Dreossi, G.,  
1946 Grigioni, P., Bonazza, M., Cagnati, A., Karlicek, D., Risi, C., Udisti, R., and Valt, M., 2016.  
1947 Three-year monitoring of stable isotopes of precipitation at Concordia Station, East  
1948 Antarctica. *Cryosphere* 10, 2415-2428, <https://doi.org/10.5194/tc-10-2415-2016>.  
1949  
1950 Stewart, C.L., Christoffersen, P., Nicholls, K.W., Williams, M.J.M., Dowdeswell, J.A., 2019.  
1951 Basal melting of Ross Ice Shelf from solar heat adsorption in an ice-front polynya. *Nature*  
1952 *Geoscience* 12, 435-440, 10.1038/s41561-019-0356-0.  
1953  
1954 Stibal, M., Box, J.E., Cameron, K.A., Langen, P.L., Yallop, M.L., Mottram, R.H., Khan,  
1955 A.L., Molotch, N.P., Christmas, N.A.M., Quaglia, F.C., Remias, D., Smeets, C.J.P.P., van den  
1956 Broeke, M.R., Ryan, J.C., Hubbard, A., Tranter, M., van As, D., Ahlstrom, A., 2017. Algae  
1957 Drive Enhanced Darkening of Bare Ice on the Greenland Ice Sheet. *Geophys Res Lett.* 44,  
1958 11463-11471, doi:10.1002/2017GL075958.  
1959  
1960 Straneo, F., Heimbach, P., Sergienko, O., Hamilton, G., Catania, G., Griffies, S., Hallberg,  
1961 R., Jenkins, A., Joughin, I., Motyka, R., Pfeffer, W.T., Price, S.F., Rignot, E., Scambos, T.,  
1962 Truffer, M., Vieli, A., 2013. Challenges to Understanding the Dynamic Response of  
1963 Greenland's Marine Terminating Glaciers to Oceanic and Atmospheric Forcing. *Bull. Amer.*  
1964 *Meteorol. Soc.* 94, 1131-1144.  
1965  
1966 Sutanudjaja, E.H., van Beek, R., Wanders, N., Wada, Y., Bosmans, J.H.C., Drost, N., van der  
1967 Ent, R. J., de Graaf, I.E.M., Hoch, J.M., de Jong, K., Karszenberg, D., López López, P.,  
1968 Peßenteiner, S., Schmitz, O., Straatsma, M.W., Vannamettee, E., Wisser, D., and Bierkens, M.  
1969 F. P., 2018. PCR-GLOBWB 2: a 5 arcmin global hydrological and water resources model.  
1970 *Geosci. Model Dev.*, 11, 2429-2453, <https://doi.org/10.5194/gmd-11-2429-2018>  
1971  
1972 Talpe, M.J., Nerem, R.S., Forootan, E., Schmidt, M., Lemoine, F.G., Enderlin, E.M.,  
1973 Landerer, F.W., 2017. Ice mass change in Greenland and Antarctica between 1993 and 2013  
1974 from satellite gravity measurements. *Journal of Geodesy* 91, 1283–1298.  
1975  
1976 Tedesco, M., Mote, T., Fettweis, X., Hanna, E., Jeyaratnam, J., Booth, J.F., Datta, R., Briggs,  
1977 K., 2016. Arctic cut-off high drives the poleward shift of a new Greenland melting record.  
1978 *Nature Commun.* 7: 11723.  
1979  
1980 Tedesco, M., Box, J.E., Cappelen, J., Fausto, R.S., Fettweis, X., Andersen, J.K., Mote, T.,  
1981 Smeets, C.J.P.P., van As, D., van de Wal, R.S.W., 2018. Greenland Ice Sheet. Arctic Report  
1982 Card: Update for 2018. NOAA, [https://arctic.noaa.gov/Report-Card/Report-Card-](https://arctic.noaa.gov/Report-Card/Report-Card-2018/ArtMID/7878/ArticleID/781/Greenland-Ice-Sheet)  
1983 [2018/ArtMID/7878/ArticleID/781/Greenland-Ice-Sheet](https://arctic.noaa.gov/Report-Card/Report-Card-2018/ArtMID/7878/ArticleID/781/Greenland-Ice-Sheet).  
1984



1985 Thomas, E.R., van Wessem, J.M., Roberts, J., Isaksson, E., Schlosser, E., Fudge, T.J.,  
1986 Vallelonga, P., Medley, B., Lenaerts, J., Bertler, N., van den Broeke, M.R., Dixon, D.A.,  
1987 Frezzotti, M., Stenni, B., Curran, M., Ekaykin, A.A., 2017. Regional Antarctic snow  
1988 accumulation over the past 1000 years. *Clim. Past*, 13, 1491-1513, [https://doi.org/10.5194/cp-](https://doi.org/10.5194/cp-13-1491-2017)  
1989 13-1491-2017.  
1990  
1991 Thomas R.H., Bentley, C.R., 1978. A model for Holocene retreat of the West Antarctic Ice  
1992 Sheet. *Quat. Res.* 10(2), 150–170, doi:10.1016/0033-5894(78)90098-4.  
1993  
1994 Thompson, D.W.J., Solomon, S., Kushner, P.J., England, M.H., Grise, K.M., Karoly, D.J.,  
1995 2011. Signatures of the Antarctic ozone hole in Southern Hemisphere surface climate change.  
1996 *Nat. Geosci.* 4, 741–749, doi:10.1038/ngeo1296.  
1997  
1998 Trusel, L.D., Das, S.B., Osman, M.B., Evans, M.J., Smith, B.E., Fettweis, X., McConnell,  
1999 J.R., Noël, B.P.Y., van den Broeke, M.R., 2018. Nonlinear rise in Greenland runoff in  
2000 response to post-industrial Arctic warming. *Nature* 564(7734), 104-108.  
2001  
2002 Turner, J., J. S. Hosking, T. J. Bracegirdle, T. Phillips, G. J. Marshall, 2016. Variability and  
2003 trends in the Southern Hemisphere high latitude, quasi-stationary planetary waves. *Int. J.*  
2004 *Climatol.* 37, 2325–2336, doi:10.1002/joc.4848.  
2005  
2006 Turner, J., Phillips, T., Thamban, M., Rahaman, W., Marshall, G.J., Wille, J.D., Favier, V.,  
2007 Winton, V.H.L., Thomas, E., Wang, Z., van den Broeke, M., Hosking, J.S., Lachlan-Cope,  
2008 T., 2019. The dominant role of extreme precipitation events in Antarctic snowfall variability.  
2009 *Geophys. Res. Lett.* 46 (6), 3502-3511, <https://doi.org/10.1029/2018GL081517>  
2010  
2011 Van den Broeke, M.R., Reijmer, C.H., Van de Wal, R.S.W., 2004. A study of the surface  
2012 mass balance in Dronning Maud Land, Antarctica, using automatic weather station S. J.  
2013 *Glaciol.* 50(171), 565-582.  
2014  
2015 van Den Broeke, M.R., Smeets, C.J.P.P., Van De Wal, R.S.W., 2011. The seasonal cycle and  
2016 interannual variability of surface energy balance and melt in the ablation zone of the west  
2017 Greenland ice sheet. *Cryosphere* 5(2), 377-390, doi:10.5194/tc-5-377-2011.  
2018  
2019 van Den Broeke, M.R., Enderlin, E.M., Howat, I.M., Kuipers Munneke, P., Noël, B.P.Y., van  
2020 de Berg, W.J., van Meijgaard, E., Wouters, B., 2016. On the recent contribution of the  
2021 Greenland ice sheet to sea level change. *Cryosphere*. 10(5). doi:10.5194/tc-10-1933-2016.  
2022  
2023 van den Broeke, M., Box, J., Fettweis, X., Hanna, E., Noel, B., Tedesco, M., van As, D., Van  
2024 de Berg, W., van Kampenhout, L., 2017. Greenland ice sheet surface mass loss: recent  
2025 developments in observation and modeling. *Curr. Clim. Change Rep.* 3, 345-356.  
2026  
2027 Van Kampenhout, L., Lenaerts, J.T.M., Lipscomb, W.H., Sacks, W.J., Lawrence, D.M.,  
2028 Slater, A.G., van den Broeke, M.R., 2017. Improving the representation of polar snow and  
2029 firn in the Community Earth System Model. *J. Adv. Model Earth Sy.* 9(7), 2583-2600.  
2030  
2031 Van Tricht, K., Lhermitte, S., Lenaerts, J.T.M., Gorodetskaya, I.V., L'Ecuyer, T.S., Noël, B.,  
2032 van den Broeke, M.R., Turner, D.D., van Lipzig, N.P.M., 2016. Clouds enhance Greenland  
2033 ice sheet meltwater runoff. *Nat Commun.* 7: 10266, doi:10.1038/ncomms10266.  
2034

2035 Van Wessem, J.M., van de Berg, W.J., Noël, B.P.Y., van Meijgaard, E., Amory, C.,  
2036 Birnbaum, G., Jakobs, C.L., Krüger, K., Lenaerts, J.T. M., Lhermitte, S., Ligtenberg, S.R.M.,  
2037 Medley, B., Reijmer, C. H., van Tricht, K., Trusel, L.D., van Uft, L.H., Wouters, B., Wuite,  
2038 J., and Van den Broeke, M.R., 2018. Modelling the climate and surface mass balance of polar  
2039 ice sheets using RACMO2 – Part 2: Antarctica (1979–2016). *Cryosphere* 12, 1479-1498.  
2040

2041 Van Wessem, J.M., Reijmer, C.H., Van De Berg, W.J., van den Broeke, M.R., Cook, A., van  
2042 Uft, L.H., van Meijgaard, E., 2015. Temperature and wind climate of the Antarctic Peninsula  
2043 as simulated by a high-resolution Regional Atmospheric Climate Model. *J Clim.* 28(18),  
2044 7306-7326, doi:10.1175/JCLI-D-15-0060.1.  
2045

2046 Vaughan, D.G., Comiso, J.C., Allison, I., Carrasco, J., Kaser, G., Kwok, R., Mote, P.,  
2047 Murray, T., Paul, F., Ren, J., Rignot, E., Solomina, O., Steffen, K., and Zhang, T., 2013.  
2048 Observations: Cryosphere, in: Stocker, T.F., Qin, D., Plattner, G.-K., Tignor, M., Allen, S.K.,  
2049 Boschung, J., Nauels, A., Xia, Y., Bex, V., Midgley, P.M. (Eds.), 2013. *Climate Change*  
2050 *2013: The Physical Science Basis. Contribution of Working Group I to the Fifth Assessment*  
2051 *Report of the Intergovernmental Panel on Climate Change.* Cambridge University Press,  
2052 Cambridge, United Kingdom and New York, NY, USA, pp. 317–382.  
2053

2054 Velicogna, I., Sutterley, T.C., van den Broeke, M.R., 2014. Regional acceleration in ice mass  
2055 loss from Greenland and Antarctica using GRACE time-variable gravity data. *Geophys. Res.*  
2056 *Lett.* 41(22), 8130-8137.  
2057

2058 Verfaillie, D., Fily, M., Le Meur, E., Magand, O., Jourdain, B., Arnaud, L., Favier, V., 2012.  
2059 Snow accumulation variability derived from radar and firn core data along a 600 km transect  
2060 in Adelie Land, East Antarctic plateau. *Cryosphere* 6, 1345–1358, doi:10.5194/tc-6-1345-  
2061 2012.  
2062

2063 Vignon, E., Genthon, C., Barral, H., Amory, C., Picard, G., Gallée, H., Casasanta, G.,  
2064 Argentini, S., 2017. Momentum- and Heat-Flux Parametrization at Dome C, Antarctica: A  
2065 Sensitivity Study. *Bound.-Layer Meteorol.* 162, 341–367, doi:10.1007/s10546-016-0192-3.  
2066

2067 Vizcaino, M., 2014. Ice sheets as interactive components of Earth System Models: progress  
2068 and challenges. *Wires Clim Change* 5(4), 557-568.  
2069

2070 Vizcaino, M., Mikolajewicz, U., Groger, M., Maier-Reimer, E., Schurgers, G., Winguth,  
2071 A.M.E., 2008. Long-term ice sheet-climate interactions under anthropogenic greenhouse  
2072 forcing simulated with a complex Earth System Model. *Clim. Dynam.* 31(6), 665-690.  
2073

2074 Vizcaino, M., Mikolajewicz, U., Jungclaus, J., Schurgers, G., 2010. Climate modification by  
2075 future ice sheet changes and consequences for ice sheet mass balance. *Clim. Dynam.* 34(2-3),  
2076 301-324.  
2077

2078 Vizcaino, M., Lipscomb, W.H., Sacks, W.J., van den Broeke, M., 2014. Greenland Surface  
2079 Mass Balance as Simulated by the Community Earth System Model. Part II: Twenty-First-  
2080 Century Changes. *J. Clim.* 27(1), 215-226.  
2081

2082 Vizcaino, M., Mikolajewicz, U., Ziemen, F., Rodehacke, C.B., Greve, R., van den Broeke,  
2083 M.R., 2015. Coupled simulations of Greenland Ice Sheet and climate change up to A.D.  
2084 2300. *Geophys. Res. Lett.* 42(10), 3927-3935.

2085  
2086 Wahr, J., Wingham, D., Bentley, C., 2000. A method of combining ICESat and GRACE  
2087 satellite data to constrain Antarctic mass balance. *J. Geophys. Res. Solid Earth* B7, 16279-  
2088 16294.

2089 Waibel, M.S., Hulbe, C.L., Jackson, C.S. & Martin, D.F., 2018. Rate of mass loss across the  
2090 instability threshold for Thwaites Glacier determines rate of mass loss for entire basin.  
2091 *Geophys. Res. Lett.* 45, 809–816.  
2092

2093 Weertman, J., 1974. Stability of the junction of an ice sheet and an ice shelf. *J Glaciol.*  
2094 13(67), 3–11, doi:10.3198/1974JoG13-67-3-11.  
2095

2096 Whitehouse, P.L., Bentley, M.J., Milne, G.A., King, M.A., Thomas, I.D., 2012. A new glacial  
2097 isostatic adjustment model for Antarctica: calibrated and tested using observations of relative  
2098 sea-level change and present-day uplift rates. *Geophysical Journal International*, 190(3),  
2099 1464-1482.  
2100

2101 Whitehouse, P.L., Gomez, N., King, M.A., Wiens, D.A., 2019. Solid Earth processes and the  
2102 evolution of the Antarctic Ice Sheet. *Nature Communications* 10:503.  
2103

2104 Wille, J.D., Favier, V., Dufour, A., Gorodetskaya, I.V., Turner, J., Agosta, C., Codron, F.,  
2105 West Antarctic surface melt triggered by atmospheric rivers. *Nature Geoscience*, in press.  
2106

2107 Williams, S.D.P., Moore, P., King, M.A., Whitehouse, P.L., 2014. Revisiting GRACE  
2108 Antarctic ice mass trends and accelerations considering autocorrelation. *Earth Planet. Sci.*  
2109 *Lett.* 385, 12-21.  
2110

2111 Wingham, D.J., Ridout, A.L., Scharroo, R., Arthern, R.J., Shum, C.K., 1998. Antarctic  
2112 elevation change 1992 to 1996. *Science* 282, 456–458.  
2113

2114 Wouters, B., Bamber, J.L., van den Broeke, M.R., Lenaerts, J.T.M., Sasgen, I., 2013. Limits  
2115 in detecting acceleration of ice sheet mass loss due to climate variability. *Nature Geosci.* 6(8),  
2116 613-616.  
2117

2118 Wouters, B., Gardner, A.S., Moholdt, G., 2019. Global glacier mass loss during the GRACE  
2119 satellite mission (2002-2016). *Front. Earth Sci.*, doi.org/10.3389/feart.2019.00096.  
2120

2121 Yi, D., Zwally, H.J., Cornejo, H.G., Barbieri, K.A., DiMarzio, J.P., 2011. Sensitivity of  
2122 elevations observed by satellite radar altimeter over ice sheets to variations in backscatter  
2123 power and derived corrections. *CryoSat Validation Workshop*, 1–3 February 2011, Frascati,  
2124 Italy. European Space Research Institute, European Space Agency, Frascati, ESA SP-693  
2125

2126 Yi, S., Sun, W., Heki, K., Qian, A., 2015. An increase in the rate of global mean sea level  
2127 since 2010. *Geophys. Res. Lett.* 42, 3998–4006, doi:10.1002/2015GL063902.  
2128

2129 Zammit-Mangion, A., Rougier, J., Schon, N., Lindgren, F., Bamber, J., 2015. Multivariate  
2130 spatio-temporal modelling for assessing Antarctica's present-day contribution to sea-level  
2131 rise. *Environmetrics* 26(3), 159-177.  
2132

2133 Zekollari, H., Huss, M., Farinotti, D., 2019. Modelling the future evolution of glaciers in the  
2134 European Alps under the EURO-CORDEX RCM ensemble. *Cryosphere* 13, 1125–1146,  
2135 doi:10.5194/tc-13-1125-2019.  
2136

2137 Zemp, M., Frey H., Gärtner-Roer, I., Nussbaumer, S.U., Hoelzle, M., Paul, F., Haeberli, W.,  
2138 Denzinger, F., Ahlstrøm, A.P., Anderson, B., Bajracharya, S., Baroni, C., Braun, L.N.,  
2139 Cáceres, B.E., Casassa, G., Cobos, G., Dávila, L.R., Delgado Granados, H., Demuth, M.N.,  
2140 Espizua, L., Fischer, A., Fujita, K., Gadek, B., Ghazanfar, A., Hagen, J.O., Holmlund, P.,  
2141 Karimi, N., Li, Z., Pelto, M., Pitte, P., Popovnin, V.V., Portocarrero, C.A., Prinz, R.,  
2142 Sangewar, C.V., Severskiy, I., Sigurdsson, O., Soruco, A., Usubaliev, R., Vincent, C., 2015.  
2143 Historically unprecedented global glacier decline in the early 21st century. *J. Glaciol.* 61,  
2144 228, 745–762, doi:10.3189/2015JoG15J017.  
2145

2146 Zemp, M., Huss, M., Thibert, E., Eckert, N., McNabb, R., Huber, J., Barandun, M.,  
2147 Machguth, H., Nussbaumer, S.U., Gärtner-Roer, I., Thomson, L., Paul, F., Maussion, F.,  
2148 Kutuzov, S., Cogley, J.G., 2019. Global glacier mass changes and their contributions to sea-  
2149 level rise from 1961 to 2016. *Nature* 568, 382–386, doi:10.1038/s41586-019-1071-0.  
2150

2151 Zhang, B., Liu, L., Khan, S.A., van Dam, T., Bjørk, A.A., Peings, Y., Zhang, E., Bevis, M.,  
2152 Yao, Y., Noël, B., 2019. Geodetic and model data reveal different spatio-temporal patterns of  
2153 transient mass changes over Greenland from 2007 to 2017. *Earth Planet. Sci. Lett.* 515, 154-  
2154 163.  
2155

2156 Zhang, B.J., Wang, Z.M., Li, F., An, J.C., Yang, Y.D., Liu, J.B., 2017. Estimation of present-  
2157 day glacial isostatic adjustment, ice mass change and elastic vertical crustal deformation over  
2158 the Antarctic ice sheet. *J. Glaciol.* 63(240), 703-715.  
2159

2160 Zwally, H.J., M.B. Giovinetto, J. Li, H.G. Cornejo, M.A. Beckley, A.C. Brenner, J.L. Saba,  
2161 D. Yi, 2005. Mass changes of the Greenland and Antarctic ice sheets and shelves and  
2162 contributions to sea-level rise: 1992–2002. *J. Glaciol.* 51, 509–527, doi: 10.3189/  
2163 172756505781829007.  
2164

2165 Zwally, H.J., Li, J., Robbins, J.W., Saba, J.L., Yi, D., Brenner, A.C., 2015. Mass gains of the  
2166 Antarctic ice sheet exceed losses. *J. Glaciol.* 61, 1019-1036.  
2167

2168 Zwally, H.J., J. Li, J.W. Robbins. J.L. Saba, D. Yi, A.C. Brenner, 2016. Response to  
2169 Comment by T. Scambos and C. Shuman (2016) on ‘Mass gains of the Antarctic ice sheet  
2170 exceed losses’ by H. J. Zwally and others (2015). *J. Glaciol.*, available on CJO 2016  
2171 doi:10.1017/jog.2016.91.  
2172  
2173  
2174  
2175  
2176  
2177  
2178  
2179  
2180  
2181  
2182

2183 **Table 1.** Probabilistic projections (5th, 25th, 50th, 75th and 95th percentiles) of Antarctic  
 2184 sea-level contribution at 2300 (in metres) under RCP8.5. Colour legend: **L14**: Simulations by  
 2185 Levermann et al. (2014), **G15**: Simulations by Golledge et al. (2015), **DP16**: Simulations by  
 2186 DeConto and Pollard (2016), **DP16BC**: Bias-corrected simulations by DeConto and Pollard  
 2187 (2016), **B19S**: Simulations with Schoof’s parameterisation by Bulthuis et al. (2019), **B19T**:  
 2188 Simulations with Tsai’s parameterisation by Bulthuis et al. (2019), **E19MICI**: Simulations  
 2189 with MICI by Edwards et al. (2019).  
 2190

	5%	25%	50%	75%	95%
<b>L14</b>	0.30	0.64	1.06	1.75	3.54
<b>G15</b>	1.61	2.07	2.28	2.50	2.96
<b>DP16</b>	6.86	7.35	9.05	11.09	11.25
<b>DP16BC</b>	6.94	7.37	9.05	11.08	11.27
<b>B19S</b>	0.27	0.61	1.04	1.47	1.81
<b>B19T</b>	0.59	1.16	1.85	2.55	3.12
<b>E19MICI</b>	7.08	8.28	8.90	9.51	10.71

2191  
 2192  
 2193  
 2194  
 2195  
 2196  
 2197  
 2198  
 2199  
 2200  
 2201  
 2202  
 2203  
 2204  
 2205  
 2206  
 2207  
 2208  
 2209  
 2210  
 2211  
 2212  
 2213  
 2214  
 2215  
 2216  
 2217

2218 **Table 2.** Pentad mass balance rates for all glaciers and ice caps, excluding the peripheral  
 2219 glaciers of Greenland and Antarctica. Modified from Bamber et al. (2018). The contributions  
 2220 from the peripheral glaciers are here excluded because in Bamber et al. (2018) the peripheral  
 2221 glacier contributions are included in those of the corresponding ice sheet because most data  
 2222 sources (many of them from GRACE) do not separate the peripheral glacier contributions.  
 2223 For reference, the mass-change rates during 2003-2009, according to Gardner et al. (2013),  
 2224 were of  $-38 \pm 7$  Gt yr<sup>-1</sup> ( $0.10 \pm 0.02$  mm SLE yr<sup>-1</sup>) for the Greenland peripheral glaciers, and of  
 2225  $-6 \pm 10$  Gt yr<sup>-1</sup> ( $0.02 \pm 0.03$  mm SLE yr<sup>-1</sup>) for the Antarctic peripheral glaciers. According to  
 2226 Zemp et al. (2019), the contributions during 2002-2016 were of  $-51 \pm 17$  Gt yr<sup>-1</sup> ( $0.14 \pm 0.05$   
 2227 mm SLE yr<sup>-1</sup>) for Greenland periphery and  $-14 \pm 108$  Gt yr<sup>-1</sup> ( $0.00 \pm 0.30$  mm SLE yr<sup>-1</sup>) for the  
 2228 Antarctic periphery.  
 2229

Pentad	1992-1996	1997-2001	2002-2006	2007-2011	2012-2016
Gt yr <sup>-1</sup>	$-117 \pm 44$	$-149 \pm 44$	$-173 \pm 33$	$-197 \pm 30$	$-227 \pm 31$
mm SLE yr <sup>-1</sup>	$0.32 \pm 0.12$	$0.42 \pm 0.12$	$0.48 \pm 0.09$	$0.55 \pm 0.08$	$0.63 \pm 0.08$

2230  
 2231  
 2232  
 2233  
 2234  
 2235  
 2236  
 2237  
 2238  
 2239  
 2240  
 2241  
 2242  
 2243  
 2244  
 2245  
 2246  
 2247  
 2248  
 2249  
 2250  
 2251  
 2252  
 2253  
 2254  
 2255  
 2256  
 2257  
 2258  
 2259  
 2260  
 2261  
 2262  
 2263

2264 **Table 3.** Estimated contributions to sea-level rise by glaciers and by ice sheets over different  
 2265 recent periods. The data sources are indicated. The percentages indicate the relative  
 2266 contributions of the glaciers and of the ice sheets with respect to the total contribution from  
 2267 the landed ice masses.  
 2268

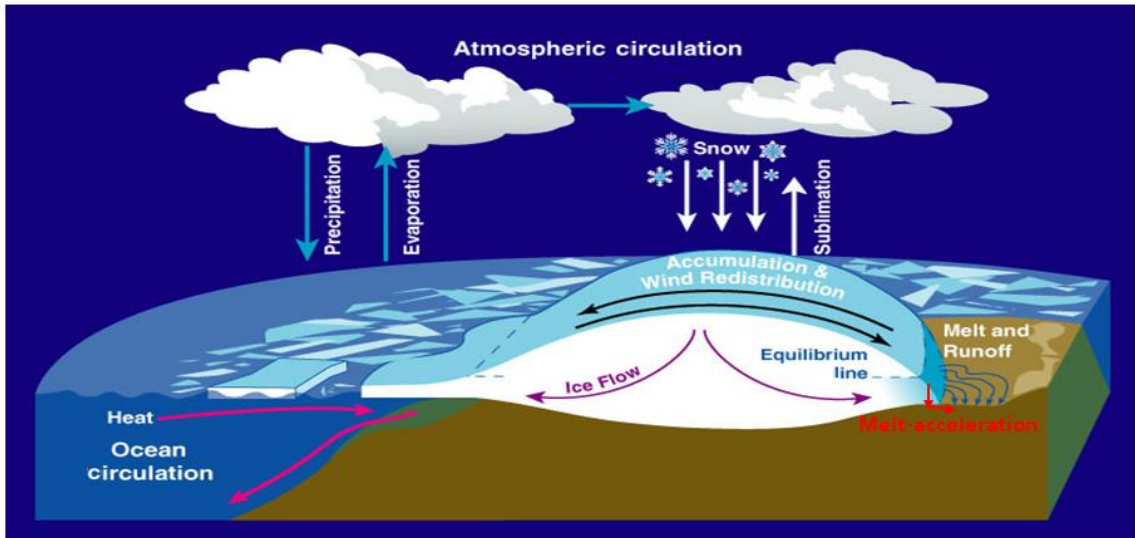
	1993-2010 Church et al. (2013) (IPCC AR5)		2003/05-2009/10 Gardner et al. (2013) Shepherd et al. (2012)		2012-2016 modified from Bamber et al. (2018)	
	mm SLE yr <sup>-1</sup>	%	mm SLE yr <sup>-1</sup>	%	mm SLE yr <sup>-1</sup>	%
Glaciers	0.86	59	0.72	43	0.73 <sup>a</sup>	40 <sup>a,b</sup>
Ice sheets	0.60	41	0.95	57	1.10 <sup>a,b</sup>	60 <sup>a,b</sup>

2269  
 2270 <sup>a</sup> Including the contributions from the peripheral glaciers of Greenland and Antarctica.  
 2271 <sup>b</sup> If the more recent estimate for the Antarctic Ice Sheet by Shepherd et al. (2018) for 2012-  
 2272 2017 were taken instead of that by Bamber et al. (2018) for 2012-2016, the contribution from  
 2273 the ice sheets would increase to 1.29 mm SLE yr<sup>-1</sup> and the relative contributions would be of  
 2274 36% for glaciers and 64% for ice sheets.  
 2275  
 2276  
 2277  
 2278  
 2279  
 2280  
 2281  
 2282  
 2283  
 2284  
 2285  
 2286  
 2287  
 2288  
 2289  
 2290  
 2291  
 2292  
 2293  
 2294  
 2295  
 2296  
 2297  
 2298  
 2299  
 2300  
 2301  
 2302  
 2303  
 2304  
 2305  
 2306  
 2307

2308 **Figures**

2309

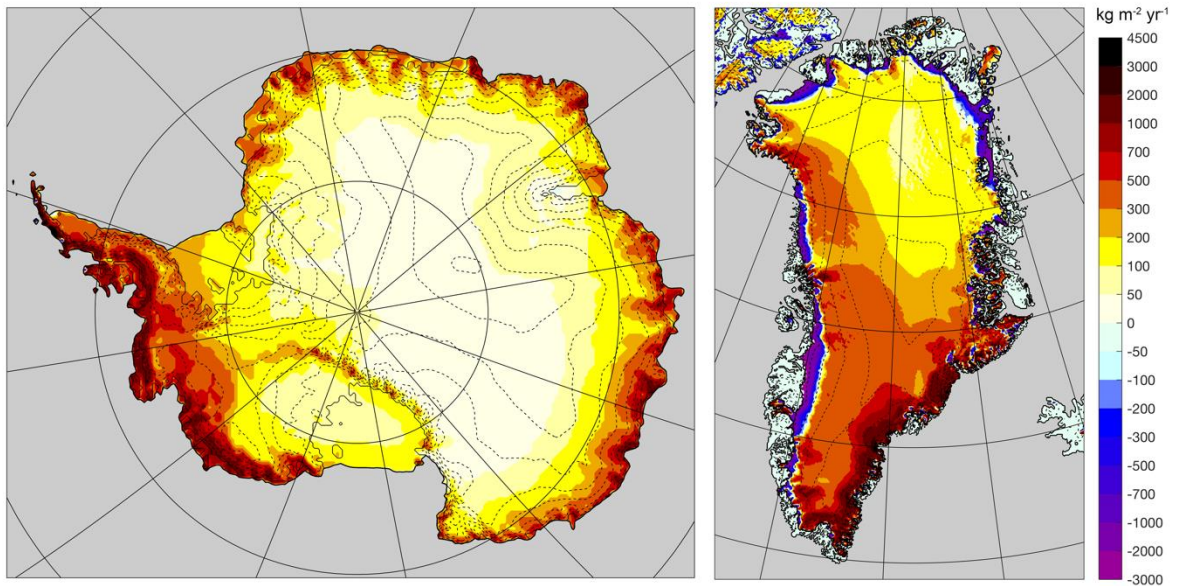
2310 **Figure 1.** The main processes affecting the mass balance and dynamics of ice sheets. Mass  
2311 input from snowfall is balanced by losses from surface meltwater runoff, sublimation and  
2312 dynamical mass losses (solid ice discharge across the grounding line). Surface melting is  
2313 highly significant for Greenland but for Antarctic grounded ice is very small and subject to  
2314 refreezing. Interaction with the ocean occurs at the undersides of the floating ice shelves and  
2315 glacier tongues, and consequent changes in thickness affect the rate of ice flow from the  
2316 grounded ice. Reproduced from Zwally et al. (2015) with the permission of Jay Zwally.



2317  
2318  
2319  
2320  
2321  
2322  
2323  
2324  
2325  
2326  
2327  
2328  
2329  
2330  
2331  
2332  
2333  
2334

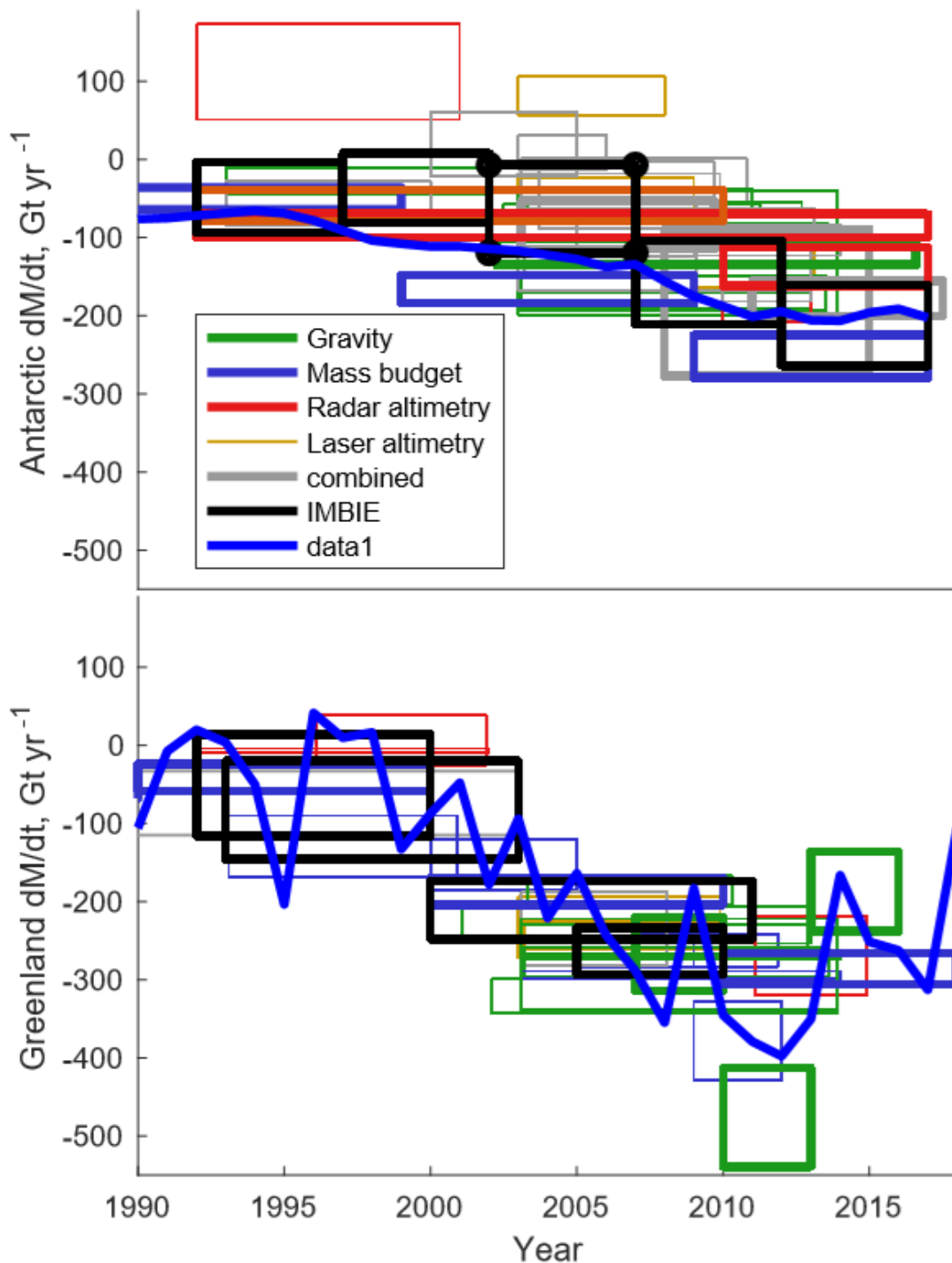


2335 **Figure 2.** Surface mass balance (averaged over the period 1989-2009) of the Antarctic ice  
2336 sheets (left) and the Greenland Ice Sheet (right) from the regional climate model  
2337 RACMO2.3p2 in  $\text{kg m}^{-2} \text{yr}^{-1}$  (van Wessem et al., 2018; Noël et al., 2018a). Elevation contour  
2338 levels (dashed) are shown every 500 m.



2339  
2340  
2341  
2342  
2343  
2344  
2345  
2346  
2347  
2348  
2349  
2350  
2351  
2352  
2353  
2354  
2355  
2356  
2357  
2358  
2359  
2360  
2361  
2362  
2363  
2364  
2365  
2366  
2367  
2368

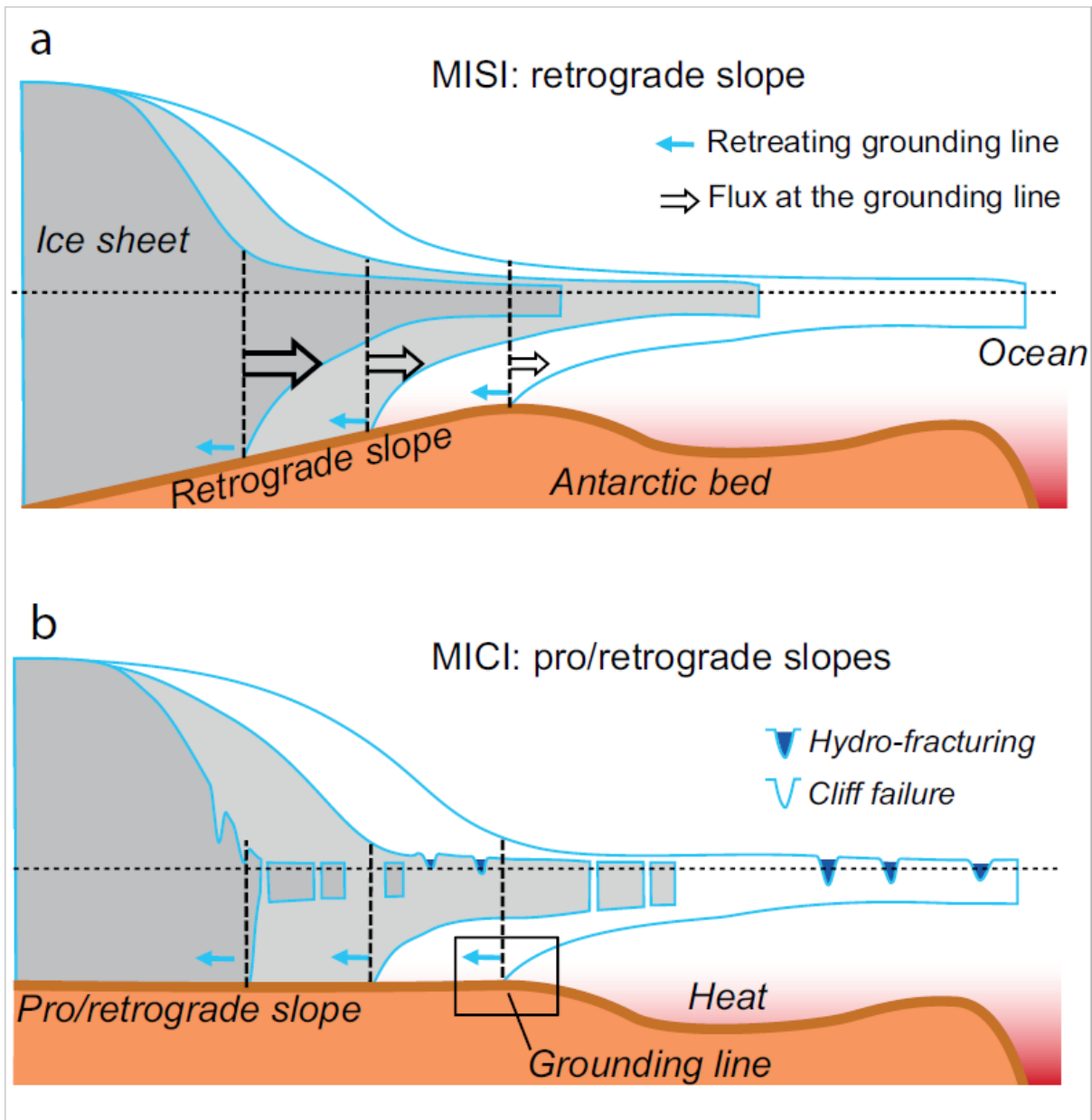
2369 **Figure 3.** Mass rates for the Antarctic (top) and Greenland (bottom) ice sheets derived from  
 2370 published studies. The horizontal extent of each rectangle indicates the period that each  
 2371 estimate spans, while the height indicates the error estimate. Studies published between 2011  
 2372 and 2017 are shown with thin lines, studies published in 2018 and early 2019 with heavier  
 2373 lines. The colour of the lines indicates the type of estimate used, and any estimate that is  
 2374 based explicitly on more than one technique is treated as a ‘combined’ estimate. The  
 2375 IMBIE (Shepherd et. al, 2012 for Greenland, Shepherd et al., 2018 for Antarctica) estimates  
 2376 are shown in black. Rectangles are overplotted with annual mass balance estimates from  
 2377 Rignot et al. (2019) for Antarctica and Mouginot et al. (2019) for Greenland, to indicate  
 2378 interannual variability. The studies cited in this plot are described in Supplemental Table I.  
 2379



2380

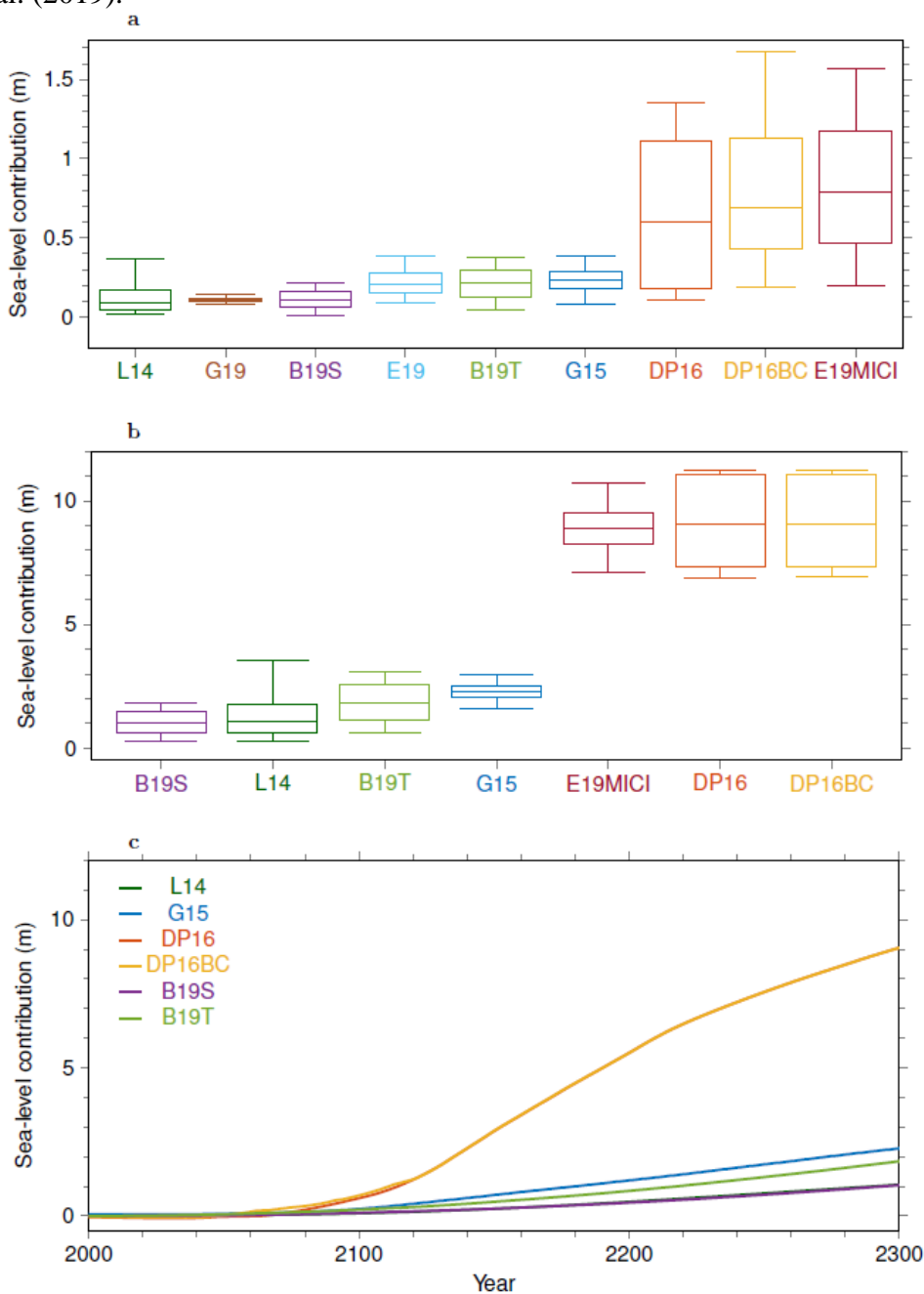
2381  
2382  
2383

**Figure 4.** Schematics of (a) Marine Ice Shelf Instability (MISI) and (b) Marine Ice Cliff Instability (MICI). The reader is referred to Section 3.1 for a discussion of MISI/MICI.



2384  
2385  
2386  
2387  
2388  
2389  
2390  
2391  
2392  
2393  
2394  
2395  
2396  
2397  
2398

2399 **Figure 5.** Projections of Antarctic sea-level contribution at (a) 2100 and (b) 2300 under  
 2400 RCP8.5. Boxes and whiskers show the 5th, 25th, 50th, 75th and 95th percentiles. The  
 2401 uncertainty range for Golledge et al. (2015) is based on a Gaussian interpretation for the  
 2402 projections with the 5th percentile given by the low scenario and the 95th percentile given by  
 2403 the high scenario. Idem for Golledge et al. (2019) with the 5th percentile given by the  
 2404 simulation without melt feedback and the 95th percentile given by the simulation with melt  
 2405 feedback. (c) Median projections of Antarctic sea-level contribution until 2300 (RCP8.5).  
 2406 Colour legend: **L14**: Simulations by Levermann et al. (2014), **G15**: Simulations by Golledge  
 2407 et al. (2015), **DP16**: Simulations by DeConto and Pollard (2016), **DP16BC**: Bias-corrected  
 2408 simulations by DeConto and Pollard (2016), **B19S**: Simulations with Schoof's  
 2409 parameterisation by Bulthuis et al. (2019), **B19T**: Simulations with Tsai's parameterisation  
 2410 by Bulthuis et al. (2019), **E19**: Simulations without MICI by Edwards et al. (2019),  
 2411 **E19MICI**: Simulations with MICI by Edwards et al. (2019), **G19**: Simulations by Golledge et  
 2412 al. (2019).



2413

## Supplementary Information

**Supplemental table I.** Details of mass-balance estimates used in Figure 4. Key for measurement type: G = gravimetry, L = laser altimetry, IOM = in/out (mass budget) method, A = airborne photogrammetry, RL and GLRIOM = combined.

### (a) Greenland Ice Sheet

Reference	Year	Type	Time 0	Time 1	Rate	Error
Zwally et al. 2011	2011	R	1992	2002	-7	3
Zwally et al. 2011	2011	L	2003.6	2007.8	-171	4
Shepherd et al. 2012	2012	GLRIOM	1992	2000	-51	65
“	2012	GLRIOM	1993	2003	-83	63
“	2012	GLRIOM	2000	2011	-211	37
“	2012	GLRIOM	2005	2010	-263	30
Wouters et al. 2013	2013	G	2003.1	2012.9	-249	20
Csatho et al. 2014	2014	L	2003.2	2010	-243	18
Enderlin et al. 2014	2014	IOM	2000	2005	-153	33
“	2014	IOM	2005	2009	-265	18
“	2014	IOM	2009	2012	-378	50
Groh et al. 2014	2014	L	2003	2009.9	-233	39
“	2014	G	2001.1	2013	-230	23.5
Hurkmans et al. 2014	2014	R	1996.1	2001.9	6	32.1
“	2014	RL	2003.1	2008.1	-235	47
Schrama et al. 2014	2014	G	2003.2	2013.6	-278	19
Velicogna et al. 2014	2014	G	2003.1	2013.9	-280	58
Andersen et al. 2015	2015	IOM	2007.1	2011.9	-262	21
Kjeldsen et al. 2015	2015	A	1983	2003	-74	41
“	2015	G	2003.3	2010.3	-186	18.9
McMillan et al. 2016	2016	R	2011.1	2014.9	-269	51
van den Broeke et al. 2016	2016	G	2003.1	2014	-270	4
“	2016	IOM	2003.1	2014	-294	5

Talpe et al. 2017	2017	G	2002.1	2013.9	-321	22
“	2017	IOM	1993.1	2000.9	-129	39
Mouginot et al. 2019	2019	IOM	1990	2000	-41.1	17
“	2019	IOM	2000	2010	-186.7	17
“	2019	IOM	2010	2018	-286.2	20
Zhang et al. 2019	2019	G	2007	2010	-267	47
“	2019	G	2010	2013	-476	63
“	2019	G	2013	2016	-187	51

**(b) Antarctic ice sheets**

<b>Reference</b>	<b>Year</b>	<b>Type</b>	<b>Time 0</b>	<b>Time 1</b>	<b>Rate</b>	<b>Error</b>
King et al. 2012	2012	G	2002.7	2010.9	-78	49
Bauer et al. 2013	2013	G	2002.5	2011.4	-104	48
Ivins et al. 2013	2013	G	2003	2012	-57	34
Sasgen et al. 2013	2013	G	2003	2012.7	-114	23
Groh et al. 2014b	2014	L	2003.1	2009.1	-126	39
Groh et al. 2014b	2014	G	2003.1	2009.1	-95	24
Gunter et al. 2014	2014	LG	2003.2	2009.1	-100	44
McMillan et al. 2014	2014	R	2010	2013	-159	48
Memin et al. 2014	2014	GR	2003.1	2010.8	-28	29
Schrama et al. 2014	2014	G	2003.1	2013.5	-171	22
Velicogna et al. 2014	2014	G	2003	2013	-180	10
Williams et al. 2014	2014	G	2003.3	2012.7	-62	7
Gao et al. 2015	2015	G	2003	2013.9	-120	80
Harig and Simons 2015	2015	G	2003.2	2013.6	-92	10
Li et al. 2016	2016	L	2003	2009	-44	21
Zamit-Magion et al. 2015	2015	LRG	2003	2009.9	-47	29
Zwally et al. 2015	2015	L	2003	2008	82	25
Zwally et al. 2015	2015	R	1992	2001	112	61
Jin et al. 2016	2016	G	1993	2002	-28	17

Jin et al. 2016	2016	G	2003	2011	-55	17
Martín-Español et al. 2016	2016	LRG	2003	2013.12	-84	22
Martín-Español et al. 2016	2016	LRG	2003	2006	9	22
Martín-Español et al. 2016	2016	LRG	2007	2009	-104	21
Martín-Español et al. 2016	2016	LRG	2010	2013	-159	22
Peng et al. 2016	2016	G	2002.5	2011.25	-65	7
Sasgen et al. 2017	2017	RG	2003	2013	-141	27
Shepherd et al. 2018	2018	LRG/IO	1992	1997	-48	45
Shepherd et al. 2018	2018	R/IO	1997	2002	-37	44
Shepherd et al. 2018	2018	LRG/IO	2002	2007	-63	56
Shepherd et al. 2018	2018	LRG/IO	2007	2012	-158	53
Shepherd et al. 2018	2018	RG/IO	2012	2017	-213	51
Talpe et al. 2017	2017	G/IO	1993	2000	-56	28
Talpe et al. 2017	2017	G/IO	2000	2005	20	41
Talpe et al. 2017	2017	G/IO	2005	2014	-103	20
Zhang et al. 2017	2017	LGG	2003.7	2009.7	-46	43
Gardner et al. 2018	2018	IO	2008	2015	-183	94
Gao et al. 2019a	2019	G	2002.25	2016.6	-119	16
Gao et al. 2019b	2019	LRG	2003.1	2009.7	-84	31
Rignot et al. 2019	2019	IOM	1979	1989	-40	9
Rignot et al. 2019	2019	IOM	1989	1999	-50	14
Rignot et al. 2019	2019	IOM	1999	2009	-166	18
Rignot et al. 2019	2019	IOM	2009	2017	-252	27
Sasgen et al. 2019	2019	RG	2011	2017.5	-178	23
Schroder et al. 2019	2019	R	1992	2017	-85	15
Schroder et al. 2019	2019	LR	1992	2010	-59	20
Schroder et al. 2019	2019	R	2010	2017	-137	25

